INTELLECTUAL SYSTEMS AND INFORMATION TECHNOLOGIES

Monograph

Edited by Prof. Yurii Gunchenko

PREMIER Publishing

Premier Publishing s.r.o.

Vienna 2021

UDC 004.9
G 94

INTELLECTUAL SYSTEMS AND INFORMATION TECHNOLOGIES: Monograph. Edited by Doctor of Technical Sciences, Profesor Yurii Gunchenko.– Vienna: Premier Publishing s.r.o. 2021. – 184 p.

ISBN 978-3-903197-27-5

DOI http://doi.org/10.29013/GunchenkoY.ISAIT.2021.184

G 94 The monograph presents materials containing original research by the authors, which reflect current trends in various areas, such as Information technologies; Systems and artificial intelligence techniques; Computers, systems, networks and their components; Automation of systems and management processes; Cybernetic and information security; Informatics and cybernetics; Project management; Electrical equipment and telecommunications; Intelligent devices and systems.

Sections of the monograph are separate extended materials, which were carefully selected and recommended for publication by the program committee on the results of the international scientific-practical conference "INTELLECTUAL SYSTEMS AND INFORMATION TECHNOLOGIES" ISIT-2019" (http://isit.odeku.edu.ua).

Subscribe to print 14/01/2021. Format 60×90/16.
Volume: 34.5 printed sheets
Offset Paper. Garinitura Minion Pro. Pec. liter. 11. Quantity: 250 copies.
Typeset in Berling by Ziegler Buchdruckerei, Linz, Austria.

Printed by Premier Publishing s.r.o. Vienna,
Vienna, Austria on acid-free paper.
Am Gestade 1, 1010 Vienna, Austria
pub@ppublishing.org, ppublishing.org

ISBN 978-3-903197-27-5

Content

ERRORS OF IMAGE COMPRESSION BY THE UAV COMPUTER BY DIFFERENT METHODS IN REAL TIME

Andrii Levchenko, Ilnara Sharipova, Yurii Shugailo,
Yurii Bercov, Hanna Korenkova, Oksana Zui

Abstract. The paper presents a comparative analysis of the effectiveness of image compression methods. A preliminary review of possible problems of representing numbers in binary code in the implementation of software in high-level programming languages. The paper summarizes the situations when the features of the representation of numbers in the computer significantly affects the results of data processing in general and images in particular. Test images of various degrees of saturation tested in known works were used as test data for the analysis of the efficiency of compression methods. Arrays of numerical data of test digital images were obtained with the help of on-board cameras of modern small-sized non-commercial drones. It is concluded that in the case of describing the original numerical data as well as Double the implementation of compression procedures in the C++ programming language. This choice is the best for further practical implementation image compression by the UAV computer for different methods. Image compression by the UAV computer in real time can be used by method with zonal-threshold selection of coefficients of fast two-dimensional Haar transformation.

Keywords: errors of image compression, programming languages, numerical data, compression method, image transformation.

Introduction and statement of the problem

The aim of image compression is to solve the problem of reducing the amount of data required for digital presentation. The basis of this process is the removal of redundant data from the original array, which reproduces the image in digital view. From a mathematical point of view, this is equivalent to converting a two-dimensional data array into a statistically uncorrelated array. The compression conversion is applied to the original image before it is saved or transmitted. Subsequently, the compressed data format is unpacked and the original image or some approximation of it is restored.

The main reason for the problems of image compression in digital data processing systems is the victory of the computing power of modern processors over the capacity limitations of storage and data transmission systems. Compression can reduce the load on data channels by converting them, which creates a load on the computer processor, because data compression is associated with large amounts of mathematical calculations.

It seemed that by increasing the bandwidth of network equipment and creating high-power computer data processing systems, the problem of limited computer resources will be a thing of the past, but social network users and technological progress are constantly evolving, leading to increased computing and restoring the problem of computer resource constraints. various conditions. For example, in the case of computer image processing by a drone, there are weight limitations. This does not allow engineering to use modern high-performance systems with high-performance processors as an on-board drone computer.

An overview of the errors in the presentation of the original data by the on-board computer

Preliminarily consider a simplified scheme for presenting graphic information in a computer (Fig. 1) image field is covered with an 8x8 grid. Compare bit 0 to those fields that are free from the image and 1 to those that are covered by image elements. If each line is interpreted as a binary number, the image can be written (encoded) in a sequence of eight decimal numbers: 0, 4, 132. 254, 254, 4, 4, 0, or in hexadecimal: 00, 04, 84, FE, FE, 04, 04, 00 and store in computer memory as bytes. Representation of numerical values in the form of bytes is the most rational in connection with features of architecture of memory chips.

The main format for presenting data in modern computers is the format for presenting binary numbers in a floating point. The format for representing binary numbers in a floating point is introduced by the IEEE754 standard [1, 2].

In engineering and programming, as a rule, 32 and 64 bit formats are used. In VB, numerical data types are represented as single (32 bits) and double (64 bits), and in C, C ++ – float (32 bits) and double (64 bits). The rest of the IEEE754 number formats are an extended version of single-precision.

0	0	0	0	0	0	0	0
0	0	0	0	0	1	0	0
1	0	0	0	0	1	0	0
1	1	1	1	1	1	1	0
1	1	1	1	1	1	1	0
0	0	0	0	0	1	0	0
0	0	0	0	0	1	0	0
0	0	0	0	0	0	0	0

Figure 1. A fragment of a digital image in binary form

To represent a number in the single-precision IEEE754 format, you must convert it to binary normalized form. To describe the procedure for converting numbers to 32-bit IEEE754 format, it makes sense to consider the appropriate steps:

– 1 bit is reserved for the sign of a number: 0-positive, 1-negative. This is the most significant bit in a 32-bit sequence;

– a bits of exponential representation follow, 1 byte (8 bits) are allocated for this. The exponent can be, like a number, with a + or – sign, although the meaning of these signs for the number, exponent and mantisa is different. To determine the sign of the exponent, so as not to introduce another sign bit, add a half-byte offset to the exponent. The offset exponent is written to the allocated 8 bits;

– the remaining 23 bits are reserved for the mantissa. But, in a normalized binary mantissa, the first bit is always 1, since the number lies in the range $1 <= M < 2$. There is no point in writing one to the allocated 23 bits, therefore, the remainder of the mantissa is written to the allocated 23 bits.

The numbers presented in the IEEE754 format represent a finite set on which an infinite set of real numbers is displayed. Therefore, the original number can be represented in IEEE754 format with an error. The graphical view of the number representation accuracy error function is presented in [2].

The absolute maximum error for a number in IEEE754 format is within half a step of the numbers. The step of the numbers doubles as the exponent of the binary number increases by one. That is, the farther from zero, the wider the step of numbers in the format IEEE754 on the numerical axis. The step of the denormalized numbers is $2^{(E-149)}$ (*Single*) and $2^{(E-1074)}$ (*Double*). Accordingly, the maximum absolute error limit for representing the original decimal number will be 1/2 of the number step: $2^{(E-150)}$ (*Single*) and $2^{(E-1075)}$ (*Double*).

The relative error expressed as a percentage will be: $(2^{(E-150)}/F)*100\%$ (*Single*) and $(2^{(E-1075)}/F)*100\%$ (*Double*).

The step of the normalized numbers is $2^{(E-150)}$ (*Single*) and $2^{(E-1075)}$ (*Double*). Accordingly, the limit of max. the absolute error will be equal to 1/2 of the number step: $2^{(E-151)}$ (*Single*) and $2^{(E-1076)}$ (*Double*). The relative error in% will be: $(2^{(E-151)}/F)*100\%$ (*Single*) and $(2^{(E-1076)}/F)*100\%$ (*Double*).

Thus, the main set of numbers in the IEEE754 format has a stable small relative error.

The maximum possible relative error for the number Single is $2^{-23}*100\%=11{,}920928955078125e^{-6}\%$. The maximum possible relative error for the number *Double* is 2^{-52}

$$*100\%=2{,}220446049250313080847263336181 6e^{-14}\%.$$

For the case of image compression by the UAV computer by different methods in real time, this means that there is a real threat of replacing the original matrices of numerical data with close to them with completely different conditionality numbers. Accordingly, small details of the original image may be lost. The task of data processing itself acquires a different nature and passes into the area, which is called incorrect tasks.

It should be noted that the IEEE754 standard provides four ways to round numbers:

- rounding tending to the nearest whole;
- rounding tending to zero;
- rounding tending to + ∞;
- rounding tending to – ∞.

When converting numbers, you must select one of the rounding methods. By default for software products, this is the first method – rounding to the nearest whole. Often in various devices use the second method – rounding to zero. When rounding to zero, you just need to discard insignificant digits of the number, so this method is the easiest in the hardware implementation [2, 3, 4].

The IEEE754 standard is widely used in engineering and programming. Most modern microprocessors are manufactured with a hardware implementation of the representation of real variables in the IEEE754 format. The programming language and the programmer cannot change this situation, there is no other representation of a real number in the microprocessor. When the IEEE754–1985 standard was created, the representation of a real variable in the form of 4 or 8 bytes seemed very large, as the amount of MS-DOS RAM was 1 MB. The program in this system could

use only 0.64 MB. For modern operating systems, the size of 8 bytes is negligible, however, the variables in most microprocessors continue to be represented in the format IEEE754–1985 [2, 4].

Currently, educational resources on the Internet present a lot of material on the features of the representation of numerical data in computers. However, in the opinion of the authors, the most complete and demonstrative from the point of view of estimating the values of transformation errors of numerical data since 2012 remains [2, 4]. As part of the solution of a number of applied problems, the authors considered some features of the representation of numbers in computer systems of technical diagnostics, navigation problems. An example of such work is [5, 6, 7].

To achieve the objectives of this work, it is advisable to summarize the known facts of computer computational errors caused by the use of numbers in the IEEE754 format.

Errors related to the accuracy of representation of real numbers in IEEE754 format. "Dangerous reduction". This error is always present in computer calculations. The reason for its occurrence is due to the lack of significant discharges. The relative error value associated with the accuracy of the representation has a dimension for single 10^{-6} for double 10^{-14}. The values of the absolute errors can be significant, for a maximum of single 1031 and double 10292, which can cause certain computational problems.

Interesting examples of specialized error calculations related to the application of the IEEE754 standard are translated in [2, 4]. Thus, for the case of errors related to the accuracy of the representation of real numbers, an example of computer and mathematical calculation of the representation of numbers is given.

For test examples, the relative error of the original numbers is approximately $3.24e^{-6}$%. As a result of one operation, the relative error of the result became 800%, ie. increased by $2.5e^{+8}$ times. The author of this work called such errors: "Dangerous reduction". The term refers to a catastrophic decrease in the accuracy of calculations in an operation where the absolute value of the result is much less than any of the input values of variables in computer calculations.

As a rule, modern programmers do not take into account the possibility of these errors when using high-level programming languages. However, they can significantly affect the final results of the calculations, and the user of the software product will sincerely believe in the correctness of the results [5].

Errors related to incorrect data type casting. "Wild mistakes". The errors are caused by the fact that the original number presented in single and double format is usually not equal to each other. For example [2]: source number 123456789,123456789, with: *Single*: 4CEB79A3=+123456792,0 (*dec*), *Double*: 419D6F34547E6B75=+123456789,123456791043281555175781 25. As it is not difficult to determine the difference between *Single* and *Double* will be: 2,87654320895671844482421875.

Therefore, it is fair to conclude that the variables and intermediate results of computer calculations should be reduced to one type of data, regardless of the expediency of different descriptions of variables in terms of saving memory in computations. Interestingly, similar requirements are imposed on software products and programming language developers (eg: C: ISO/EC9899: 1999). It should be noted that it is not enough to simply reduce all source data to one type. It is also necessary to reduce the results of intermediate operations to one type [2, 4].

The same source points to the fact that the result of the calculations may depend on the type and version of the compiler of a particular language. For test examples, the conclusion is made that the VC ++ compiler automatically lists the types of variables, and an attempt to force them to one type ends in a compilation error.

Calculation errors caused by failure to specify data types in [2] are proposed to be called "wild mistakes". These errors in the implementation of software products in high-level programming languages are due to ignorance of standards and programming theory (ie, poor basic education). That is why we support the use of the word "mistakes" when referring to such errors in the implementation of software products.

Mantiss shift errors. "Cyclic holes". These errors are due to the loss of accuracy of the result when the mantissa numbers on the numerical axis do not intersect. If the mantises of numbers do not intersect on the numerical axis, then the operations of addition and subtraction between these numbers are impossible.

According to the results of test examples, the shift error occurs if the original normalized numbers have different exponents. If the numbers differ by more than 2^{23} (for single) and 2^{52} (for double), then the operations of addition and subtraction between these numbers are not possible.

The maximum relative error of the operation result is approximately 5.96^{e-6}%, which does not exceed the relative error of the number representation.

The value of the relative error is small, but there are problems with programming. First, at the specified numerical values of the initial data it is possible to work with numbers only in a narrow range of a numerical axis where mantises intersect. Second, for each initial number, there is a cycle execution limit called a "cyclic hole". That is, if there is a cycle in which the original number is summed to the sum, then there is a numerical limit of the sum for this number. The sum, having reached a certain value, ceases to increase from its addition to the original number.

An example of a "cyclic hole" in an automatic control system is given in [2].

Rounding errors. "Dirty zero". In computer calculations, two types of rounding are always implemented. Either the numerical value of the performed arithmetic operation is rounded as a result of calculations and features of data representation or rounding occurs with the output and input of a real number in the window of operating system.

In the first case, the variable is rounded by one of the 4 types of rounding IEEE754, by default rounding occurs to the nearest whole. In this case, the variable takes a new rounded value different from the actual value.

In the second case, Windows has the following problems [4, 8]; there is no technical possibility to display or enter exact values of variables in windows of the graphic interface of the user, there are serious errors like "dirty zero".

Source [8] points to the fact that this kind of error often occurs in the "operator-machine" interface for various commercial applications in high-level programming languages. As a confirmation, this source indicates a fragment of the interface of the "logistic weight program" when resetting the container.

"Dirty zero" errors are situations where the numeric value of a variable is not actually zero in the program code. Whereas when creating programs, a variable equal to zero is considered according to mathematical relations. The relative error of the result is infinity.

In logical comparison operations, this non-zero can lead program execution to another branch of the algorithm. If for cases of presence of the interface of the operator there is a possibility to react to emergence of an error, for cases of automated processing of digital data such possibility is absent. This case includes image compression by the UAV computer by different methods in real time.

Errors at the norm/denor limit of the number. "Numbers –net-killer". These errors occur when working with numbers that are on the border

of the normalized representation of numbers. They are related to the difference in the representation of numbers in the IEEE754 format and in the difference in the formulas for translating the IEEE754 format into real numbers. That is, devices (or programs) must use different algorithms depending on the position of the real number on the numerical axis of the format. In addition to complicating devices and algorithms, there is also uncertainty in the transition zone. The uncertainty of the transition zone is that the standard does not specify a specific value of the transition boundary. In fact, the transition boundary is between two real numbers.

Since the boundary is a real number, its accuracy can be set indefinitely and the digital device or program does not have enough bit to decide to which range to assign this number.

In [2], as an example is the bug № 53632 for PHP, which caused panic in early 2011.

Entering the number $2.2250738585072011e^{-308}$ caused the process to hang with almost 100% CPU usage. Other numbers in this range did not cause problems. The same source indicates that the message about the bug was received on 30.12.2010, the message about its correction by the developer was received on 10.01.2011. Since the PHP preprocessor is used by most servers, any network user had the opportunity to "cut down" any server within 10 days. According to the developers, this bug only works in 32-bit systems. It is suggested that if you increase the accuracy of the limit number, modern 64-bit systems will also hang. Although for commercial reasons, the developers deny this possibility. The reason for the denial is clear: any user of the network, with a certain level of persistence, has the potential to "cut down" most of the information resources of the world community within ten days.

Comparison of image compression methods

Errors of image compression by the UAV computer by different methods in real time. The description of the problem of presenting numerical data led to restrictions on further comparative analysis errors of image compression by the uav computer by different methods in real time.

As models of image compression and recovery procedures, their software implementations in the C++ programming language were used. The elements of the test images were represented by 32-bit code. Both original

and restored images were recorded. The evaluation of compression methods for efficiency was carried out on the basis of private indicators, which include:

– σ – is the standard deviation of the restored image;

– $K_{+/-}$ – is the number of addition/subtraction operations when performing compression-recovery operations;

– $K_{m/d}$ – is the number of multiplication / division operations when performing compression-recovery operations;

– t_t – is the time of transformation of the original image (from the moment of reading the original image to writing to the file of the obtained compressed sequence);

– K_t – is the compression ratio of the original image.

The modified method of arithmetic coding with a fixed model of image compression (szsdv&iqrp) [10, 11] was tested in the following variants: with (szsdv&iqrp+) and without (szsdv&iqrp-) subquantization and using zonal-threshold selection at different values of the image quality restoration parameter (szsdv & iqrp).

The original images were used in the standard 4: 3 format with a dimension of 640 × 480 image samples, which allowed when dividing the image into 8 × 8 blocks to obtain an integer number of blocks and avoid the recovery error introduced by the addition of samples of the original image.

When performing research, a comparative evaluation of image compression efficiency [12, 13, 14, 15] for varieties of the method with zonal threshold selection and compression methods widely used in practice in image processing, such as:

– JPEG [16, 17], which includes two-dimensional discrete-cosine conversion of samples of the original image;

– JPEG-2 [15], which includes wavelet transform and statistical coding when changing the parameter "compression" in the range from 0 to 100;

– WI, which includes performing wavelet transform and statistical coding when changing the parameter "compression" in the range from 0 to 100.

In the general case, the transformation of the image by the algorithms of the JPEG method involves the following steps:

– change of color space of representation of RGB samples on YCrCb;

– two-dimensional discrete-cosine transformation of samples of the original image;

– quantization of the transformant in accordance with the selected parameter "compression" in the range from 0 to 100;

– coding of series lengths (RLE) of the obtained sequences;
– Huffman statistical coding;

In the methods JPEG, JPEG-2, the "compression" (Z) parameter is used to control the compression ratio.

A separate comparison is made with image compression methods, which implement procedures similar to those used in the compression method with zonal-threshold selection. Such methods include compression methods based on the zonal selection of the coefficients of two-dimensional discrete-cosine transformation (2-ddcost) [19] and the zonal selection of the coefficients of fast integer two-dimensional Haar transformation (zscfastint2-dtHaar).

The analysis of the values K_t and σ obtained when processing images with different degrees of saturation, depending on the values of Z, showed that the analyzed compression methods provide σ of less than 3% with Z values less than 70, 60 and 50 when processing low-, medium- and highly saturated images respectively.

Compression ratios for this value σ range from 3 to 25 times for the JPEG method, from 5 to 35 times for JPEG-2000, and from 5 to 30 times for WI. Note that when using the WI compression method at compression values of 50 and 70, significant compression ratios were obtained (of the order of 50–80 times), but the σ value in this case increases 2–3 times in relation to the σ values of the JPEG methods. The analysis of the results of image compression shows that the JPEG-2000 method was the most effective in terms of σ and K_t.

Analysis of indicators for compression methods 2-ddcost, zscfastint2-dtHaar showed that the methods provide σ less than 3% at values of $W_S \geq 5$ when processing highly saturated images and at values $W_S \geq 3$ for low- and medium-saturated images. Compression coefficients for such an σ value lie in the intervals: from 1 to 12 times for the 2-ddcost method, from 1.8 to 18 times for zscfastint2-dtHaar, from 1.8 to 23 times for the szsdv&iqrp method.

With $WS = 1$ and 2, the RMS value increases sharply, so it is advisable to use such values of the quality parameter only to obtain large compression ratios. This conclusion confirms the results for the known test data [11], however, it requires verification for other images, where the numerical values of the intensity of the color components have different sizes.

Analysis of the nature of the change in compression ratios shows that when processing "low-saturated" images, the szsdv&iqrp method [10]

provides less compression at WS = 5–10 than the 2-ddcost compression method with zonal selection. However, when using the 2-ddcost method, much worse σ values were obtained for szsdv & iqrp method.

In [11], this is due to the presence of a large number of "natural" zeros, i.e. zero values of the conversion coefficients before selection. We can conclude that the selected test images are inadequate for the totality of all possible situations. When processing medium and highly saturated images, the szsdv & iqrp method provides high values of K_t.

In a comparative analysis of compression methods, the ratio of the obtained K_t and σ is of greatest interest. The main tasks of image processing in the interests of object recognition, therefore, will analyze those settings of compression methods at which the σ value takes on a value of no more than 2%. The analysis shows that the JPEG-2 compression method is characterized by the best K_t / σ ratio. In addition, it should be noted that the maximum values of the compression ratios for such methods as JPEG, JPEG-2, WI are significantly superior to other compression methods.

Since the evaluation of the compression parameters – K_t and σ for images with different degrees of saturation is carried out using a limited number of experiments (n = 900), then the error of the method itself is introduced into the determination of these parameters.

The values of the probability that the error will not exceed in the assessment of K_t and σ – P are presented in table 1.

Table 1. – Values of the probability P for the investigated compression efficiency indicators for the test case

K_t			σ		
p = 0,95	q = 0,05	n = 900	p = 0,9	q = 0,1	n = 900
P = 0,99			P = 0,95		

The values given in the table based on the results [11] are estimates, since one value of the number of tests is taken into account. The dependence of the studied parameters of image compression on the number of results is subject to further study.

Computational complexity is an important parameter for comparing image compression methods that characterize the time of their implementation. To determine its value, two approaches are used: an estimation of the number of elementary operations performed (addition, subtraction, multiplication, division, etc.) or the execution time of the method procedures.

When using the first approach, addition/subtraction and multiplication/division operations are considered separately. This is due to the fact that to perform multiplication/division operations, more clock cycles of computational elements are required and their technical feasibility is more complicated. So, when processing images by the analyzed methods, it is necessary to perform:

When using the first approach, addition/subtraction $K_{+/-}$ and multiplication/division $K_{m/d}$ operations are considered separately. This is due to the fact that to perform multiplication/division operations, more clock cycles of computational elements are required and their technical feasibility is more complicated. So, when processing images by the analyzed methods, it is necessary to perform:

14680064 operations addition/subtraction and 16777216 operations multiplication/division when using the method based on the 2-ddcost transformation;

3670016 operations addition/subtraction and 2097152 operations multiplication/division when using the method based on the zscfastint2-dtHaar transform method;

5155016 addition/subtraction operations and 3582152 multiplication/division operations when using the szsdv & iqrp transform method.

Thus, the computational complexity of the image compression method szsdv&iqrp is 5 times less than that of the method based on 2-ddcost transformation, but about 1.5 times more than with zscfastint2-dtHaar transform. This is due to the need to carry out additional calculations to find the threshold of the breeding. However, the proposed method provides higher compression ratios with lower σ compared to the zscfastint2-dtHaar transform method.

An analysis of the computational complexity of image compression methods from a practical point of view, in terms of the number of operations performed, is not advisable and is of interest in studying the computer implementation of mathematical methods.

Evaluation of the effectiveness of compression methods from the point of view of the expediency of using image compression by the computer UAV in real time procedures will be carried out according to the value of the time for transforming an image into a file. By the time indicator of compression methods we mean the time spent on the execution of compression procedures [11].

The time depends on the computational complexity of the compression procedures used, on the performance of computational elements and

storage devices, as well as on the efficiency of the program code that implements the algorithm in the software implementation of the compression method [19]. In (Fig. 2) shows the results of a comparative analysis of the compression time of images by the known algorithms JPEG, JPEG-2, WI and software implementation szsdv&iqrp transform method.

It should be noted that the szsdv&iqrp procedures for arithmetic operations are integer. In terms of the study errors in the presentation of the original data by the on-board computer, this is a significant advantage.

At the same time, according to the sources [3, 9, 10, 11], allows obtaining at $\sigma < 3\%$:

- for a highly saturated image $K_t = 3.5$ times;
- for the medium-saturated image $K_t = 7$ times;
- for the low-saturated image $K_t = 23$ times.

The use of subquantization of coefficients in direct transformation according to the Haar basis makes it possible to increase the compression ratio by reducing the dynamic range of the conversion coefficients in relation to the range of samples of the original image. However, this leads to a significant increase in the values of the standard deviation. At sub-quantization levels $V = 1$ or 2, the compression ratio increases by 10–25% due to a decrease in the alphabet of the encoded source.

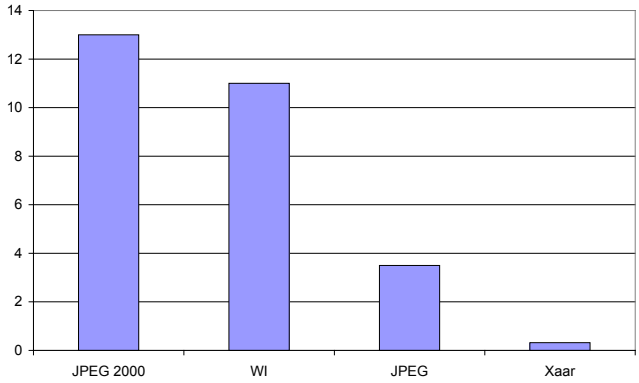

Figure 2. Time of images compression for different methods

It should be noted that the proposed recommendations for choosing the values of the parameters of the developed compression method make it possible to minimize the visibility of introduced distortions in the processed images when reaching relatively low compression ratios 5.5–10 times.

Conclusions

1. It is false to believe that floating-point calculations are within the relative error of representing the largest number. The magnitude of errors is cumulative. Numerical values are added to each other. The postulate of metrology on mutual error compensation during data averaging does not work in the case of computer processing of decimal data.

2. When processing data by programs written in high-level programming languages with converting values from decimal to binary number system, the tendency of the averaged value of the measurement results to the true value of the physical quantity does not occur. Errors such as dirty zero and dangerous reduction make the amount of computational error unacceptable. When programming computer calculations, special attention should be paid to the transformation of values close.

3. The main job of programmers is to deal with errors, and not in mathematical solutions to the problem. The programmer needs to calculate the error of the result in each cycle in order to take it into account in the next cycle. The programmer must be absolutely prepared for the fact that some basic concepts of mathematics are not carried out in calculations in the IEEE754 format. For example, the rules of algebraic commutativity $(a + b) + c = (a + c) + b$ are usually not met in such calculations. Unfortunately, in modern fundamental mathematics education, little attention is paid to this issue, leaving the solution of the toolbox problems to the applied programmer.

4. The results of various independent studies presented in the work allow us to conclude that the selected test images are inadequate for the totality of all possible situations.

5. The values given according to the results of [11] are estimates, since one value of the number of tests is taken into account. The dependence of the studied parameters of image compression on the number of results is subject to further study.

References:

1. EEE Standard for Binary Floating-Point Arithmetic. Copyright 1985 by The Institute of Electrical and Electronics Engineers, Inc 345 East 47th Street, – New York, NY10017, USA.
2. *Yashkardin V.* IEEE754 – binary floating point arithmetic standard/ IEEE754 – стандарт двоичной арифметики с плавающей точкой: [Online].– Access mode: URL: https: //i www.softelectro.ru, 02.11.2020.

3. *Salnik Yu. P.* Modified method of arithmetic coding with a fixed model/Модифицированный метод арифметического кодирования с фиксированной моделью in Radioelectronic and computer systems, 2005. – Issue 5. – P. 50–54.
4. The IEEE754 program is a converter of numbers in the IEEE754 format with an absolute precision of the result representation: [Online].– Access mode: URL: // http://www.softelectro.ru/pr_ieee754.htm.
5. *Levchenko A., Voitenkov R.* Origins of disability of diagnostic systems of weapons of the second kind with representation of numbers with a floating point / Витоки втрати працездатності систем діагностики ОВТ другого роду з представленням чисел з плаваючою комою, SWorld scientific works, – Vol. 1(38). – Part 3. – P. 108–115. – March, 2015.
6. *Levchenko A., Voitenkov R.* Method of representation of numbers for software tools of guaranteeing information technologies of decision support systems for weapons management / Метод представлення чисел для програмних засобів гарантоздатних інформаційних технологій систем підтримки прийняття рішень для керування станом ОВТ, in Proc. 19th conference "Problems of creation, development and application of special purpose information systems", Zhytomyr, ZMI NAU, 2012. – P. 142–143.
7. *Semchac O., Levchenko A.* Disadvanteges of computer implementation of SLAM-metods of local navigation autonovus mobile objects, SWorld journal, – Vol. 2. – Part 2. – P. 108–115. – October, 2019.
8. *Yurovitsky V. M.* IEEE754-tick threatens humanity/IEEE754-тика угрожает человечеству: [Online].– Access mode: URL: https: // IEEE754.htm, 14.10.2020.
9. *Korolev A. V., Bokhan K. A., Salnik Yu. P.* Subquantization of the transformer of a two-dimensional integer Haar transformation in Modeling and information technologies, – Kyiv: IPME, NASU, 2004. – Issue 26. – Vol. 1. – P. 3–7.
10. *Korolev A. V., Bokhan K. A., Salnik Yu. P.* Zonal-threshold selection of coefficients of fast two-dimensional Haar transformation in Information processing systems, NASU, 2004. – Issue 4. – Vol. 1. – P. 109–113.
11. *Bokhan K. A., Koroleva N. A., Salnik Yu. P.* Evaluation of the effectiveness of the zonal-threshold selection for the Haar transformation coefficients / Оценка эффективности зонально-пороговой селекции коэффициентов преобразования Хаара in Systems of processing information, NASU, 2004. – Issue 6. – P. 13–17.

12. *Bondarev V. N., Trester G., Chernega V. S.* Digital signal processing: methods and tools: 2nd ed., H, Cosinus, 2001. – 398 c.
13. *Klimenko L. A., Malakhov S. V.* Video encoding methods / Методы кодирования видеоданных in Information and control systems in railway transport, 1998. – Issue 2. – P. 59–62.
14. *Pratt W. C.* Image transfer methods. Reduction of redundancy / Методы передачи изображений. Сокращение избыточности, – M., Radio and communication, 1983. – 264 p.
15. *Vatolin D., Ratushnyak A., Smirnov M., Yukin V. M.* Methods of data compression: The device of archivers, compression of images and video / Методы сжатия данных: Устройство архиваторов, сжатие изображений и видео, Dialog–MIFI, 2002. – 384 c.
16. *Miano J.* Image compression formats in action, – M., Triumf, 2003. – 354 c.
17. *Wallace G. K.* The JPEG Still Picture Compression Standard // Communication of the ACM, 1991. – Vol. 34. – Issue 4.
18. *Korolev A. V., Malakhov S. V., Linnik N. F.* Modified zonal compression of images with partial elimination of phase components of the spectrum / Модифицированное зональное сжатие изображений при частичном устранении фазовых составляющих спектра in Systems of processing information, HMU, 2001. – Issue 5(15). – P. 176–180.
19. *Levchenko A.* The structure of the information technology of the guaranteed development of the tasks of forecasting the state of the defense system / Структура інформаційної технології гарантованого розв'язання задачі прогнозу стану системи озброєння in Problems of opening, testing, storage and operation of folding information systems, ZMI NAU, 2010. – Issue 3. – P. 96–110.

Andrii Levchenko, C.t.s., as.prof, assistant professor of the Computer science and technologies department, Odesa National University, 2 Dvoryanska str., Odesa, Ukraine
E-mail: katyaandreylev@gmail.com, a.levchenko@onu.edu.ua.
ORCID: https://orcid.org/0000-0001-5550-0027,

Yurii Shugailo, C.f-m.s., assistant professor of the Computer science and technologies department, Odesa National University, 2 Dvoryanska str., Odesa, Ukraine
E-mail: y.shugailo@gmail.
ORCID: https://orcid.org/0000-0003-2144-0930

Hanna Korenkova, C.f-m.s., assistant professor of the Computer science and technologies department, Odesa National University, 2 Dvoryanska str., Odesa, Ukrain
E-mail: nitsuk@onu.edu.ua
ORCID: https://orcid.org/0000-0001-7207-3688

Ilnara Sharipova, Master of metrology, Postgraduate student of the Computer science and technologies department, Odesa National University, 2 Dvoryanska str., Odesa, Ukraine
E-mail: iln.sharipova@ukr.net.
ORCID: https://orcid.org/0000-0003-0521-1299

Yurii Bercov, Master of computer science, senior master of the Computer science and technologies department, Odesa National University, 2 Dvoryanska str., Odesa, Ukraine
E-mail: bercov@gmail.com.
ORCID: https://orcid.org/0000-0001-9704-1121

Oksana Zui, Odesa National University, 2 Dvoryanska str., Odesa, Ukraine
E-mail: oks.zuj@gmail.com
ORCID: https://orcid.org/0000-0001-9520-4441

HIGH-PRECISION TECHNOLOGIES FOR HYDRO-ACOUSTIC STUDIES OF COMPLEX BOTTOM RELIEF ARE ONE OF THE AREAS OF THE SPECIAL ECONOMIC ZONE FOR THE HIGH-TECH PARK

Nataliia Punchenko, Oleksandra Tsyra

Abstract. Modern control systems are built on an integrated principle and use the data received from the onboard sonar equipment. The most promising in this regard is multi-beam echo sounders, which allows to solve both search and research problems and to correct the generation of navigation parameters of the onboard control system.

Keywords: multi-beam echo sounder, single-beam echo sounder, sound beam, navigation, positioning.

Introduction and statement of the problem

The role of the oceans for humanity is growing rapidly. Land – the hard shell of the Earth, makes up about 30% of the surface of our planet – is becoming increasingly crowded for its growing population. A human enriched with knowledge is becoming ever firmer in his intentions to more actively develop the use of all resources of the seas and oceans. Scientists and engineers have developed a variety of systems and instruments, which are equipped with a large research fleet. A versatile technique, located in the hands of people who study the water space, allows to study physical processes in the entire thickness of ocean waters, biological communities of the seas, the bottom and its deep layers. The main technical means providing the most complete and comprehensive information on the water masses of the seas and oceans are hydroacoustic systems and various devices based on acoustic principles. Human began to learn the water element a long time ago. And even though in his hands are the perfect research methods, aquatic life is fraught with a lot of unknowns. Academician L. M. Brekhovskikh today calls the World Ocean the Big Unknown. And indeed, most recently, a little more than 30 years ago, peculiar sound waveguides called underwater sound channels were discovered in the thickness of oceanic waters. In

these channels the sound power is slightly weakened, which determines its ultra-long distribution. In the 70-s, a new important discovery was registered – the presence of huge synoptic vortices in the ocean. The priority of this discovery belongs to a group of Soviet oceanologists led by L. M. Brekhovskikh. According to experts, these vortices accumulate 90% of the kinetic energy of the ocean and significantly affect its parameters. Thermohydrodynamic conditions affecting sound propagation disturb biological life. Today, many economic problems are associated with the ocean. Among the most important problems facing science is the study of the oceans, including the Black Sea shelf, with the aim of rational use of its resources.

The aim of the work is the Black Sea bathymetric maps, reflecting the average features of the dismemberment of the underwater relief, where the details are not partially recorded. Based on this circumstance, the main source when studying dissection are bottom topography profiles, which are based on the obtained echograms.

At present, it is generally recognized that it is necessary to solve a complex of major scientific and technical problems to improve the safety of navigation in modern conditions. In the general complex of problems, an important link is the development of autonomous passive and active navigation systems, which include sonar navigation systems. A complementary complex subsystem in the general automated navigation system is the subsystem of hydroacoustic navigation devices, which includes sonar logs and echo sounders.

The scientific basis for solving such problems is laid in the publications of the works of such scientists as B. G. Abramovich, N. I. Andermo, M. K. Borkus, A. N. Bochkarev, D. V. Vasiliev, V. I. Volov, P. N. Denbigh, F. R. Dickey, S. F. Kozubovskaya, A. A. Krasovsky, V. P. Tarasenko, etc., where, on correlation extreme systems, it is concluded that there are several methods for measuring speed and structural implementations of these methods. Some aspects of special studies of equipment using random processes are described in the works of J. Bendat, V. V. Bykov, Yu. I. Gribanov, A. P. Zhukovsky, S. G. Zubkovich, G. Ya. Mirsky, Yu. I. Feldman et al., where problems related to the analysis of random processes, the formation of realizations of random processes with given spectral characteristics, and the development of hardware for analyzing the correlation and spectral characteristics of random processes are considered.

Main part

To ensure navigational safety, the navigator needs to know the depth of the place under the keel of the ship. For this purpose, navigation echo sounders are installed on ships, because of all known types of radiation, sound propagates into the sea with the least loss compared to radio waves and light, which attenuate much more in muddy and salty sea water [1]. For this purpose, bottom topography surveys are carried out, which can be divided into classes: 1. bottom topography surveys are a set of hydrographic works performed with the aim of constructing a digital bottom topography model, identifying navigational hazards and then assembling them based on the received navigation charts and navigation aids to ensure the safety of navigation; 2. navigational danger is a natural or artificial underwater or drying obstacle (raising the bottom or underwater object) with depths above it that are hazardous to ships. Signs of navigational danger are considered to be depths that differ from the surrounding depths to a lower side: at depths from 0 to 40 m inclusive – more than 1 m; at depths of more than 40 to 100 m inclusive – more than 2 m; at depths of more than 100 m – more than 10% with a smooth bottom relief; more than 20% with hilly bottom topography; more than 30% with complex bottom topography.

Navigational hazards also include the coastline and surface obstacles (natural and artificial), the position and characteristics of which must also be determined when shooting the bottom topography.

3. To make the bottom relief depending on the importance of the water area in terms of shipping, the ratio of the depths in the shipping part with the maximum draft of the vessels and the characteristics of the bottom soil is determined by four survey classes: 1, 2, 3 and 4, differing in: accuracy of the survey – permissible uncertainties of depth measurement and their location; survey detail – discreteness of depth readings over the water area.

Class 1 survey is carried out in areas of navigable water areas with depths from 0 to 40 m inclusive. When survey the 1st class, the discreteness of the depth reading should ensure the identification of relief details that differ from the surrounding depths by the amount specified in paragraph 2, and the detection of objects at the bottom in size equivalent to a cube with an edge of 1 m or more.

Examples of areas in which class 1 surveys are conducted are shallow harbors, water moorings, mooring places, shallow fairways and sea channels, the most important sections of shipping channels (fairways) and rivers

with minimal depths under the keel. Class 2 survey is performed in navigable waters with depths of less than 100 m with detail, which ensures the detection of objects at the bottom in size equivalent to a cube with an edge of at least 2 m at a depth of up to 40 m, and in depth, different from the surrounding depths value specified in paragraph 2. The 2nd class of surveying is used for areas in which the natural features of the relief or artificial objects at the bottom have minimal depths and do not create obstacles for vessels passing through this area (the depth under the keel is uncritical). Class 3 survey is carried out for navigable water areas with depths up to 200 m inclusive. This class of survey is recommended only for those areas of the water area where the depth under the keel is not considered significant, and the likelihood of artificial or natural obstacles at the bottom is low. Class 4 survey is carried out in marine areas with depths of more than 200 m.

In some cases, one class may not be suitable for the entire area. In these cases, in the survey project, it is necessary to clearly define the areas of the water area where other classes should be used.

The situation detected by the hydrograph in the field can be so different from the expected that it can serve as a basis for changing the survey class. For example, in the area through which vessels with a displacement of 200,000 tons or more pass and which has a depth of more than 40 m, a second-class survey may be set. However, if the hydrograph detects shallows with depths less than 40 m, then in this place it is necessary to take a first-class survey.

The bottom topography is divided into:

a) the areal survey. Survey with equally high discreteness of uniform depth reports in two mutually perpendicular directions: maximum and minimum depth gradient. It consists in measuring the depths on the survey strips, the overlap of which provides a uniform at least a one-time coverage (taking into account double coverage in the zones of overlapping survey strips) by counting the depths of the bottom for the water area over the entire survey area. The areal surveying can be performed: by the multi-beam echo sounder; by the multichannel echo sounder (echo sounder have a number of transceiving transducers of vertical radiation and reception); by the aviation laser bathymetric systems; by the according to aerial and space photographing of the water area using aerial cameras, digital aerial cameras, scanning optoelectronic systems; by the according to radar survey of water areas.

b) The meter, which consists in measuring depths using a single-beam echo sounder, manual lot, basting with maximum discreteness of readings,

which are sequentially laid along the general direction of the maximum gradient of depths for parallel profiles (tacks), which are located on distances from each other and are set depending on the spatial variability of depths in direction perpendicular to the profile direction (tack).

c) The meter with a hydroacoustic examination of the intergalse bottom sections consists in simultaneously measuring the depths on successive profiles (tacks) and sonar sounding of the bottom between the tacks in order to identify navigational hazards and their subsequent survey with higher detail.

Using aviation laser bathymetric systems, surveys of classes 2 and 3 are allowed. Measurement with a hydroacoustic examination of the inter-galley sections of the bottom should be used only when survey 2 and 3 classes. The meter should only be used for survey 3rd and 4th grade.

When considering navigational safety, it is impossible to ignore the systemic unification of a finite set of sciences, the theoretical and practical aspects of which are in certain relations and correlations with each other, serve to achieve the unified goal of scientific and technological progress as a particular industry of material production and act as a whole with respect to other sciences and branches of the national economy – megascience metrology [2].

For navigational safety, at depths, it is necessary to specify the accuracy requirements for positioning. It is necessary to consider the requirements for clarifying the magnitude of the error in the location of the depth, depending on the magnitude of the error in its measurement.

When monitoring the status of underwater objects and solving several other tasks, they impose serious requirements for conducting a detailed survey of the bottom topography with high, almost centimeter, accuracy.

The survey error (μ) can be determined by the formula [1]:

$$\mu^2 = m_c^2 \delta_t^2 + m_z^2 + m_i^2 \quad (1)$$

where m_c – mean square error (MSE) of determining the ship's position on the tack;

δ_t – vertical ruggedness indicator;

m_z – MSE of the depth measurements;

m_i – MSE of the interpolation, depends on the distance between the tracks, the nature of the separation of the field and the adopted method of interpolation.

This formula can be applied when measuring using a single-beam echo sounder, when it is impossible to obtain data on the depths between

the spans. When performing areal surveys of the bottom topography of multi-beam echo sounders, i.e., if there is a very high density of data on the depths in the survey strip, there is probably no need to take into account the vertical field division indicator (δt), as well as to interpolate the depth values in the survey strip. Based on the foregoing, expression 1 may acquire a different form:

$$\mu^2 = m_c^2 + m_z^2 \quad (2)$$

From this we can conclude that the accuracy of survey depends on the error in measuring the depths, the error in determining the location. If one of the errors is 0.33 times smaller than the other, then the smaller error in the calculations is neglected.

Nowadays, one must not forget that international organizations use the concept of measurement uncertainty. Total horizontal (planned) uncertainty (THU): component of the total transferred uncertainty calculated in the horizontal plane. Even though the total horizontal (planned) uncertainty is given as a single value, it has a dimension of 2D. It is assumed that the uncertainty is anisotropic (i.e., the correlation between latitude and longitude errors can be neglected). This moment allows us to assume that the normal distribution is symmetric in a circle and allows us to characterize the radial distribution of errors in true value by one number. Total Vertical (Altitude) Uncertainty (TVU): component of the total transferred uncertainty calculated in the vertical plane. Total Vertical (Altitude) Uncertainty is a1D Dimension.

Along with these concepts, the terms are used – the total error of determining the location of depth and the total error of measuring depth, since we assume that, in essence – the uncertainty corresponds to the concept of error.

The total vertical (altitude) uncertainty (the total error of the depth measurement) should not exceed the value, calculated by the formula 2.

The total horizontal (planned) uncertainty (total depth location error) at the 95% confidence level should be no more than 2 m. This approach to assessing the depth measurement errors and its location in the S-44 standard is due to the requirements for ensuring the safety of navigation, where the assessment is important depth measurement accuracy.

First consideration of shipping safety using marine acoustics essays of oceanographic work in the Black Sea.

The history of oceanographic work in the Black Sea is usually divided into temporary stages: until the 70 s of the 18th century, 1770–1870, 1870–1917, 1917–1941, 1946–1995, 1995 – to this day.

The first period was marked by the general interest of the basin of the Black and Azov Seas. As a result of these works, a map of the coast of the Black and Azov Seas appeared. The result of such oceanographic work was hydrographic and hydrometeorological work, which resulted in atlases – indicate the depth of up to 500 m and the soil of the seabed.

1. In 1808, the description of "Lotsiya or a guide to the Black and Azov Seas" by I. Budishchev.

Hydrometeorological stations were opened, a depot of maps of the Black Sea Fleet was created, in 1842 a new atlas was published on the work of the expedition of Yegor Pavlovich Mangarani. In 1851, the depot of cards published the first Black Sea.

The next period can be called as a more systematic study of the Black Sea basin, a powerful foundation was laid for cartography and study of the waters of the Black Sea. Where, in a certain area, it was concluded that the flow depends on the winds, the temperature and density – on the direction of the current. We checked that the density of the Black Sea waters is lower than oceanological. This assessment of water metabolism. Got information about the coastal course.

New hydrological stations opened. The first oceanographic Black Sea expedition was organized under the leadership of Joseph Bernardovich Spindler. One of the components of the result is the study of the seabed topography. All findings of the expedition research were important for science.

The next period began with the signing decree by the V. I. Lenin SNK RSFSR "On the organization of the meteorological service of the RSFSR". According to the results after revolutionary expeditions, data were obtained on the state of water: hydrological and biological, and vertical and horizontal exchanges. In 1932, Nikolai Mikhailovich Knipovich issued the first monograph on the hydrology of the Black Sea, which included the results of studies of 20 years of the 20th century. This work, on some issues, is relevant today. In 1935, a full oceanographic survey was conducted in the winter of the Black Sea. Hydrometeorological reference books issued. The hypothesis was tested that the Black Sea basin consists of two unconnected balls, it is confirmed that the thickness of the sea's waters is dynamically one and that horizontal and vertical movement of water occurs in it. The next period is characterized by the fact that in the late forties of the last century, ultrasonic echo sounders appeared on the armament of hydrographs. The sea was considered as aspects of oceanography and hydrobiology. In 1957, four seasonal surveys were conducted. Once again,

they confirmed that at the depth of the sea there are processes of circulation of water exchange [3, 4]. Created navigational aids. A radio navigation coordinate system has been introduced. At the end of the 20th century, according to the results of research after the Second World War on the topography and soil bottom, current navigation maps were created. In these studies, a qualitatively new approach was used a comprehensiveness based on autonomous and remotely controlled equipment, non-contact observation methods. The research results introduce new results of water circulation, turbulent exchange, water pollution and chemical composition. The manuals "Climatic Fields of Salinity and Water Temperatures of the Black Sea", "Typical Wind Fields and Waves of the Black Sea" were issued.

At present, remote methods for observing the sea are used for research, based on such studies – cartography of various parameters.

The section on marine acoustics includes hydroacoustics. This is the section of acoustics that studies the propagation of sound waves in a real marine environment for purposes of underwater location, communication, etc. A distinctive feature of underwater sounds is low attenuation, this feature allows sound to propagate under water for much greater distances than in air. In the range of audible sounds that bulding on frequencies of 500–2000 Hz, the range of distribution of medium-intensity sounds under water reaches 15–20 km, and in the ultrasound region – 3–5 km. Based on the values of sound attenuation, which can be observed in laboratory studies in small volumes of water, significantly greater distances could be expected. However, in natural conditions, in addition to attenuation due to the properties of the water itself (viscous attenuation), the refraction of sound and its scattering and absorption by various inhomogeneities of the mediums have a significant effect.

Sound refraction, in other words, when it comes to distorting the path of a sound beam, can be caused by the heterogeneity of the properties of water, mainly along the vertical, caused by three main reasons:

1) changes in hydrostatic pressure with depth; 2) changes in salinity; 3) temperature changes due to uneven heating of the mass of water by the sun's rays.

As a result of superposition of the main causes, the speed of sound propagation is: – 1450 m/s for fresh water; – 1500 m/s for sea water.

Changes occur depending on the depth, while the law of change depends on natural conditions: season, time of day, depth and several other reasons. Sound rays emerging at an angle to the horizon are bent, and their

direction of bend is determined by the distribution of sound velocities in the medium. In the warmer months, the upper layers are always warmer than the lower layers, the rays bend downward and are mainly reflected from the bottom, losing with this display most of their energy. In the cold season, the lower layers of water retain their temperature, and the upper layers of water are cooled, the rays bend upward and undergo multiple reflections from the surface of the water, the energy loss of which is much less. From this it follows that in the cold season, the range of sound propagation increases, in contrast to the warm season. Thanks to refraction, viscous attenuation of the dead zones is formed, i.e., areas located near the source where there is no audibility.

The presence of refraction leads to an increase in the range of sound propagation – the phenomenon of ultra-long propagation of sounds under water. At a certain depth below the surface of the water is a layer in which sound travels at the lowest speed; above this depth, the speed of sound increases due to an increase in temperature, and below – due to an increase in hydrostatic pressure with depth. Such a layer is a kind of underwater sound channel. A beam that deviates from the channel axis up or down, as a result of refraction, always tries to get back. By placing the sound source and receiver in this layer, medium-strength sounds (explosions of small charges of 1–2 kg) can be recorded and determined that their range is hundreds and thousands of kilometers. A significant increase in the range of sound propagation in the presence of an underwater sound channel will be located at the location of the sound source and receiver, but it is not at all necessary that the channel axis will be located at the surface. Under these conditions, the rays, refracting downward, go into the deep-water layers, where there is a deviation upward and tend again to the surface at several tens of kilometers from the source. Next, an iteration of the propagation of rays occurs, as a result of which is the formation of a sequence of viscous attenuation of suddenly illuminated zones, which can be tracked at several hundred kilometers. The phenomenon of ultra-long sound propagation in the sea was discovered independently by American scientists M. Iving and J. Worzel (1944) and Soviet scientists L. M. Brekhovskikh and L. D. Rosenberg (1946).

When amplifying high-frequency sounds, in our case Ultrasonic, at a very short wavelength, which is affected by small inhomogeneities found in natural bodies of water: microorganisms, gas bubbles, etc. Such heterogeneities have a double effect: 1. absorb the energy of sound waves; 2. scatter the energy of sound waves.

As a result, such a pattern is observed that with an increase in the frequency of sound vibrations, the propagation range of sound waves is reduced. This property increases in the surface water layer, where many inhomogeneities can be fixed by the natural properties of the layer. The scattering of sound by inhomogeneities, as well as irregularities in the surface of the water and the bottom, affects the appearance of underwater reverberation that accompanies the sending of a sound pulse: sound waves, reflected from a set of inhomogeneities and which merging, give an extension of the sound pulse that continues after it ends, similar to the reverberation that can be observed in enclosed spaces. Underwater reverb is one of the main obstacles for several practical applications of hydroacoustic.

The propagation limit of underwater sounds is limited by the intrinsic noise of the sea, which have a different origin: 1. part of the noise arises from the impact of waves on the surface of the water, from the surf, from the noise of the movement of stones, etc. 2. part of the noise is associated with marine fauna; this includes sounds made by fish and other marine animals.

Hydroacoustics has a large-scale practical application, since no types of electromagnetic waves, including light waves, propagate in water (due to its electrical conductivity) over any considerable distance. From here it follows that sound is the only means of providing communication under water. For such purposes need use: 1. sound frequencies from 300 to 10,000 Hz; 2. ultrasonic frequencies from 10000 Hz and above.

As emitters and receivers, electrodynamic and piezoelectric emitters and hydrophones are used in the sound field, and piezoelectric and magnetostrictive ones are used in the ultrasonic region. Significant use of sonar when using echo sounders, which are designed: 1. to solve civilian as well as military tasks (search for enemy submarines, non-atomic torpedo attack, etc.); 2. for seaworthy purposes (swimming near rocks, stones, etc.), fishing reconnaissance and prospecting, etc.

To create the Black Sea spatial data, as well as provide real map information, it is necessary to provide the Black Sea zones of Ukraine with a survey of the seabed topography using modern hydroacoustic equipment of the high-tech park.

Today, the problem in creating automated control systems is quite obvious that when it comes to system reliability parameters and the reliability parameters of constituent elements, they should not be considered independently, that is, the reliability of the system should depend on the reliability parameters of the constituent elements [5]. Here, to ensure navigational

safety, echo-sounders are installed on ships, which are selected in accordance with the parameters of computer-integrated navigation systems.

It should be noted that a multi-beam echo sounder, unlike a single-beam echo sounder, measures not the depths, but the inclined ranges from the bottom to the receiving antenna and the angular deviation of the axis of each beam from the vertical, on the basis of which the depth for each beam is calculated. Modern designs of multi-beam echo sounders are also able to measure the intensity of the reflected signal for each beam and, based on this information, create a geometrically correct acoustic image of the bottom in the form of sonar images [1].

In a multi-beam echo sounder, to determine the depth, it is possible to use a single approach when acoustic illumination of the viewing band is carried out, where the width is directly proportional to the depth. When calculating the depths within the field of view, which is based on the echo signal, can be produced by oblique rays with known reception rays. When calculating the depth, the distance from the center of the antenna of each spot for the acoustic contact of the beam with the bottom surface is also taken into account the propagation time of the acoustic signal for each beam, it is transferred to the oblique range, then taking into account the beam angle and sound velocity profile data.

Today, one can trace the development pattern in such a way that in the modern information society, information technologies play an important strategic role in the development of each industry. This role is growing rapidly due to the fact that information technology:

– plays a key role in the processes of obtaining, accumulating, disseminating new knowledge based on artificial intelligence methods, allows you to find solutions to poorly formalized tasks, tasks with incomplete information and fuzzy source data, by analogy with the creation of metaprocedures used by the human brain [6]. Such an excellent strategy can be traced in an area such as maritime navigation. Where are integrated areas such as navigation, cartography and hydrography (coordination of underwater objects. Currently, such work is carried out in accordance with the standard of the International Hydrographic Organization for hydrographic surveys (IHO Standards for Hydrographis Survey) – SP – 44. 1998 [7]. To achieve safe navigation, in our time, more and more offensively, multi-beam echo sounder displaces single-beam echo sounder. When considering the measurement of multi-beam echo sounder, you immediately see the advantages over single-beam echo sounder. But first, let's define what

measurement means and what measurement groups do, for what tasks they are created.

Measurement works are special methods of survey the bottom topography when the depth is measured on tacks located at a given distance from each other. The bathymetric method was first applied in the 17th century dutch scientist P. Anselin for the image of the depths of the river Meuse on the plan of Rotterdam in 1697. Measurement depending on the volume of work, the nature of the bottom topography, are carried out using a manual lot or a special echo sounder. After which it is possible to draw up bathymetric bottom maps. The underwater relief is depicted using isobaths (lines that connect the depth level), and the color depends on the degree of heights, the greater the depth, the darker the image.

The main objectives of the measurement are: to identify the state of the dimensions of the shipping facilities of the sea routes (canals, fairways, raids, shipping passages of port and harbor water areas); determine the volumes of the planned and completed dredging operations; identifying the magnitude and intensity of the record of shipping facilities of sea routes providing dredging projects with a planned breakdown and designation on the territory of the Border of work sites with a given design accuracy; provision of dredging facilities with measuring materials; control over the condition of places of dumps of soil and access routes to them; quality control of dredgers; provision of dredging facilities, if necessary, time level posts.

Since the invention of the echo sounder and its use in the practice of marine research, the performance of surveying has increased many times. The principle of operation of the echo sounder is based on measuring the travel time in the water column of an acoustic signal reflected from the bottom. The speed of sound in water is taken, as a rule, equal to 1500 m/s. The first samples of echo sounders were quite primitive. Measurement of depths with their use could be carried out only when the ship stopped. However, by the beginning of the thirties of the twentieth century, echo sounders were created that allow continuous measurement of the depths along the ship. It was with the use of such means of measuring technology over the next decades that a gigantic amount of sonar measurement data was obtained, which let prepare and issue detailed bathymetric maps.

The development of society is compared with an accelerating spiral, where each next coil is wider than the previous one, thereby forming the idea of an expanding spiral from the base up, that is, an inverted cone. So there is a constructive change in the echo sounders, where in the analy-

sis of measuring equipment the following is carried out: 1. elimination, rejection of the old, outdated, that does not meet modern requirements; 2. absorbs, holds and retains everything viable, promising; 3. gives a brand new development.

Enrichment of the improvement by substantive, functional, structural and other characteristics of echo sounders is occurs.

In a spiral form of development, the result point and the return point do not coincide, the repeatability is not absolute, but relative, partial and, of course, there is no certainty or mystical return to past constructions. Any position on a given coil of the spiral is above the corresponding position of the previous coil.

The design of some echo sounders allows to continuously measure depths along the course of the survey vessels and automatically record them in scale on a paper tape – an echogram. On the echogram, special operational assessments indicate the depths measured at the time of coordination of the planned position of the survey vessel. In modern echo sounders, the measured depths are presented on the indicator in digital form, and their storage is provided on various media. The accuracy of measuring depths with an echo sounder in the range of 0.2–20 m is 0.05–0.1 m.

Measurement echo sounders can be divided into single-beam, with which can measure the depth of the place directly below the vessel, and multi-beam, the purpose of which depth measurements are not only under the vessel, but also at a considerable distance from it. Depending on their purpose and technical characteristics, echo sounders are divided into echo sounders for shallow and large depths. Separation of professional and amateur echo sounders is recommended, since when using a narrow emitter and carefully calibrated sounder, it is possible to achieve even greater accuracy in determining depths [8–18].

Single-beam measuring echo-sounders are more effective because they measure the depth in the transverse direction on both sides of the acoustic antenna, forming a fan of narrow acoustic rays in the transverse plane of the ship and therefore obtain a topographic view of the seabed, build digital model of the bottom topography or its pseudo-volumetric image [8].

For a more visual vision, we compare single-beam and multi-beam echo sounders that are included in the measurement complexes.

Measurement systems based on one/two beam echo sounders can allow depth measurements to be made over a tack grid. The result of such a measurement will be a file with depths and coordinates on the basis of

which a spatial model of the bottom topography is built, reporting tablets and maps are formed. Measurement complex can be placed on almost any ship, starting from a small boat.

Measurement complex consists of echo sounder, GNSS receiver, laptop with measuring software, heading sensor (optional), sound velocity probe (optional), software for building a 3D model of the bottom topography (optional).

For multipath systems, the basis of wide-range multipath speakers is taken. Which can create conditions for scanning the bottom topography in the band of the sector of view with a width of 10 ° to 160 ° with high resolution.

A multi-beam echo sounder measures slant ranges with a predetermined angle of inclination; this property can make it possible to turn the obtained data into a spatial coordinate model of the relief in real time. In addition, a multi-beam echo sounder can determine the intensity of the reflected acoustic signal for each beam, after which a geometrically correct image of the bottom topography is constructed, which can be compared with a similar image of the side view.

The forward-looking function of the sonar allows you to search and detect underwater objects. High frequency option – 700 kHz, allows you to use the echo sounder as a profilograph.

A wide scanning sector – up to 160 ° allows you to perfectly perform high-precision surveys of the side surfaces – walls of moorings, breakwaters, bridge supports and the bases of drilling platforms, etc.

The composition of the complex based on a multi-beam echo sounder: underwater transceiver unit, on-board interface model, GNSS receiver with GPS compass function, pitch compensator, inertial system (optional), sound speed probe, sound speed probe for installation on the transceiver unit, laptop processor (not required for Sonic MBE), a laptop with software for monitoring the sonar and software for collecting data, a receiver-emitter bracket with a cowl, a rod for installing a receiver-emitter (optional).

To date, multi-beam echo sounders have been universally recognized as a means of areal bathymetric surveying, due to the high accuracy of depth measurement. When using a multi-beam echo sounder, the bottom can be almost completely acoustically mastered, this possibility really allows to use it for a detailed view of the bottom. Eventual detection of objects on the bottom surface has appeared. This means of measuring technology confidently positioned itself to measure any geometric parameters of underwater objects.

The principle of operation of the bag-beam echo sounder is to scan the surface with rays that reach a width of 0.5 to 2 degrees, the width of the field of view extends within the range of 2.5–3 depths under the keel. The processing of the multi-beam echo sounder data starts from the moment when the measured bottom-to-bottom information, using the profiling data of the vertical propagation of the speed of sound, can calculate the depth for each beam. The sonic beam sonar software generates the processing of the information received: the data is filtered, which means the removal of emissions, constant running obstacles, bottom reverb and other random error components, after which a digital model of the bottom topography can be formed, where each point of the measured depth corresponds to its geographical coordinates. Digital elevation models are of two types: irregular triangulation; regular rectangular or rotary.

With constantly changing geomorphological forms of the bottom, created by hydrographic services the reference digital relief model of the Black Sea allows, at an acceptable level, data leveling, to a greater extent, where there are areas with a dissected bottom topography. When the digital elevation model is superimposed on the marine navigation chart, the digital elevation model is compared with the reference digital elevation model (reference digital elevation model of the area of work): the sets of measured and reference depths are compared, and correspondingly, the sets of coordinates identified with them are compared on the basis of which the calculation of corrections to reckoning coordinates is performed and the data are adjusted.

Advantages of the multi-beam echo sounder: 1. the accuracy of the correction is determined by the accuracy of the reference digital terrain model; 2. the availability of technical solutions and operational experience in the use of a bag-beam echo sounder; 3. the ability to hide the use; 4. synergistic effect: search, survey, classification – it is possible to analyze changes.

Disadvantages of the work of a beam-beam echo sounder: 1. the quality of the hydrographic service; 2. prototypes of a multi-beam echo sounder, which provide survey and processing of data of appropriate quality, are in the development stage.

Conclusion

An analysis of the technical properties of single-beam and multi-beam echo sounders to obtain the results of depth measurements can be argued that the ability of these systems to take a picture of the bottom with accuracy of depth calculation is sufficient ensure of the safety of navigation.

The use of a multi-beam echo sounder is proposed, since this system allows to completely solve the problem of detailed bathymetric surveys, in contrast to single-beam ones. Even though a large source of error for a multipath echo sounder is an incorrectly measured sound velocity profile. But this effect of the incorrectly entered sound velocity profile can be immediately seen on the bottom profile – it will have a curved appearance, especially at the extreme rays of a flat equal bottom. Information is provided in real time to ensure the safety of navigation and is stored for hydrographic services, that is, during post-processing, the output data does not change, but new ones are created considering the amendments introduced. After each performed depth correction operation, a control file is created, so there is always the opportunity to monitor the post-processing.

References:

1. *Punchenko N. O.* An experimental study of the accuracy of depth measurement with echo sounders / N. O. Punchenko // The Caucasus economic & social analysis journal United Kingdom, – London, 2019. May- july, 2019. – Vol. 32. – Issue 05.– P. 135–139. ISSN: 2298–0946, E-ISSN: 1987–6114; DOI Prefix: 10.36962.
2. *Kondratov V. T.* The structure of metrology of the XXI century / V. T. Kondratov // Measuring and computing equipment in technological processes.2010.– No. 2.– P. 7–23.
3. *Altman E. N.* From the experience of conducting case studies of the sea using a new oceanographic technique // Technical Information Bulletin.1962.– No. 11.– P. 58–63.
4. *Altman E. N.* Sea research using a new oceanographic technique // Meteorology and Hydrology.1962.– No. 12.– P. 33–38.
5. *Punchenko N. O.* Technical and economic evaluation of automated control systems in the development of a high-tech park / N. O. Punchenko // Materials of the international scientific-practical conference Information Technologies and Computer Modeling. Ivano-Frankivsk 20–25.05.2019 року.– P. 36–39.
6. *Punchenko N. O.* Reliability of the components of the Information System / N. O. Punchenko // Bulletin of the Khmelnitsky National University.2019.– No. 1. – P. 162–164. ISSN2307–5732. DOI:10.31891/2307-5732-2019-269-1-162-164.

7. IHO Standards for Hydrographis Survey. Special Publication SP – 44, 4th Edition [Text]. Monaco, 1998.
8. *Demidenko P. P.* Shipborne radar and radio navigation systems: Textbook. – Odessa, 2009. – 372 p.
9. *Lurton X., Lamarche G.* Backscatter measurements by seafloor-mapping sonars: Guidelines and Recommendations // A collective report by members of the GeoHab Backscatter Working Group. 2015. – 200 p.
10. *Koryakin Yu. A., Smirnov S. A., Yakovlev G. V.* Ship sonar equipment. SPb.: Science, 2004. – 410 p.
11. *Churkin O. F., Starozhitsky V. V.* The current state of technical equipment for surveying the topography and bottom soil, the ways of their development until 2010 // Proceedings of the international conference "Current State, Problems of Navigation and Oceanography" (NO-2001). – Vol. 2. – SPb. 2001. – P. 95–98.
12. Multibeam echo sounders shallow water // Hydro International. – July/August. 2003. – P. 38–41.
13. Multibeam echo sounders deep water // Hydro International. 2003. – September. – P. 42–45.
14. *Michel B.* Brissette. The Application of Multibeam Sonars in Route Survey. – The university of new Braunswick, 1997.
15. *Sozer M., Stojanovic M., Proakis J. G.* Underwater acoustic networks // IEEE J. Oceanic Eng. 2000. – 25. – P. 72–82.
16. *Markovich I. I., Dushenin Yu. V., Shelestenko E. Yu.* The use of modern computing facilities in advanced forward-looking sonars. Supercomputer technology (SCT-2012) // Mater. The second All-Russian scientific and technical. conf. Rostov-on-Don: Publishing House of SFU, 2012. – P. 230–234.
17. *Markovich I. I.* Digital signal processing in systems and devices: monograph. Rostov-on-Don: Publishing house of SFU, 2012. – 236 p.
18. *Koryakin Yu. A., Smirnov S. A., Yakovlev G. V.* Ship hydroacoustic equipment: state and current problems – SPb.: Science, 2004. – 410 p.

Nataliia Punchenko, Engineering Science Ph.D., associate professor, Dept. of automated systems and information-measuring technology, Odessa State Academy of Technical Regulation and Quality, 15 Kuznechna str., Odesa Ukraine
E-mail: iioonn24@rambler.ru.
ORCID: https://orcid.org/0000-0003-1382-4490

Oleksandra Tsyra, PhD in Philosophy, associate professor, Dept. of Communication Networks, O. S. Popov Odesa National Academy of Telecommunications, 1 Kuznechna Str, Odesa Ukraine
E-mail: Aleksandra.tsyra@gmail.com
ORCID: https://orcid.org/0000-0003-3552-2039

INFORMATION MODEL FOR POTENTIALLY DETONATIVE OBJECT

Viktor Volkov, Anastasiia Pavlenko

Abstract. Arbitrary potentially detonative object is considered from the point of view of the system analysis as the complex hierarchical system. The first stages of elaboration of the information model for this complex system are fulfilled: the system is structurized, its elements are described with their attributes and relationships, and appropriate information structure diagrams are composed.

Keywords. detonation, potentially detonative object, elementary potentially detonative object, information model, structuring.

Introduction and statement of the problem

Extremely fast progress in computing machinery and telecommunicational equipment enlarged greatly the human potentialities in sphere of the decision making for solving different problems. It concerns also the problems of prevention and mitigation of industrial and transport explosions.

The explosion prevention is one of the most topical and most difficult problems of the present-day industry and up-to-date transport. There are two kinds of explosions: deflagration explosion (sometimes called simply "explosion") and detonation. Deflagration explosions in industrial plants and transport systems occur much more often than detonations. But detonations are more devastating and less studied, and, as a result, more unpredictable than deflagration explosions.

It is obvious the necessity of creating special program-technical systems to prevent detonations. Such a system (the computer complex) may be the decision support system (DSS). But to construct suitable DSS it is necessary to compose general information model for potentially detonative object of arbitrary type. Constructing of such information model is the main purpose of this study.

Main part

Let us call **potentially detonative object** (PDO) an arbitrary object (industrial, transport, laboratory, domestic), on which a detonation explosion can take place as a result of random causes. An object, the detonation of which can be caused only artificially, i.e. deliberately (for example, a charge of cast TNT) is not considered as PDO. This is due to the fact that deflagration explosions and detonations, which can only be caused intentionally, do not make sense to consider from the standpoint of ensuring explosion safety.

An arbitrary PDO can be viewed from the standpoint of system analysis as a complex system. The architecture of this system consists of some components (subsystems) and of the hierarchical relationships between these components. As a matter of fact, hierarchy is the first feature of a complex system, since only systems with a hierarchical structure can be in principle investigated [1].

Attention should be paid to the fact that the nature of the PDO does not play an essential role for further reasoning and can be completely arbitrary. Both an elevator and a silo building (silo block) or a separate silo, both a chemical plant and a powder warehouse, can be considered as a potentially detonating object.

The first stage for the development of an information model of every system is its structuring. The information model of the PDO is no exception.

The complex potentially detonative object (complex PDO) is considered a PDO of the zero level, which is numbered 0, i.e. its number is 0 (PDO_0). This object is the main, "global" object. There is only one PDO_0.

In the vast majority of cases this complex object (PDO_0) can be divided into subsystems (components, elements); those subsystems (components, elements) are PDOs of the 1st level (PDO _1), each of which has its own individual number n_1 ($1 \le n_1 \le m_1$), where the general number of PDO _1 equals to m_1; these potentially detonative objects of the 1st level are marked as

$$\text{PDO\_1\_1, PDO \_1\_2, ..., PDO \_1\_ } m_1.$$

By the way, the nature of any two different PDOs of the 1st level can be either the same or completely different.

Some of the PDOs of the 1st level, i.e. PDO_1 (for example, PDO _1_ i_1, PDO _1_i_2, ..., PDO _1_i_κ, where $1 \le i_1 \le ... \le i_k \le m_1$), are also complex PDOs. They can also be divided into subsystems. These subsystems are potentially explosive objects of the 2nd level (PDO_2), which are numbered as follows:

$$\text{PDO\_2\_ 1\_}i_1\text{\_1, PDO\_2\_ 1\_}i_1\text{\_2, ..., PDO\_2\_ 1\_}i_1\text{\_ } m_{2,1};$$

PDO_2_ 1_i_2_1, PDO_2_ 1_i_2_2, ..., PDO_2_ 1_i_2_$m_{2,2}$;
PDO_2_ 1_i_k_1, PDO_2_ 1_i_k_2, ..., PDO_2_ 1_i_k_$m_{2,k}$.

The general number of PDO_2 is equal to

$$m_2 = m_{2,1} + m_{2,2} + \ldots + m_{2,k}.$$

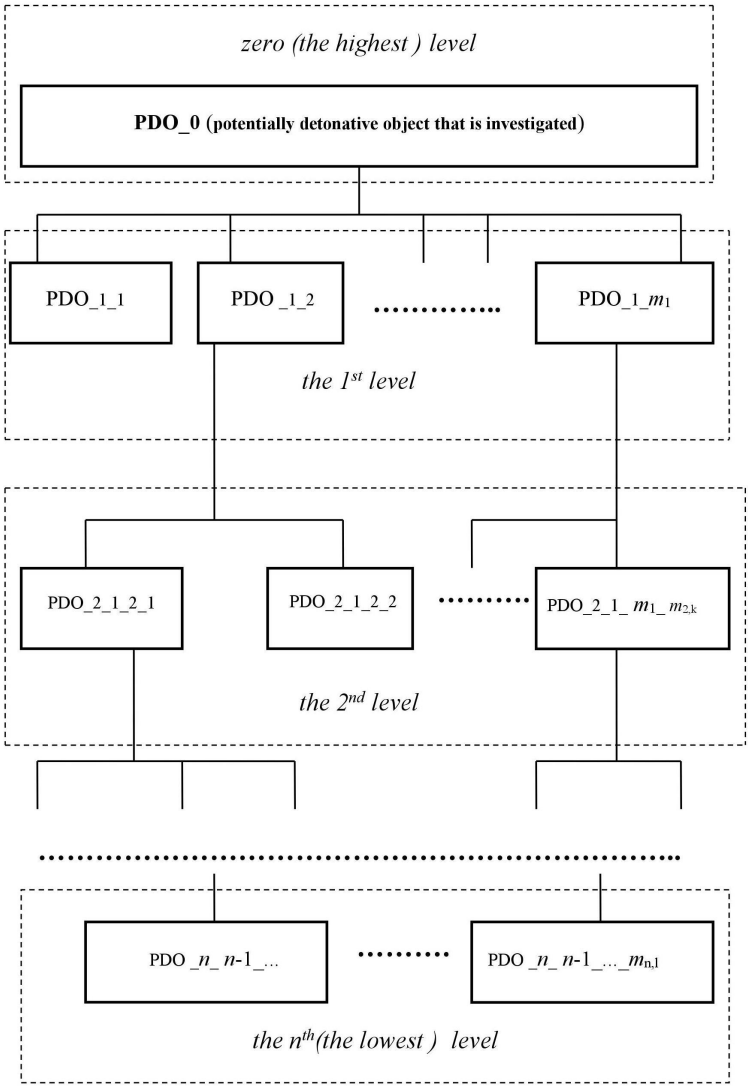

Figure 1. The general structure of the complex potentially detonative object

Some of the PDOs of the 2nd level, i.e. PDO_2, can also be divided into subsystems (components, elements) – potentially explosive objects of the 3rd level (PDO_3) in the general number of m_3, and so on (Fig. 1).

For example, an elevator as a whole can be considered as a PDO of the zero level, as a PDO of the 1st level – silo buildings, separate bunkers, a working tower, elevator shafts, an aspiration system, as PDO of the 2nd level – individual silos (as components of silo buildings), aspiration shafts (as components of an aspiration system), etc.

The total number of sublevels in a complex PDO (which itself is considered an object of the zero level) is not limited in principle. This number is largely determined by the developer of the information model. The developer, in turn, focuses on the specifics of the object and features of the formulation of the problem of ensuring detonation safety. For PDO of any level, when identifying its components as PDOs of a lower level (next level with a larger number), the geometric, physicochemical and technological properties of both individual sublevel components (objects) and the PDO as a whole containing these components are taken into account.

The general structure of a complex potentially detonative object is shown in (Fig. 1). The numbering of the levels is "top-down", i.e. the lower level has a larger number.

It is quite obvious that the generalized structure of a complex potentially detonative object can be represented by an oriented tree (a connected directed acyclic graph) [2] with a root corresponding to PDO_0. This graph (tree) can be sorted [2]; the outgoing degrees of all vertices, except the external ones (i.e., except the terminal nodes or leaves) are at least 2.

Figure 2 shows a graph image for the structure of a complex potentially detonative object. The external vertices (terminal nodes) of the graph (tree) shown in (Fig. 2) are vertices 2, 4, 7, 8, 9, 10, 11, 12. It is obvious that terminal vertices can be in any level, except zero level. The subsystems corresponding to the terminal nodes of the graph in the graph representation of the structure of a potentially detonative object, considered as a complex system, are the elementary components of the system. These components are called elementary potentially detonative objects (EPDO).

According to [1], the choice of elementary components of the system under study is relatively arbitrary and is largely determined by the researcher himself. However, such arbitrariness in the choice of the researcher is actually always limited: such a restriction is primarily dictated by the need to have all the information required for solving the task set

about each of the elementary components of the system – its characteristics, possible states and reactions to the effects of other components of the system or external influences.

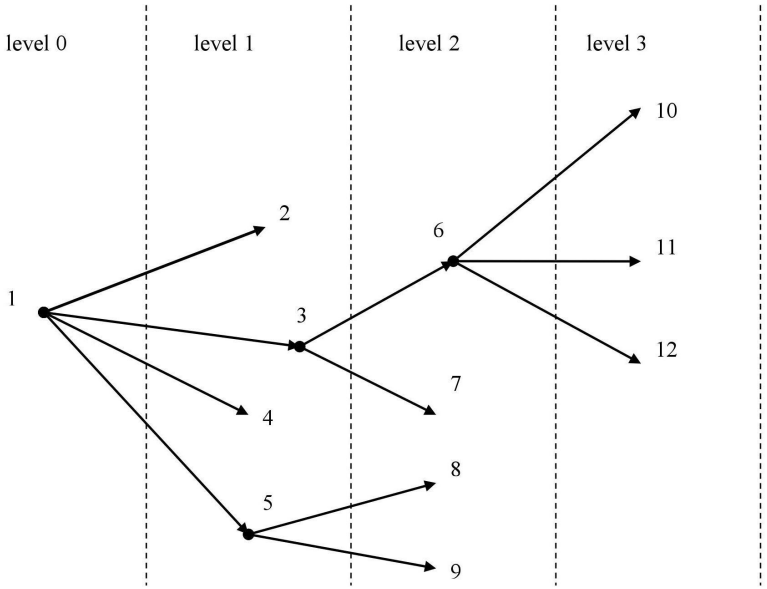

Figure 2. Graph of the complex potentially detonative object structure

In the case of modeling a PDO of an arbitrary nature, one of the following objects should be (to a certain extent) considered as an EPDO (model of a real object):

1. Open space;
2. Flat channel:
   a) infinite (unlocked),
   b) of the finite length, half-open (closed at one end),
   c) of the finite length, closed (closed at both ends),
   d) of the finite length, open (open at both ends).
3. Round cylindrical tube:
   a) infinite (open),
   b) of the finite length, half-open (closed at one end),
   c) finite length, closed (closed at both ends),
   d) finite length, closed (closed at both ends).
4. Joint of two different objects of type 1-3 (for example, joint of two tubes with different diameters or channel output in the open space).

The choice of such potentially detonative objects as elementary is due to the following considerations:

- For objects of type 1–3, mathematical models have been developed [3–7], allowing to evaluate the possibility of the detonation explosion developing in each of such objects. These mathematical models are based on solving problems on the hydrodynamic stability of combustion and detonation waves. Solving the problems of the stability of combustion waves makes it possible to evaluate, on the one hand, the possibility of autoturbulization of the flame and the transition of slow combustion into a (deflagration) explosion, and on the other hand, the possibility of the formation of detonation waves. Solving the problems of the stability of detonation waves makes it possible to define more exactly the detonation limits and determine the detonation modes [8] (if detonation takes place at all).
- For objects of type 4 there are investigations [5, 8] for estimating the possibility of the detonation transition from one object of type 1–3 to another. Object of type 4 is principally new object in comparison with the information model of potentially explosive object [9]. The necessity of considering such object is connected with possibility of the detonation attenuation during the transition of detonation wave from tube or channel to open space or from tube or channel to another tube or channel with larger diameter [8]. The study of these problems is based on calculating the number of detonation cells (in the mode of cellular detonation), which fits along the width of the channel or along the diameter of a round pipe [5, 7]. In turn, the size of the detonation cell (and, consequently, the number of cells that fit along the width of the channel or along the diameter of the tube) is determined by solving the problem of the detonation wave stability [5, 7].
- Any real PDO can be virtually modeled by a composition (combination) of these elementary potentially detonative objects.
- Real potentially detonative objects or their components (subsystems) are easily identified as the above mentioned elementary potentially detonative objects.

Any PDO is characterized by physicochemical properties (these are dynamic properties) and geometry of its borders (walls) (these are static properties). It is the type of boundary geometry that allows (as was done above) to identify and simultaneously classify EPDOs. The above classifi-

cation of EPDOs can be considered a topological classification (as opposed to other types of classification – systemic and parametric).

Thus, 10 classes of objects are distinguished. The object of each of these 10 classes of EPDOs can be a model of some element (subsystem) of a real explosive system. The details about 9 classes of types 1–3 are outlined before [9].

Note that EPDOs of class 2 and class 3 can simulate not only channels of rectangular cross section and pipes of circular cross section, respectively, but also pipes of elliptical cross section. Moreover, if the length of the major semiaxis of the ellipse in the section of the pipe slightly exceeds the length of its minor axis, then the pipe can be modeled with a circular section pipe with a radius of a circle equal to the length of the major axis of the ellipse, i.e. potentially explosive class 3 facility; if the length of the major semiaxis of the ellipse in the section of the pipe significantly exceeds the length of its minor semiaxis, then the pipe can be modeled with a rectangular channel with a rectangle within which this ellipse can be inscribed, and such a channel, in turn, is modeled as one of the potentially explosive objects of class 2.

Note also, that channels with (regular) polygonal cross-sections can, as a rule, be modeled by rectangular channels or pipes of round diameter. Channels of rectangular cross-section and pipes of circular diameter cannot simulate only channels with a triangular cross-section, but such channels are extremely rare in engineering practice (at least for explosive objects).

Consider the completeness of the classification of EPDO. It is quite obvious that the only often-observed common element of real PDO not covered by the 10 classes mentioned above is a round tube with a bend. The detonative hazard of pipes even with a smooth bend is significantly higher than for straight pipes [8]. A detailed consideration of this problem shows [8,10,11] that the analysis of the detonation hazard of an object simulated by a curved circular tube, in one way or another, boils down to an analysis of the detonation hazard of an object that is simulated by a straight circular tube, i.e. one of the PDOs of class 3. But at the same time, the obtained estimates of the detonation hazard are very approximate [8].

So the first stage of development of the information model for real PDO is its decomposition, which must be done by the rules described above. The indisputable advantages of such decomposition are its naturalness and the possibility of obtaining, along with the assessment of the detonation hazard of a complex PDO as a whole, the explosion rating of each of its subsystems. However, such a multi-level decomposition of PDO as a complex system is in most cases superfluous.

In fact, in many cases if one particularly evaluates the detonation hazard of each technological or technical subsystem of a complex PDO, then this object can be considered a simple set of EPDO. It should proceed from a simple postulate that the level of the detonation ability of a complex PDO as a whole corresponds (equal to or not less) to the level of the detonation ability which among all the elementary potentially detonative objects this PDO contains is maximum. Then a complex PDO (PDO_0) is represented by a system with only one sublevel containing "equal" EPDO, denoted as EPDO_1, EPDO_2, ..., EPDO_*m*, where *m* is the total number of such objects (Fig. 3).

Thus, the hierarchical structuring of a complex detonative system has been carried out.

The next step after structuring in the information model developing is the identification of conceptual entities, or objects, which constitute the subsystem for analysis [12]. In the case of PDOs, first of all it is necessary to identify the EPDOs (with their attributes and relationships).

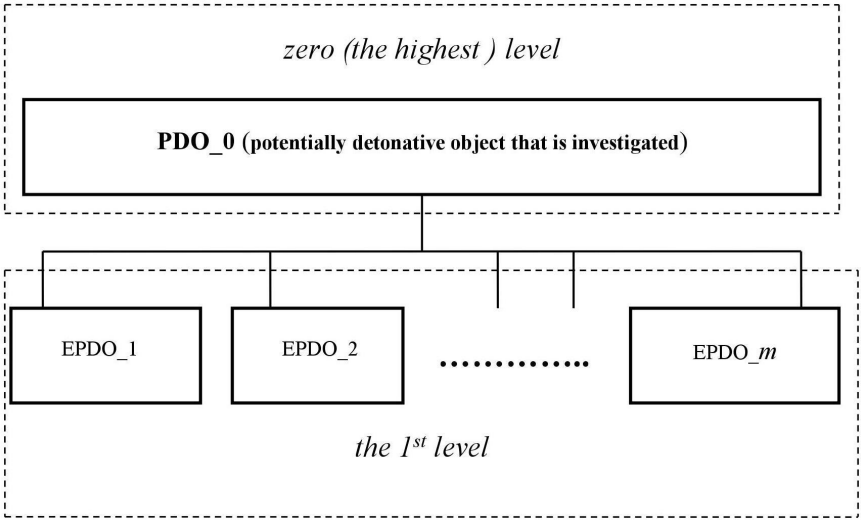

Figure 3. Simplified structure of the complex potentially detonative object

As a matter of fact it is done as it was done in [13]. The major difference is replacing of notions (and attributes) Explosion hazard and Relative explosion hazard by notions (and attributes) Detonation hazard and Relative detonation hazard. But it should be borne in mind that Relative explosion hazard means the possibility of a deflagration explosion if a fire already

takes place, and Relative detonation hazard means the possibility of a detonation if an ignition or a deflagration explosion already takes place.

Explosion hazard is fuzzy variable for estimation of the possibility of explosion (deflagration or detonation), Detonation hazard is fuzzy variable for estimation of the possibility of detonation [14]. Algorithms for calculating these estimations are described before [13, 14].

Relative explosion hazard is fuzzy variable for estimation of the possibility of explosion when ignition already takes place. Relative detonation hazard is fuzzy variable for estimation of the possibility of detonation when ignition or deflagrative explosion already takes place. Algorithms for calculating of these estimations are also developed before [13, 14].

Passing to fuzzy variables and fuzzy logic is due to the impossibility of taking into account mathematically (with the required accuracy) such factors as the roughness of the walls of pipes and channels, the complexity of the kinetics of chemical reactions, etc. For example, according to experimental studies [8], the roughnesses of the walls of pipes and channels (especially if these roughnesses are periodically repeated on the walls) significantly (sometimes several times) increase the possibility of detonation. In this case, the length of the detonation induction distance is reduced by 10-20 times, and in some cases - up to 50 times [7, 8]. This factor plays a very significant role, since if the length of the detonation induction distance exceeds the maximum size of the EPDO (the length of the channel or pipe), then the deflagration-to-detonation transition will not occur even if all other necessary conditions are fulfilled.

The application of fuzzy logic allows us to use the proposed mathematical model and information model of the transition from combustion to deflagration explosion and from the deflagration explosion to detonation, or directly from combustion to detonation, for the mathematical and information support and software (that is based on this support) of decision support systems on the issues of explosion (detonation) safety and explosion (detonation) protection of the real industrial and transport facilities.

The advantage of the decision support system of this type is that it allows the decision makers to do without experts. This is especially important, since it is well known that working with experts has always been and remains a weak link in decision support systems. The ability to “get rid” of experts is due to the fact that in this case the decision-making model under uncertainty is combined with the classical decision-making model [14].

All kinds of EPDOs are described with their attributes and with the relationships between them and between each of them and the complex PDO.

Information structure diagram [12] for complex PDO is composed for general case. Information structure diagrams for different kinds of PDO are also built in general terms.

Conclusion

Arbitrary potentially detonative object is considered from the point of view of the system analysis as the complex hierarchical system. This complex system is structurized.

Elementary potentially detonative objects are indicated. Differences between a potentially explosive object and a potentially detonative object, between elementary potentially explosive object and elementary potentially detonative object are pointed out.

Ten classes of the elementary potentially detonative objects are determined. In this regard, the classification is based on geometric features, since the PDO geometry largely determines the danger of the detonation explosion. The fact that the classification is based on obvious geometric criteria greatly simplifies the process of designing an information model of a specific real potentially detonative object.

All kinds of elementary potentially explosive objects are described with their attributes and relationships. Information structure diagrams are also built.

The information model for potentially detonative object proposed in this study can serve as a basis for mathematical and information support of the automated control systems for the dangerously explosive objects, in particular for the dangerously detonative objects.

This information model for potentially detonative object is universal. The universality of this information model lies in the fact that it is applicable to almost all real objects (industrial, transport, domestic) and does not depend on what kind of potentially explosive medium is (heterogeneous or homogeneous, gaseous, liquid or solid). This information model is also independent of the chemical nature of the explosive medium.

The development of this study is associated with the possible application of the information model for the real potentially detonative objects and projecting decision support systems for the decision making on the explosion safety problems and detonation safety problems. This decision support system must help a decision maker to answer these questions about:

1) the possibility of the transition of combustion to detonation if there is a fire (as a result of accidental ignition or spontaneous combustion);

2) the time for transition of combustion to detonation (or of deflagration explosion to detonation) if such transition is possible;

3) measures (technical, technological, or organizational) that can be taken to prevent an explosion or detonation timely, or, in extreme cases, minimize damages from the consequences of detonation or explosion.

References:

1. *Booch G.* Object-oriented Analysis and Design With Applications, Santa Clara, – California: Addison Wesley Longman, Inc., 1998.
2. *Reinhard D.* Graph Theory, Berlin, – New-York: Springer-Verlag, 2005.
3. *Aslanov S. K., Volkov V. E.* Integral method for study of hydrodynamic stability of a laminar flame, Combustion, Explosion and Shock Waves, Springer, – Vol. 27. – No. 5. 1991. – P. 553–558.
4. *Aslanov S., Volkov V.* On the instability and cell structure of flames, Archivum combustionis, – Vol. 12. – No. 1–4. 1992. – P. 81–90.
5. *Aslanov S., Volkov V.* Instability and Structure of Detonation in a Model Combustor, in Application of Detonation to Propulsion, – Moscow: TORUS PRESS, 2004. – P. 17–25.
6. *Volkov V. E.* Instability of Flames in Cylindrical Tubes and Combustors. Third International Symposium of Nonequlibrium Processes, Plasma, Combustion and Atmospheric Phenomena. Abstracts of presentations, – Moscow: TORUS PRESS, 2007. – 46 p.
7. *Volkov V.* Deflagration-to-detonation transition and the detonation induction distance estimation. Proceedings of Odessa Polytechnical University, – No. 1(43). 2014. – P. 120–126.
8. *Nettleton M. A.* Gaseous detonations: their nature and control, Springer, 2013.
9. *Volkov V. E.* Information model of potentially explosive object. Part 1. Automation of technological and business-processes, – No. 9–10. 2012. – P. 3–11.
10. *Frolov S. M., Aksenov V. S., Shamshin I. O.* Detonation Propagation Through U-Bends in Nonequlibrium Processes. – Vol. 1. Combustion and Detonation, – Moscow: TORUS PRESS, 2005. – P. 348–364.
11. *Frolov S. M., Aksenov V. S., Shamshin I. O.* Shock-to-detonation Transition In Tubes With U-Bends in Pulsed and Continuous Detonations, – Moscow: TORUS PRESS, 2006. – P. 146–158.

12. *Shlaer S., Mellor S. J.* Object-Oriented Systems Analysis: Modeling the World in Data, Prentice Hall, 1988.
13. *Volkov V. E.* Information model of potentially explosive object. Part 2. Automation of technological and business-processes, 2012.– No. 9–10. – P. 3–9.
14. *Volkov V. E.* Decision Support Systems on Hazards of Industrial Explosions. Seventh International Symposium on Hazards, Prevention and Mitigation of Industrial Explosions: Thirteeenth International Colloquium on Dust Explosions & Eighth Colloquim on Gas, Vapor, Liquid, and Hybrid Explosions. – Vol. 3. – St. Petersburg, 2008. – P. 343–347.

Viktor Volkov, Doc. Tech. Science, Prof., Head of the Theoretical Mechanics department, Odesa I. I. Mechnikov National University, Dvoryanska str., 2, Odesa, Ukraine
E-mail: viktor@te.net.ua
ORCID: http://orcid.org/0000-0002-3990-8126

Anastasiia Pavlenko, Educational department, Odesa National Academy of Food Technologies, Kanatnaya str., 112, Odesa, Ukraine
E-mail: virgonass@gmail.com
ORCID: https://orcid.org/0000-0002-0563-6150

INTELLIGENCE SYSTEM FOR THE HUMAN STATE INSPECTION

Viktor Sineglazov, Roman Pantyeyev, Mykola Vasylenko
Yuriy Opanasiuk, Roman Manuilenko

Abstract. The problem of customs control intelligence security system creations is considered. The necessity of the passenger'svoice and the emotions face changes analysis during control in airports is shown. The voice and the emotional changes of a human face correspond to internal reaction of the person on the posed control questions. As the solution of this problem it's proposed to apply the convolutional neural network at the stage of micro emotion identification and the indistinct qualifier – at the stage of decision making for potential threats of passenger. As the indistinct qualifier it is offered to use the NEFCLASS neural network. The example of practical approach for micro emotion recognition by means of convolutional neural network is given.

Keywords: Combined convolutional neural network, voice analysis, micro expressions, facial state recognition, information security, information infrastructure.

Introduction and formulation of the problem

The artificial intelligence for image processing and especially facial recognition is the highly discussed theme in modern world. There a lot spheres requires the tool that allows recognizing the person, its own parameters as age, gender, expressions, psychological state and any other features. For example it's widely used in security systems for verification the person and allows it to enter the building or use the application. Also, it's can be applied in sociological statistics formation or during the interview on the psychologically related working place. The main idea of this work is to understand and find the optimal ways for application the artificial intelligence systems as for example neural networks to solve the recognition problem in the better way. In addition, it's necessary to set what kind of features needed to be recognized and its recognition accuracy [1].

Main problem of this work is to discover the approaches to recognize and track changing of face features relatively to some parameters.

Current problem could be solved in different ways [2]. Nowadays, there already exists a good enough number of already realized systems. Most popular of them are the following ones:

– automated border processing system "SmartGate' that is used to compare the face with the e-passport database;

– "DeepFace" facial recognition system used in Facebook;

– "Face ID" introduced by Apply to allow the person authentication in their devices;

"Next Generation Identification" system is formed by FBI for the identification of the person through huge database.

Nowadays, the real importance is given to increasing the aircraft safety conditions, in particular during the passenger control. Commonly, the number of people for each security officer is too high to deal with them in restricted period of time. The employee of aircraft company is faced by a hard task, to ask the number of special questions to understand the emotional state of the passenger to successful admission of the flight.

The main features that allow solving this problem is emotional changes of the passenger during the control conversation. The most successful application of this approach was done by El Al aircraft company (Israel).

The challenge is to detect and recognize the facial micro changings. It's very difficult task especially with a large number of passengers (about 20–30 people on one security officer) and demand considerable preparation. In this work as the solution of given problem offered to use an intellectual analysis system which consists of the two-level neural networks of deep learning based on micro emotion recognition: at the first level the convolution neural network [1], on the second – the qualifier constructed with use of indistinct neural network, for example NEFCLASS [2] is applied.

The main tools on which modern image classification algorithms are based are Deep Learning and CNN (convolutional neural networks).

Convolutional neural networks are similar to conventional neural networks, but they are designed with the assumption that the input is fedimage. This allowed to lay down certain characteristics in the architecture, which are aimed at improving the classification. Unlike conventional neural networks, the layers of convolutional neural networks are three-dimensional. Neurons in one layer are associated only with a specific area of the next layer.

The first input layer of the network has the dimension $w \times h \times d$, where w is the width of the image, h is the height, and d is the number of color channels. Each layer of such a network transforms the received input using

a differentiation function. The following types of layers are used in a convolutional neural network: CONV (convolutional), POOL (pooling), FC (fully-connected).

Convolution layer parameters – a set of filters. A typical filter can have a dimension of $5 \times 5 \times 3$. During a direct pass, this filter moves along the input layer and calculates the product between the filter elements and the area of the input image. Thus, a so-called activation card is formed, which contains the filter response to the input layer in each position. It is intuitively clear that in the process of learning filters are formed that respond to certain characteristics, for example, an edge, a spot of a certain color, and so on. In fact, the problem of interpreting the work of the neural network is complex and unsolved at the moment, but such an analogy allows us to better understand the principle of operation. Several filters are used for each area of the input layer, each of which potentially has to recognize different characteristics of this area.

Each filter produces a two-dimensional activation card, which is then layered on top of each other along the depth of the source layer. The considered concept can be clearly shown in (Fig. 4). The input layer (red) has a dimension of $32 \times 32 \times 3$, ie the image is supplied with a 32×32 image with three color channels. Each neuron of the convolutional layer is associated only with a certain area of the input layer, but with full depth. An example of a convolutional layer using 5 filters for each region is given.

It should be noted that the filters can move with different steps (1, 2, etc.) so we can vary the dimension of the output layer, the larger the step, the smaller the dimension of the layer. Sometimes zero elements are added to the input image at the edges to standardize all images to a certain size for which the neural network is designed.

Voice recognition

The main definitions describing the parameters of a person's speech, as well as those associated with the shape, size, dynamics of transformation of the timbre that forms it and the emotions (emotional state) of a person, are divided into four groups of signs that allow to objectively distinguish speech signals: spectral-temporal, amplitude-frequency, cepstral and the latter are nonlinear dynamics.

According to the type of speech, continuous speech recognition systems and speech signals are distinguished. In the latter case, discrete

(special) pronunciation of speech commands is required, where the pauses between them are much larger than the intra-word pauses. Typically, the duration of such separation pauses is half a second.

During continuous speech recognition, the words of phrases are pronounced naturally, without inserting any special pauses between words. There is also a third variant of the operation of recognition systems, where they must detect the pronunciation in the sound stream of the given words, regardless of the "noise" in other words or highlighting with pauses. This mode is called keyword search [1–3].

Basically, two options are used in speech recognition:

1. A measure of the proximity of parameters.
2. Recognition using neural networks.

Neural networks do not make assumptions about the statistical properties of objects and have several qualities that make them attractive models for speech recognition. When used to assess the probability of a speech segment, neural networks allow discriminatory training to be conducted in a natural and efficient manner. Few assumptions about the statistics of input functions are made with neural networks. However, despite their effectiveness in classifying short-term time units such as single phonemes and single words, neural networks are rarely successful for continuous recognition tasks, mainly due to their lack of the ability to model temporal relationships. A variant of deep learning of neural networks has been used in experiments to solve this problem.

Due to the inability of the original neural networks to model temporal dependencies, an alternative approach is to use neural networks as preprocessing, for example, for transforming features, decreasing the dimension [2, 5].

Another approach is a time-lagged neural network. He used a modified training variant to capture spatial variances and temporal deformations in the function sequence. One input layer, two hidden layers and one output layer were used to classify different phonemes created by native speakers. The weights were determined in such a way that the system was somewhat invariant to temporal distortions in the speech signal. It recognized only phoneme speech and was not used for decisions over longer periods of time, that is, it was not used directly for word recognition.

Syllables and words are essentially sequential. This means that both techniques are very powerful in a different context. As in a neural network, the task is to establish the appropriate connection weights, the task of the Markov model is to find the corresponding transition and obser-

vation probabilities. In many speech recognition systems, both methods are implemented together and work in a symbiotic relationship. Neural networks do a very good job of learning the probability of a phoneme from highly parallel audio input, while Markov models can use the probabilities of observing phonemes that neural networks provide to derive the most likely sequence or word of a phoneme. This underlies the hybrid approach to understanding natural language [4].

The first step consists of an acoustic environment, including equipment for receiving speech. This environment can have a profound effect on the generated speech representations. For example, it can have an additional effect arising from additive noise or room vibration.

The second step is intended to solve these problems, as well as to obtain acoustic representations in which it is necessary to separate classes of speech sounds and effectively suppress irrelevant sources of variation.

The third step is to highlight the specific features of the preprocessed signal. This can be done using various methods such as cepstrum analysis and spectrogram.

The fourth step classifies the extracted features and associates the input sound with the best fit sound into a known "word set" and presents this as a result.

It is important to feed a neural network with normalized input. Recorded samples never reproduce identical waveforms; length, amplitude, background noise may vary. Therefore, we need to do some preprocessing of the signal to extract only the information related to speech. This means that using the correct features is critical to a successful classification. Good functions simplify the design of the classifier, while weak functions (with a small degree of discrimination) can hardly be compensated for by any classifier.

In the first step, it is important to properly filter out the noise in order to obtain the correct spectrum. The input signal can be cleaned using a special filter specified by formula 1.

$$x_i = (x_i - 0,9 * x_{i-1})[0,54 - 0,46 * \cos((i-6) * \frac{2\pi}{180})] \quad (1)$$

where: x_i – input sound values

The next step is usually to obtain a correct spectrogram that can be used later. The Fourier transform method (formula 2) is suitable for this task.

$$x_k = \sum_{n=0}^{N-1} x_n e^{-\frac{2\pi i}{N} kn} k = 0,..., N-1 \quad (2)$$

where:

N – frame length;
x_n – signal amplitude;
x_k – complex signal amplitude.
There are two main approaches:
1. Fixed point approach.

This approach translates the time-varying trajectory to a point in space, reducing the trajectory classification problem to a one-point classification. Since the statements showed significant variability, not only in function, but also in time, they were normalized so that all temporary deformations were canceled. All trajectories on the training and test sets were normalized to a trajectory of 100 points, so that the Euclidean distance between adjacent points in the reduced object space was always one hundredth of the length of the trajectory projected into the reduced space.

2. Approach with a different trajectory.

This approach, instead of reducing the problem to point classification, has a lot to do with normalized trajectories. The trajectories are fed directly to the recognizer, which at the same time continuously produces an output that can be used for classification purposes.

While none of the approaches were good enough for practical purposes at the current stage of development, they were good enough to prove that translation of speech in trajectory in object space works for recognition purposes. Human speech is a dynamic process that can be correctly described as a trajectory in a specific feature space.

Moreover, the dimensionality reduction scheme proved dimensionality reduction while maintaining some initial topology of the trajectories, i.e. it has stored enough information to provide good recognition accuracy. It is interesting to note that although this approach has been used in the speech recognition field for over a decade, no one has used it to generate trajectories, but only to generate sequences of labels.

Finally, the new approach developed for teaching neural network architecture has proven to be simple and very effective. This significantly reduced the number of calculations required to find the correct set of parameters [2, 4].

For recognition, the most commonly used neural network is the multilayer perceptron. Its general structure consists of several layers. The neurons in its structure often function according to the McCulloch-Pitts model, corresponding to the following function, shown in the form of formula 3 [9].

$$y_k(t) = f(u_k(t)) \quad (3)$$

The most famous learning algorithm for a multilayer perceptron is the one described by Frank Rosenblatt in 1959 and as a modification proposed by David Rumelhart as a back propagation error that allows supervised learning (learning "with a teacher").

The main point in training is the correction of the weights; it is performed according to the following objective function shown in formula 4.

$$w_{ij}(t+1) = \eta \frac{\delta E}{\delta w_{ij}(t)} x_i(t) \quad (4)$$

where: η – коэффициентобучения.

Convolutional neural networks are also often used in voice recognition tasks. A convolutional neural network is a special type of feed forward neural network.

Forward propagation means that the variable neurons in this network are divided into groups called layers.

The main point is to create a convolution, which can be described by the following formula 5.

$$(f * g)[m,n] = \sum_{k,l} f[m-k, n-l] * g[k,l] \quad (5)$$

where f – original matrix.

The neural network approach involves first getting the speech data itself.

After the first step, when we have received a certain set of data, we can build a table (Table 1), in which each element corresponds to a set of numbers [1].

Table 1. – Data set

Segment	**1. result**	**2. result**	**…**	***i* – result**
1. segment	x_{11}	x_{21}	…	x_{1i}
2. segment	x_{21}	x_{22}	…	x_{2i}
…			…	
j – segment	x_{N1}	x_{N2}	…	x_{Ni}

It turns out that a set of values is defined for each neuron. But on the last layer, we will only have one neuron.

This is the so-called feedback neural network.

Thus, the whole algorithm can be structured as follows:

1. First, define a set of values for each segment.

2. At the second step, the initial values are fed to the input of the system, in accordance with formula 6.

$$y_j = f(\sum_{i=1}^{I} w_{ij} x_{ij} + \beta_j + w_j x_j) \quad (6)$$

where: *f(x)* – nonlinear function

3. Next, calculate the last layer (formula 7)

$$y_k = f(\sum_{j=1}^{J} w_{jk} y_i + \beta_k) \quad (7)$$

In general, the general algorithm will look like this: a step-by-step construction of a matrix with weights is performed and a gradual decrease in the probability of getting an error.

The learning process itself is as follows: a sample is fed to the input of the neural network and the necessary weights are adjusted. The process is repeated until the error rate reaches a minimum.

The error function is calculated by formula 8.

$$E = \frac{1}{2N} \sum_{i=1}^{N} (y_{ki} + d_i)^2 \quad (8)$$

N – the total number of subjects at the input of the neural network of samples;

Thus, the above model can become the basis for speech recognition at the level of neural networks.

Review of existing solutionsfor the human emotional state recognition

During the analysis of human emotional state recognition, it's necessary to consider "profiling" [3]. This is a set of psychological approaches for analyzing and predicting a person's behavior, based on particular features, appearance and verbal behavior. This technique can be successfully applied in computer vision due to the classification of these features for potential danger prevention. Using the profiling method it is necessary to use a coding system of facial movements (SKLiD) [4]. By using the SKLID, it is possible to create a facial model based on units of actions and a fixed period of time needed to act any emotion. Here, the units of action are the movements performed by individual muscles or a group of muscles.

The system also has a limited number of descriptors (unitary movements performed by a group of muscles: tightening the cheeks, stretching the eyelids, raising the wings of the nose, raising the upper lip, deepening the nose-labial fold, raising the corners of the lips, dimpling the lips, lowering the corners of the mouth, lowering the lower lip, pulling off the lips)

[5]. Each manifestation of facial emotions of a person can be described by a set of descriptors. As the apparent facial changes there also occurs the micro emotions. They can be taken into account in more complicated recognition approaches. Table 2 describes the main facial changes relatively to the six standard types of emotions [6].

Motion units of the person can be divided into three groups conditionally:

1) static – recognition using only the photo is possible;

2) dynamic – it is necessary to continuous frame changing, key points initialization or obtaining the average value of distances between motion units;

3) empty – actively participate in manifestation of emotions, however are not registered search algorithms (dimples on cheeks).

Now it is possible to review the following recognition methods of the human emotional state using a profiling approach. The most efficient ones are: holistic methods, local methods, methods of calculation of forms of objects, methods of calculation of dynamics of objects (Table 3) [7]. For the human face it is possible to initialize up to 80 facial landmarks. Commonly, it is borders of eyes, mouth and eyebrows. Malar muscles are not important feature for human expression recognition and its analysis. Each of emotions has the unique dynamics parameters.

Table 2. – Relations of emotional facial features changing

Emotion	Eyebrow	Mouth
Surprise	Rise	Open
Fear	Rise and wrinkled	Open and stretch
Disgust	Decrease	Rise and ends will decrease
Anger	Decrease and wrinkled	Opens and ends will decrease
Happiness	Bends down	Ends will rise
Sadness	End part will decrease	Ends will decrease

Therefore, profiling is the relevant method for emotional identifying and analyzing of an individual features, which makes it possible to significantly increase the level of security, for example, at airports.

These approaches were implemented in the following software for processing video images of a human face subject to emotions [7]:

1) Face Reader – developed by "Nold us Information Technology" (The Netherlands), requires the facial video for proper identification. System capabilities: recognition of emotions, the definition of ethnicity, the use of the Active Template method, the creation of an artificial face model. Ad-

vantages: recognition with an accuracy of 89%; you can define emotions by frames or completely (video), full visualization (histograms, diagrams of emotions). Disadvantages: does not recognize children under five; inaccurate definition of emotions in a person with glasses; different skin color is perceived by the system in different ways; turned face is not detected.

Table 3. – Methods for facial emotional state recognition of human face

Methods	Holistic methods	Local methods
Methods for shapes calculations	Classificators: Artificial Neural network, Random Forest, Adaboost, Gabor filters, 2D face models: AAM, ASM EBGM.	Classificators: Artificial Neural network, Bayes Classificator, Adaboost, Geometric face models. Own vectors: PCA. Local histograms: HoG, LBP.
Methods for dynamics calculations	Optical flow, Dynamic models.	3D dynamic models Statistical models: HMM, DBN.

2) Emotion Software and GladOrs application – developed by "Visual Recognition" (Netherlands). System capabilities: the system creates a 3D model of the face with the identification of 12 key areas, such as the corners of the eye and the corners of the mouth. Pluses: recognizes anger, sadness, fear, surprise, disgust and happiness. The software is not demanding on the computer. Disadvantages: unknown details of the implementation algorithm (no defects identified).

3) Face Analysis System – developed by "MMER-Systems" (Germany). System features: Face overlay a certain deformable mask that allows you to calculate the necessary parameters in real time. Advantages: recognizes six basic emotions, determines gender, age, ethnicity; identifies the person if the photo was previously uploaded to the database; has additional modules. Disadvantages: incomplete coverage of the loaded data, since you can work with a webcam; inaccurate results for uploading data.

The task of recognizing emotions is part of a comprehensive system for image analysis. For its proper operation, it is important to clearly identify

the person's face in the image and properly extract it for further processing, relay on a number of dynamic parameters.

Face detection algorithms can be divided into four categories [8]:

- empirical method;
- method of invariant signs;
- recognition on the template implemented by the developer;
- a method detection on external signs (the training systems).

The main stages of algorithms of empirical approach are:

- stay on the image of the person: eye, nose, mouth;
- detection: borders of the person, form, brightness, texture, color;
- combination of all found invariant signs and their verification.

Shortcoming is that this algorithm is very sensitive to degree of an inclination and turn of the head.

Mathematical problem statement for facial state recognition

Mimic reactions of each person have a certain set of standard manifestation parameters and are divided into two categories: geometric and behavioral.

To describe the quantitative and qualitative parameters of the face (voluntary and involuntary) use a coding system of facial movements. In this case, the quantitative parameter is the intensity of movement from *A* to *E*.

The video data stream is a sequential set of frames. The goal of recognition is to merge faces on images into disjoint classes. The task of face recognition is formulated as follows: it is required to build a recognition function (formula 1) output that determines the image class *w*, presented by a vector of sign $(x_1(w),\ldots, x_n(w))$.

$$F(w) = (F_1(w), F_2(w)\ldots, F_k(w)) \tag{9}$$

In this case a class is the one of six basic emotions of the person.

$$F_k(w) = \begin{cases} 1, if w \in \Omega_k \\ 0, if w \notin \Omega_k \end{cases} \tag{10}$$

Search of a solution is carried out by using of artificial neural networks.

The invariant is the property of some class (set) of mathematical objects remaining invariable at conversions of a certain type [7].

The invariant moments represent characteristic signs which can meet in each picture. Most often persons on video frames are exposed

to the different deformations inherent to a mimicry of the person. In such conditions it is necessary to tell about "pseudo-invariants" [4].

It is reasonable to convert the color images in a gray-scale style. After preprocessing and normalization the sample represents a matrix of pixels, each of which matters brightness in the range [0.1].

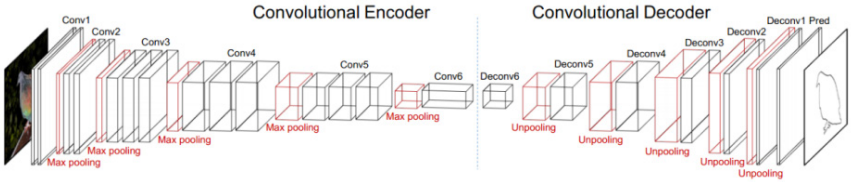

Figure 1. Structural scheme of combined convolutional neural network

Problem solution

The solution of a problem of recognition of emotions belongs to a problem of classification, i.e. the neural network should carry the received data set to emotions, answering to the set of parameters. Let's consider the mathematical description of a problem of recognition:

Let the set of *M* of images of persons (emotion, for example surprise) be given as $\{w_1,\ldots, n\}$, each of which has a vector of values of signs (mimic signs): [9]

$$x_i = (x_{ij},\ldots,x_{im}) \tag{11}$$

Vector of signs are carried by experts to some classes:

$$\Omega_1 = \{w_1,\ldots,w_{m1}\}, \Omega_2 = \{w_{m1+1},\ldots,w_{m1+m2}\},\ldots, \tag{12}$$

where $m_1 + m_2 + \ldots + m_k = m$, $m = |M|$.

For a solution of this task in work the combined convolution neural network which consists of convolution neural network, the qualifier and re-convolution neural network is used. Use of this network allows selecting emotional reaction of each of above-mentioned features. Data of exits of this network are inputs of the indistinct qualifier which allows making on the basis of the analysis of reaction of separate elements of the person decisions concerning threats which this passenger can represent.

The combined convolution neural network solves such problems as:

1) Recognition and description of features of the person.

This task demands definition of position of bodies (eyes, a nose, a mouth, etc.) on a face and also forms of these bodies should be defined.

2) Classification.

According to information on features of the person it is necessary to define what type of emotion is present at the image. Then it is necessary to define information on mood for further development of the intelligent interface.

The combined network consists of convolutional neural network, some qualifier and re-convolutional neural network. The conceptual structure of such network presented on the figure 1. Such architecture allows not only to distinguish image elements, but also to notice on it recognition elements. Re-convolutional neural network is specular reflection of convolutional neural network.

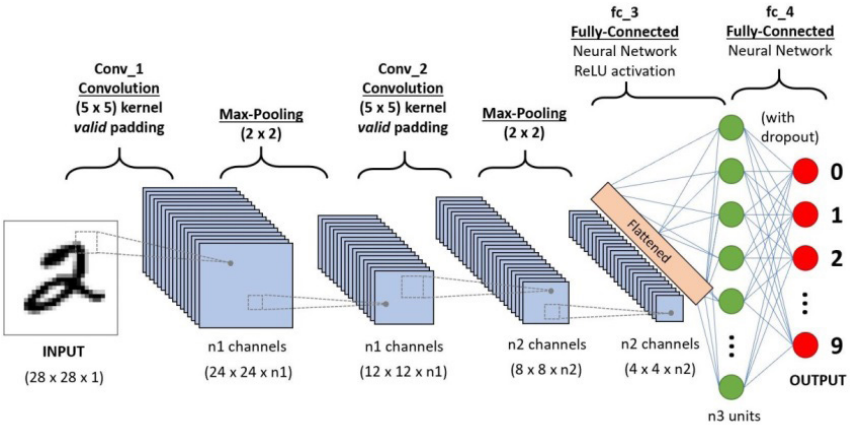

Figure 2. Structural scheme of single covolutional neural network

The ability of the multilayer neural networks trained by method of gradient descent to creation of difficult multidimensional areas on the basis of a large number of the training examples allows applying them as the qualifier to image identification.

Despite it, in traditional full-meshed neural network there is a number of the shortcomings lowering efficiency of their work. First of all, it is the big size of images (the image is understood as the graphical representation of a recognizable image presented in the form of set of pixels), which can reach several hundred. For correct training in such data it is required to increase number of the hidden neurons that leads to increase in number of parameters, and, as a result, lowers training speed, demands the big training selection. But the biggest restriction of such networks is that they do

not differ in invariance to different deformations, for example, to transfer or insignificant distortion of an input signal.

The convolutional neural network systems (ConvNets or CNNs) are the logical instrument receives an input parameters as image in the set of pixels view, finds some features on it and due to it sets the parameters (weighted coefficients) to wide data objects in the images and be able to highlight any special things among all over objects. ConvNets requires the less clean processing power relatively to other processing algorithms. Unlike to standard filter methods that working as hard-engineered unit, the convolutional neural network can achieve it through the training processes.

The structure of a ConvNets is same as connectivity image of human brain biological neurons and was based on group of the "Visual Cortex". Each one neuron responds to stimuli only in a specially-restricted area of the visual field known as the receptive area. A set of such areas overlap to cover the entire visual area. TheConvNets are able to clearly capture the spatial and temporal dependencies in any input image data through the application based on relevant filters. CNN structure performs a great setting to the image dataset with help of reduction in the number of parameters involved and reusability of weights. Therefore, the neural network can be trained to understand the sophistication of the image better. On the figure 2 presented the conceptual structure of convolutional neural network.

As the input commonly we will get the RNG image which means R – red color, G – greed and B – blue. Also, image can be in different color types: gray-scale, HSV, RGB, CMYK, etc.

For the while, take into the mind which the computational power needed for process the image of 8K (7680×4320) sizes. The main purpose of ConvNets is to compress it into much more lighter state without losing important parts (features). It's necessary to take care when we're designing structure with low features learning possibilities and huge data sets.

On the basis of results of check of the combined convolution neural network on test selection it is possible to determine a number of significant parameters:

1. Number of convolution layers.
2. Number of aggregation layers.
3. Mutual placement of convolution layers and aggregation layers.
4. Convolutional layers (for each layer separately):
5. Aggregation layers (for each layer separately):

6. Fully-connected layers (for each layer separately):
7. Existence of extracting operation for each layer: – extracting percent and random function.

For optimization of structure and parameters of convolution neural network the genetic algorithm is used [10].

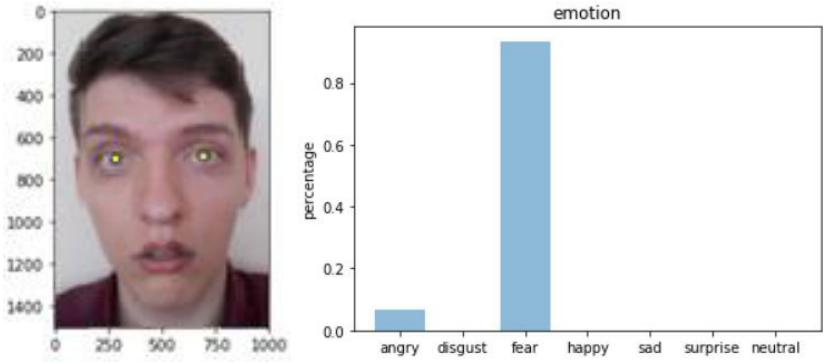

Figure 3. Facial expression recognition example obtained using complex CNN

Conclusions

In this work the effective approach for emotional state recognition of human face using digital images analysis is proposed. It is developed the ways of application the combined convolutional neural network for assigned task and algorithms of digital image processing was applied.

For the solution of the classification task it is used fuzzy neural network classifier such as "NEFCLASS", inputs of which are outputs of CNN. Given approach has the acceptable recognition level and good enough accuracy. This system can be successfully applied to perform the security purposes in the airports and able to increase the security level.

However, the system has some limitations as the sensitivity to lightning level, dependence on head rotation degree. These limitations will be eliminated at continuation of this work in the following directions: gain of compensation of light difference using the complication of an algorithm of adaptive filtering; expansion the range of emotions.

In (Fig. 3) presented the result of combined convolutional neural network for expression and analysis of human emotional state.

References:

1. *Krizhevsky A., Sutskeyever I. and Hinton G. E.* ImageNet Classification with Deep Convolutional Neural Network 2012.
2. *Nauck D., Cruse R.* NEFCLASS – a neuro-fuzzy approach for classification of data, Junuary 1995.
3. *Volinsky-Bosmanov Y. M.* Profiling. Technology for preventing crime acts in Magnetism, – Vol. III. G. T. Rado and H. Suhl, Eds. – New York: Academic, 2015. – 220 p.
4. *Li R., Ma S.* Impact of depression on response to comedy: A dynamic facial coding analysis. Journal of abnormal psychology, – 116(4). 2007. – P. 804–9.
5. *Knyazev B. A., Gapanyuk Y. E.* Recognition of aberrant behavior of the person. Journal of engineering, 2013. – 512 p.
6. *Ekman P. and Friesen W.* Facial Action Coding System: A Technique for the Measurement of Facial Movement, consulting Psychologists Press, Palo Alto, 1978.
7. *Stutz D.* Introduction to Neural Networks. Seminar on Selected Topics in Human Language Technology and Pattern Recognition, 2014.
8. *Tatarenkov D. A.* Analysis of face recognition methods on images, 2015. – 270 p.
9. *Deco G. and Obradovic D.* An Information-theoretic Approach to Neural Computing, Springer, – New-York, 1996.
10. *Voronosky G. K. , Petrashev S. N., Sergeev S. A.* Genetic algorithms. Artificial intelligence systems and problems of virtual reality, 1997.

Viktor Sineglazov, Dr. Sci., Professor, head of department, aviation computer integrated complexes department, National aviation university, Liubomyra Huzara ave., 1, Kyiv, 03058, Ukraine.
E-mail: svm@nau.edu.ua

Roman Pantyeyev, Ph.D., assistant professor, senior lecturer, aviation computer integrated complexes department, National aviation university. Liubomyra Huzara ave., 1, Kyiv, 03058, Ukraine
E-mail: romanpanteevmail@gmail.com
ORCID: https://orcid.org/0000-0003-4707-4608

Mykola Vasylenko, Ph.D., senior lecturer, aviation computer integrated complexes department, National aviation university. Liubomyra Huzara ave., 1, Kyiv, 03058, Ukraine.
E-mail: m.p.vasylenko@nau.edu.ua
ORCID0000-0003-4937-8082

Yuriy Opanasiuk, senior lecturer, aviation computer integrated complexes department, National aviation university. Liubomyra Huzara ave., 1, Kyiv, 03058, Ukraine.
E-mail: yuriy.opanasiuk@gmail.com

Roman Manuilenko, Ph.D., scientific employee, systems control theory department, Institute of applied mathematics and mechanics, National academy of sciences, Henerala Batyuka str., 19, Slovyansk, 84116, Ukraine.
E-mail: ronma2016@gmail.com

INTELLIGENT BIOMASS COLLECTION PROCESSES MANAGEMENT SYSTEM FOR BIOGAS HARVESTS BY AUTONOMOUS UNMANNED AERIAL VEHICLES

Yurii Gunchenko, Sergey Shvorov, Taras Davidenko,
Anna Yukhimenko, Dmytro Slutskyi, Larysa Martynovych

Abstract. The work aim is developing the functional structure of the intelligent control system (ICS) of biomass collection processes for biogas plants (BGP) by unmanned harvesters. To achieve this goal, a method for determining the volume and density of yields of energy crops (EC) in the fields using unmanned aerial vehicles (drons) and scientific substantiation of the method of synthesis of compromise-optimal routes and speed of robotic harvesting equipment with a minimum length of autonomous combine harvesters (ACH) in the process of biomass collection and taking into account the density of changes in the yield of EC, as well as various obstacles.

Keywords: intelligent control system, unmanned combine harvesters, biomass, biogas.

Introduction and problem statement

One of the most important tasks today is the development and implementation of promising technologies for the industrial production of biomethane to replace natural gas. As a rule, not only waste from agricultural farms, agro-firms, sugar factories and poultry farms, but also specially grown energy crops for biogas plants are used to obtain the maximum volumes of biomethane. Solving this problem on a large industrial scale involves the development and application of intelligent control systems for EC harvesting processes using unmanned harvesters. As practice shows, suboptimal planning of field works leads to the imposition of routes of harvesting equipment, delays in its work and, as a consequence, excessive fuel consumption. In order to eliminate these shortcomings with the help of ISC should be performed planning of harvesting works and calculation of optimal trajectories of harvesting equipment, which are introduced into the navigation equipment of each harvesting tool. Implementation

of optimal trajectories in the process of harvesting involves reducing fuel consumption by minimizing time delays of harvesting equipment and the number of overlapping routes of their movement, taking into account the characteristics and geometric shape of the field.

However, at present, methods for determining the volume and density of yields of energy crops from UAVs, harvesting planning, synthesis of compromise-optimal routes of promising unmanned robotic harvesting equipment and construction of intelligent control systems for harvesting energy crops for biogas plants (complexes and factories). Analysis of recent work [1–8] shows that currently known global and local methods of navigation BZK. Global methods are characterized by the fact that before the BZK movement, field maps are fully known. With the help of GPS receivers the location of each BOD, the finish point, as well as the location of all obstacles is determined. At present, methods of wave front, A *, visible graph and tree of squares are known for navigation of harvesting equipment [1–4]. The disadvantages of such methods include the need to save a map of large fields and considerable computational complexity. Local navigation methods are used in cases where stationary (passive) and moving (active) obstacles are unknown, which can appear and disappear and change their location. In this case, BZK receives navigation information about the local area of the environment, being within the range of its sensors. Such methods of MR navigation include: methods based on the use of potential interference fields [2], methods of the BUG family [5, 6], which use tactile sensors to obtain navigation information, as well as methods of the VisBUG family [6–8], which involve obtaining navigation information from ultrasonic sensors.

The advantages of local navigation methods include their computational simplicity. The disadvantages of these methods, compared with the methods of global navigation, are the deviation of the real trajectory of the BZK from the optimal route and a more complex procedure for localizing BZK in space. Both groups of BZK navigation methods are characterized by the problem of timely identification of passive and, especially, active obstacles in the way of ACH movement. In addition, the existing methods and algorithms for solving problems of planning the trajectories of ground BZK are used in two stages: first there is a global trajectory of cartographic data, which is then periodically updated according to the onboard technical vision system (OTVS) ACH. This approach is characterized by contradictions and shortcomings due to the significant difference

in the scale of information at these two stages. The advantages of local navigation methods include their computational simplicity. The disadvantages of these methods, compared with the methods of global navigation, are the deviation of the real trajectory of the ACH from the optimal route and a more complex procedure for localizing ACH in space. Both groups of ACH navigation methods are characterized by the problem of timely identification of passive and, especially, active obstacles in the way of ACH movement. In addition, the existing methods and algorithms for solving problems of planning the trajectories of ground ACH are used in two stages: first there is a global trajectory of cartographic data, which is then periodically updated according to the onboard technical vision system (OTVS) ACH. This approach is characterized by contradictions and shortcomings due to the significant difference in the scale of information at these two stages.

Traditional raw materials for biogas reactors, in particular livestock and poultry waste due to declining livestock, may not be enough to produce the required amount of energy. As additional sources for biogas production in the EU countries use vegetable raw materials, namely energy crops and crop waste, as shown in the works of A. Meyer et al. (2017) [9] and P. Schröder et al. (2018) [10]. Crops of energy crops are planned taking into account, first of all, the areas of unsuitable lands for crop production, such as peatlands (K. Laasasenaho et al., 2017) [11], as well as logistics for existing biogas reactors. Technologies developed for the production of biogas from waste that accumulates in processing sites are adapted to specific raw materials (R. Ciccoli et al., 2018) [12], which limits its use for seasonal raw materials. In the work of K. Sahoo et al. (2018) [13] it is shown that crop residues in the fields have a certain economic potential for biogas production, but there is a problem of monitoring the volume of these raw materials and optimizing the logistics for its transportation to the reactors. The issue of optimizing the transport of biomass within the region was considered by J. Höhn et al. (2014) [14] for Finland, in the work of V. Burg et al. (2018) [15] – for Switzerland, but evaluated, first of all, the sites of promising construction of stationary biogas reactors. The works show that from year to year the location of biomass sources changes, which complicates the solution of the issue of operational monitoring of the state and volume of biomass during the year to optimize logistics.

The experience of using biogas plants and plants in European countries, especially in Germany, shows that a significant increase in biogas

production requires the use of hybrids of energy corn. The proportion of corn silage in a mixture with other co-substrates can be from 2 to 99%. Analysis of existing biogas technologies shows that in Germany in 2012 for the cultivation of energy crops (mainly corn) for the production of biogas used about 1 million hectares of land. At the same time there is a need for further research of methods and technologies of EC collection. One of the promising ways to increase the efficiency of BSU is the use of specially grown maize hybrids for biogas production, as well as the use of corn production waste for grain, sunflower and straw, which is one of the most important and widespread crops in the world, including in Ukraine.

The highest yield of biogas, as research shows, gives a hybrid of corn Monica 350 MW. This hybrid with a grain yield of 13.0–13.5 t/ha and silage 48.0–76.0 t/ha, is tall (250–290 cm), has become widespread in the steppe of Ukraine.

Harvesting sunflowers involves collecting them in a digger after threshing the baskets, and the stems are crushed with disc peelers, raked into rolls and formed in the field of cops.

Currently in Ukraine, the non-grain part (NGP) of sunflower is burned in boilers, however, one of the promising areas of use of NZCH sunflower is the production of pellets / briquettes with their subsequent use in ACH.

Annual volumes of straw in the agro-industrial complex are close to the total production of grain crops in Ukraine. Depending on the condition of the breads, the availability of machinery and agronomic conditions, direct combining (single-phase method of harvesting) or stacking of bread in rolls followed by threshing (two-phase method of harvesting) is used. The grain part of the crop is separated from the stem part during harvesting, and the other part of the straw that remains in the field is plowed into the soil.

Analysis of the processes of harvesting, transportation and storage of NGP requires 2–3 times more money than harvesting grain. At the same time, labor costs for harvesting the non-grain part reach 70% of all costs for harvesting the entire grain crop. This can be explained by the fact that the development of existing EC harvesting technologies lags far behind the development of grain harvesting technologies.

Requires research on the automation of the processes of harvesting and further use of NGP for energy needs and, above all, the efficient use of straw as the largest part of the EC.

Cereal straw can be used for livestock needs or as an organic fertilizer, as well as for energy needs (combustion in boilers, production of pellets /

briquettes for biogas plants). At the same time, there is a need to substantiate a promising highly efficient technology for harvesting energy crops.

Based on the above, the **purpose of the research** is to develop a functional structure of an intelligent control system for biomass collection processes for biogas plants by unmanned harvesters.

To achieve this goal the **following tasks are solved**:

– development of a method for determining the volume and density of changes in the yield of energy crops of biomass in the fields using unmanned aerial vehicles;

– substantiation of the method of synthesis of compromise-optimal routes and speed of robotic harvesting equipment with the minimum length of ACH paths in the process of biomass collection and taking into account the density of EC yield change, as well as passive (stationary) obstacles;

– development of methodical bases of planning of routes of movement of unmanned combine harvesters;

– development of methodical bases of the organization of speed control of movement of unmanned combines.

With the help of the proposed ISC the following tasks should be solved: monitoring the process of growing EC, determining the volume and density of changes in the yield of energy crops EC based on the use of UAVs; recognition of EC, active and passive obstacles in the way of ACH movement, planning of optimal routes of their movement for EC collection; operational management of processes of loading and delivery of raw materials to ACH.

To address these issues, the CPI should include subsystems for monitoring, planning and operational management of energy collection processes. In addition, one of the most important tasks, which is solved with the help of ISC, is the placement of crops of different energy crops, monitoring their condition and their differential fertilization in a specially defined area, taking into account geophysical features for each crop.

Development of a method for determining the volume and density of changes in the yield of biomass energy crops in the fields using unmanned aerial vehicles

Currently, more and more attention is paid to "precision farming", which ensures maximum productivity of agricultural work. The most promising is the use of unmanned aerial vehicles to plan and control the

movement of unmanned aerial vehicles depending on the presence of crops and obstacles in each section of the field.

The planning process content and time of work is divided into several stages, namely: sowing of early winter crops and their harvesting, sowing of subsequent EC and their harvesting. Each of these stages of planning has its own characteristics, and for their implementation it is advisable to provide in the ISC appropriate database and knowledge.

The EC monitoring subsystem is a geographic information system that receives data on the quantity and quality of raw materials from information sensors located on the UAV, as well as from other information sources. Based on these data, a set of acceptable solutions for improving the condition of energy crops, as well as the organization of collection and subsequent use of organic raw materials at BSU.

According to the results of experimental studies, conventional digital UAV cameras can be used effectively in determining crop volumes and identifying various obstacles to the movement of BZK in each part of the field. After photographing on an electronic map of the field on the basis of statistical processing of RGB-signals several contrasting zones on optical characteristics (sites) are defined. For each of these zones, the control yields used to train the neural network are calculated experimentally. With the help of special software for processing the spectral characteristics of digital images of each area using neural networks, the volume and density of crop changes in the movement of unmanned harvesters are determined, which provides prompt decision-making for their distribution, route planning and speed control.

The basis of the subsystem are special methods and algorithms for pattern recognition, which provide the following tasks: image perception (technical measurement), pre-processing of the received signal (filtering), selection of the required characteristics and image classification (decision making). For this purpose, the neural network structure was synthesized and the corresponding multilayer perceptron was tested for adequacy. Processing of graphic data based on the results of UAV photography is carried out using information technology based on the use of special software manufactured by NULES LDE – Land damage expert. The program has the ability based on statistical processing of RGB signals to determine the coordinates of the interference for BZK on the electronic map of the area and the volume of the EC.

It is important to correctly organize the sequence of actions for monitoring the condition of energy plants based on the use of UAVs. Analyzing the methodology of using UAVs for spectral monitoring of vegetation in relation

to reflected radiation (leaf diagnostics), it should be noted its fundamental differences from similar satellite, aircraft or ground platforms. The specifics of the use of satellite and aircraft platforms have led to technical decisions on the choice of spectral channels and methods of radio frequency correction, ie correction for changes in lighting. Near-infrared (NIR) channels are commonly used for satellite platforms, but conventional digital or multi-channel UAV cameras are more effective in determining crop yields.

Specialized geographic information systems (GIS), which take into account both spatial reference and special information about the EC, play a significant role in solving the problem of clarifying the condition of energy crops with the help of unmanned aerial vehicles. As practice shows, UAV surveys not only increase the accuracy, homogeneity, objectivity and frequency of observations, but also allow to significantly improve the methods of operational control over the condition of crops and forecasting the yield of energy crops.

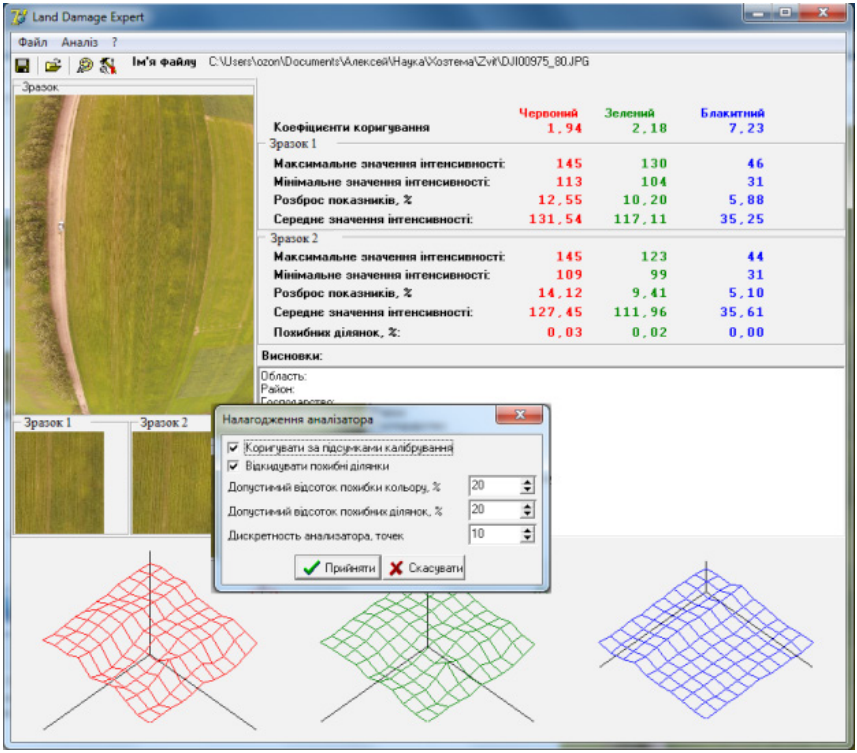

Figure 1. Interface and debugging unit of the Land damage expert program

Effective management of BZK requires the solution of many complex tasks, including data collection from UAVs, their processing using special software for monitoring the state of fields and volumes of energy crops.

Solving the problems of analysis, forecasting and optimization of BC management should be carried out comprehensively using digital slope maps with a model of terrain and slope exposures, yields and type of crops, power lines and other stationary obstacles in the way of ACH.

Processing of graphic data based on the results of UAV photography is carried out using special software manufactured by NULES LDE – Land damage expert, the interface and debugging unit of which are shown in (Fig. 1).

The LDE program allows you to use a manipulator (mouse) on an electronic map of the area to select research areas for which statistical processing of graphic data. Because the standard JPEG format defines RGB values not for each specific pixel, but for areas with the same parameters, LDE converts data from JPEG format to BMP format, in which the brightness values of the components of the additive color model are determined for each pixel.

The program has the ability to determine the coordinates of obstacles on the electronic map of the area, the RGB values of which differ from the average by a percentage (10–15%), which is taken into account when setting up the program. To plan the movement of BC, the known information is the coordinates of the area where the harvest is planned, the initial location of each ACH and the end points of their route, the coordinates of obstacles and areas without harvest, obtained by UAVs and processed by Land damage expert software.

In the technological aspect, Land damage expert is a means of collecting, storing, analyzing, visualizing space-time data and related information about GIS objects. It is GIS technology that allows to give a detailed description of the structure of the surface of the assessed area, the features of soil cover and land use, creates real preconditions for their cultivation.

Among the existing data sources for GIS are known: cartographic sources, photographic data of field searches and various cadastres, data from the Internet and statistical data.

With the help of special software for monitoring the status and determining the volume of the EC, the following tasks are solved:

1. Binding to the location of images obtained from UAVs and entering information about the volume and status of the EC in the GIS database.

2. Information processing using the method and algorithm for determining the volume of EC for planning and optimization of routes BC.

3. Determining the geometric shape of the field and obstacles for planning BC routes.

4. Issuance of recommendations on the use of BC.

Figure 2. Linking UAV images to reference points

The task of positioning the UAV is to determine the two landmarks that fall into the camera field of view, and the drons position (X_c, Y_c, Z_c) and orientation (α, β, δ).

Under the imposed restrictions, system (1) is significantly simplified: the angles β and δ become equal to zero, which means that the orientation of the UAV is given by one angle α.

The UAV orientation matrix is formed using Euler angles (Fig. 2):

Figure 3. Contrasting optical characteristics of sections 1–3

The results of experimental studies show that standard digital cameras can be used to predict the yield in each section of the field and identify different types of obstacles in the way of UC. After photographing the field based on the processing of RGB signals using GIS, several different contrasting zones (areas) are determined by optical characteristics. For each of these zones (Fig. 3, sections 1–3) are measured control yields for neural network training.

$$R(\alpha,\beta,\delta) = R_{\delta}^{Z''} R_{\beta}^{X'} R_{\alpha}^{Z} = \begin{pmatrix} \cos\delta & \sin\delta & 0 \\ -\sin\delta & \cos\delta & 0 \\ 0 & 0 & 1 \end{pmatrix} \begin{pmatrix} 1 & 0 & 0 \\ 0 & \cos\beta & \sin\beta \\ 0 & -\sin\beta & \cos\beta \end{pmatrix} \tilde{O}$$
$$\tilde{O} \begin{pmatrix} \cos\alpha & \sin\alpha & 0 \\ -\sin\alpha & \cos\alpha & 0 \\ 0 & 0 & 1 \end{pmatrix} \quad (1)$$

where $\alpha \in [0,2\pi]$, $\beta \in [0,\pi/2]$, $\delta \in [0,2\pi]$.

$$x_i = -f_x \frac{r_{11}(X_i - X_c) + r_{12}(X_i - X_c) + r_{13}(X_i - X_c)}{r_{31}(X_i - X_c) + r_{32}(X_i - X_c) + r_{33}(X_i - X_c)} + \alpha_x$$
$$y_i = f_y \frac{r_{21}(X_i - X_c) + r_{22}(X_i - X_c) + r_{23}(X_i - X_c)}{r_{31}(X_i - X_c) + r_{32}(X_i - X_c) + r_{33}(X_i - X_c)} + \alpha_y \quad , \quad (2)$$

where $r_{ij} = r_{ij}(\alpha,\beta,\delta), i, j = 1,2,3.$

Studies have shown that EC plants at study points 1–3 differed in density, height and development (table 1).

The height of the plants is determined by measuring the average height of the 20 plants closest to the measuring point.

The studies were performed using DJI Phantom 2 and CD600 or Slantrange 3p quadcopters on the DJI Matrice 600 Pro platform.

Table 1. – Characteristics of EC crops at contrasting points of the image

Points No.	Plant height, sm	Plant density, pcs. on m²	Average weight one plant, kg	Estimated biomass, kg/m²
1.	165	10	1,9	19,0
2.	20	1	0,1	1
3.	175	10	2,1	21,0

The accuracy of determining the number of plants on the map at the early stage of vegetation depends most on the height of the UAV and the relationship between plant size and pixel size (Fig. 4).

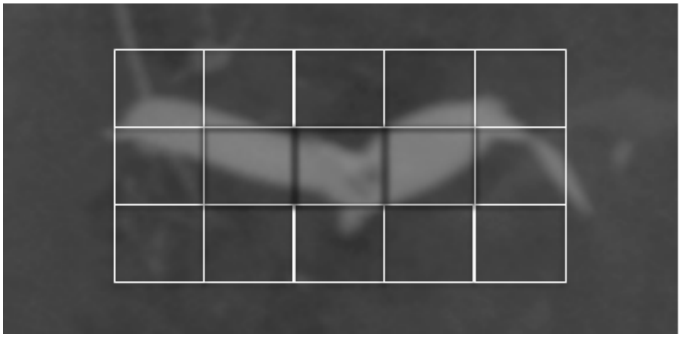

Figure 4. Corn at an early stage of vegetation with the representation of pixels from a great height

As can be seen from (Fig. 4), the three central highlighted pixels are filled with a larger percentage of the whole plant, and therefore to get a good result on the number of plants, you need to have about 5 pixels per plant.

In the (table 2) shows the pixel size on the earth's surface as a function of the height of the UAV above the earth's surface, which makes it possible to determine the correct flight altitude for data collection.

Table 2. – Pixel size on the earth's surface (GSD) as a function of height above the earth's surface

Height (м)	**25**	**30**	**35**	**45**	**60**	**90**	**120**
1p – GSD (м)	0.019	0.023	0.026	0.034	0.045	0.068	0.090
2i, 2p – GSD (м)	0.010	0.012	0.014	0.018	0.024	0.036	0.048

On the basis of application of the device of neural networks volumes of a crop on a way of movement of ACH (Fig. 5) are defined.

The formation of the neural network is effectively carried out using the software STATISTICA.

Substantiation of the method of synthesis of compromise-optimal routes and speed of robotic harvesting equipment with the minimum length of BZK paths in the process of biomass collection and taking into account the density of EC yield change, as well as passive (stationary) obstacles

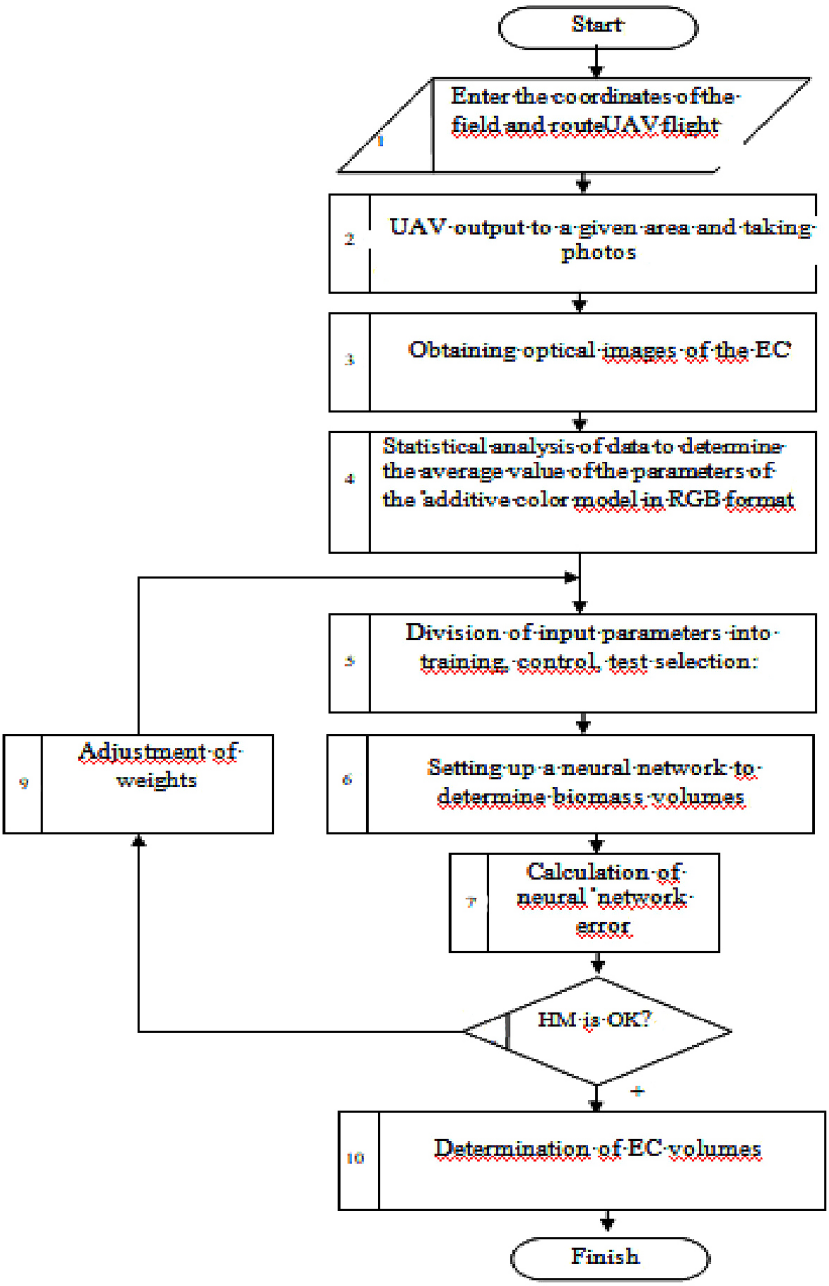

Figure 5. Algorithm for statistical processing of RGB signals

One of the most promising areas of robotics is route planning or navigation ACH. Navigation is the theory and practice of guiding moving objects along a given trajectory. The purpose of ACH navigation is to find the optimal (according to the specified criteria) routes of its movement between the given points of space taking into account stationary (passive) and mobile (active) obstacles. Based on this, the development of new models, methods and algorithms for navigating autonomous mobile robots, taking into account different types of obstacles is an urgent scientific and technical task.

So-called global and local methods of navigating moving objects are currently known and widely used. A characteristic feature of global methods is that the map of the area from the location of all obstacles before the start of the ACH is fully known. In cases where passive and active obstacles can change their coordinates, local navigation methods are used.

For the given groups of methods of navigation of ACH there is a necessity of timely definition of these obstacles on a way of movement of BK.

As the results of monitoring the actual situation of the movement of equipment in the field, the existing system of planning and management of harvesting equipment has the following shortcomings, namely:

1) disregard for the volume of EC and the geometric shape of the fields;
2) overlapping routes of harvesting machines;
3) loss of time due to ST delays;
4) there is no single control.

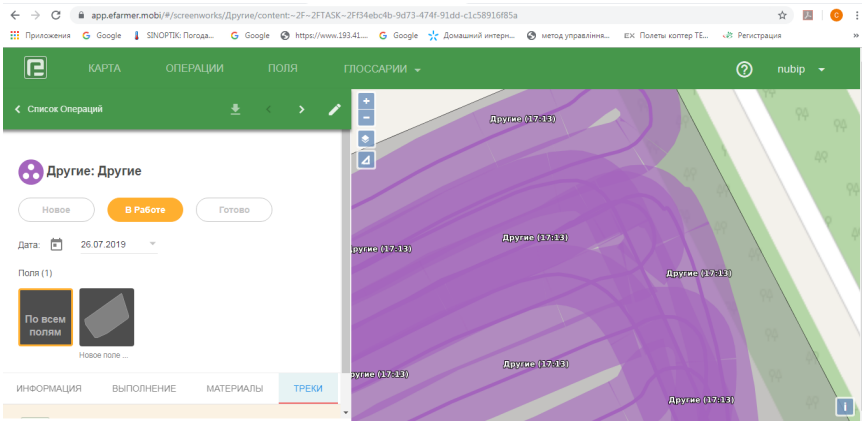

Figure 6. Overlay of routes of movement of combines

In (Fig. 6) shows the overlap of the routes of movement of combines during harvesting.

In order to eliminate this shortcoming, the solution of the problem of synthesis of optimal routes of unmanned combines is as follows.

The process of planning the content and time of planning the trajectories of ACH is divided into several stages, namely: the formation of an electronic map of the terrain and identification of all types of obstacles in each section of the UAV based on statistical analysis and artificial intelligence, as well as determining optimal routes of ACH obstacles using the method of situational control.

The paper proposes a combined method of ACH navigation, based on a combination of approaches typical for both global and local navigation methods. In the presence of STZ on the basis of the UAV the option of planning of trajectories of movement of ACH in three stages is possible: with use of cartographic data (global trajectory); based on UAV data based on UAVs (tactical trajectory); using STZ ACH data (local trajectory). The tactical trajectory, which is built according to the data from the UAV-based STZ, is a closed trajectory passing through the folds of the terrain. The target point at the global planning level is the end point of the BZK route task, the target points at the tactical planning level will be a sequence of points belonging to the global trajectory, and the target points at the local planning level will be sequences of points belonging to trajectories built at the tactical planning level. Thus, the district on which BZK moves, consists of sites of two types: open sites and obstacles which ACH cannot overcome directly. If an obstacle is found in the way of ACH, he must go around it. Procedures of this type are present not only in the tasks of photographic analysis, but also in data processing using GIS. As the scope of application of geoinformation technologies expands and the procedures of geoinformation modeling become more complicated, the procedures of analysis and classification of data sets, objects and structures occupy an increasingly important place in the new generation of GIS.

Virtually the entire process of thematic decoding of photographic images consists of a step-by-step grouping and subsequent transformation of data in order to create a completely definite, problem-oriented picture of the earth's surface. Much of these steps are provided by the methods and algorithms included in the specialized toolkits, and the task of the processor is to create the most efficient data classification scheme.

The problem is solved with the help of special information technology, which involves obtaining data on the area from an unmanned aerial ve-

hicle in the optical range and processing photos using GIS. Photographing of a certain surface is carried out from a height of 1 to 250 m with the possibility of obtaining images with high resolution. With the help of special software the movement of the UAV (quadcopter) is controlled. After photographing for each pixel or elementary area (square) of the field, statistical processing of graphic data of the brightness of the components of the additive model of color formation is performed. Thus, the coordinates of the interference are determined (specified) if the RGB values of which differ from the set value in the GIS by a corresponding percentage.

For planning the movement of ACH known information is the initial location and the end point of the route of ACH movement, the coordinates of the obstacles obtained by the UAV.

It is necessary to find the following optimal routes of ACH traffic, which provide: a) the minimum path of ACH traffic; b) bypassing passive and active obstacles.

The solution of this problem is reduced to a discrete form on a network of elementary squares of the field with coordinates (x_m, y_j) at the j–th level of the network and with the coordinates of the BC (x_j, y_{j-1}) at the (j–1)-th level of the network.

It is believed that the BC can move only from one node of this network to another.

The problem of synthesis of optimal trajectories in given conditions is solved using the method of situational control and multiagent apparatus, which includes a combination of neural networks and odd blocks, as well as the method of dynamic programming, which minimizes the trajectory of ACH [16, 17]:

$$D_{j-1,j}^{j,m} = (x_m - x_j)^2 + (y_j - y_{j-1})^2, \tag{3}$$

$$\begin{gathered} x_m = x_{j-1} + \Delta S_m \cdot \cos\left(\alpha 0 + \sum_i^N \frac{S}{L}\sin(\psi_c)\right); \\ y_j = Y_{j-1} + \Delta S_m \cdot \sin\left(\alpha 0 + \sum_i^N \frac{S}{L}\sin(\psi_c)\right); \\ \psi_c = \frac{\psi_{\bar{E}} + \psi_{\bar{I}}}{2}, \end{gathered} \tag{4}$$

$$F(j,m) = \min_{i \in I_{j-1}} [\Delta F_{j-1}^{j,m} + F(j-1,i)], j \in [1,J], \tag{5}$$

$$\Delta F_{j-1,j}^{j,m} = \frac{k_1 B_{\max}}{B_{\max} - B_{j,m}} + \frac{k_2 D_{\max}}{D_{\max} - D_{j-1,i}^{j,m}} + \frac{k_3 \lambda_{\max}}{\lambda_{\max} - \lambda_{j-1,i}^{j,m}}, \quad (6)$$

where k_1, k_2, k_3 – is weighting factors, B – is assessment of the danger of approaching ACH to passive obstacles, D – is the length of the route of unmanned harvesters, λ – is assessment of the probability of ACH entering the area of EC absence, L – is the distance between the axles of the front and rear wheels, the size of the base BC, α_0 – is the initial value of the angle between the direction of the longitudinal axis and one of the axes of the reference rectangular coordinate system, ΔS_m – is the distance between two passed points, S – is element of the path traveled, Ψ_c – is the arithmetic mean of the rotary wheels between the left angle of rotation $\Psi_л$ and the right angle of rotation Ψ_n.

As the optimal at level j is selected and the allowable point of this level, which corresponds to the minimum length of the trajectory of the ACH, which is transmitted to the navigation equipment ACH.

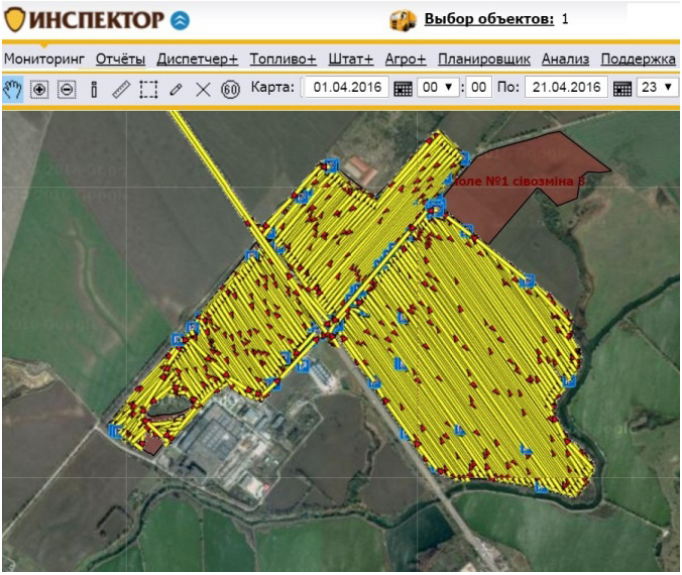

Figure 7. Planning of global trajectories of BZK

The geometrical characteristics of the maneuvering zone are remotely determined by the STZ created on the basis of the 3D-laser sensor which allows to receive the image of external environment before ACH, in the range of distances 0 … 50 m, with an accuracy of 5 cm. taking into account

the angular and linear displacements of the ACH, local trajectories of the ACH movement are constructed.

When planning global trajectories, a cartographic database is used (Fig. 7), which allows not only to store information about large areas of possible maneuvering, but also to adjust it in the process of movement according to UAV STZ.

Thus, the navigation system is created on the basis of a combination of satellite navigation, UAV sensors and ACH. In addition, the method of situational control and the device of multiagents is used, which provides a timely response of ACH to unforeseen obstacles that appear in its path (Fig. 8).

Figure 8. Determination of obstacles according to the UAV STZ

It is also possible to separate the contours of the obstacle with the help of – laser radars (LiDAR), which, in addition to the spectral indicators, determine the distance to the object.

The integrated use of various sensors and navigation methods allows to reliably solve the navigation problem by on-board means of ACH in the conditions of obstacles on the ground, and the executive system to work out the found trajectories taking into account the kinematic and dynamic characteristics of UC.

Experimental studies conducted in the Separate subdivision of NULES of Ukraine "Agronomic Research Station" showed the advantages in the efficiency and reliability of the results of the proposed technology and in the use of the combined method compared to traditional navigation methods.

Thus, the proposed method of planning routes ACH depending on the presence of obstacles to their movement, identified by UAVs, provides higher reliability and efficiency of information and accuracy of control UC,

as well as reducing the total length of ACH and fuel consumption. The obtained data from the UAV make it possible to quickly identify obstacles to the movement of the BC based on the use of the developed technology, which reduces the time spent on planning the routes of a group of mobile robots.

Methodical bases of planning of routes of movement of unmanned combine harvesters

To obtain, in accordance with the established requirements, topographic maps at a scale of 1: 2000 is prepared photo basis with an extension of 15 cm / pixel and with an error in determining the coordinates at any point not more than 18 cm. Yes, such a camera is included in the set of DJI Phantom 3+ UAVs or shooting can be done with a GoProHero camera, which provides an expansion of 10–15 cm/pixel from a height of 100–120 m.

The required anchoring accuracy is achieved by measuring the coordinates of the photographic centers using high-precision GNSS, GPS receivers within the defined reference network, or by using a terrestrial reference network, or RTK stations, which provide coordinates with an error of not more than 4 cm.

Agisoft PhotoScan software is used to create an orthophoto plan in order to lay the optimal BZK routes when assembling the EC. This determines the height matrix, as well as orthophoto plans with optimal trajectories of ACH. The operator of the PhotoScan software environment is responsible only for the management and control of the program operation modes.

Binding in the model program to the terrain consists of three main stages:

– automatic determination of boundaries and points of overlap of images, as well as the coordinates of the centers of photography, calculation of parameters that describe the optical system (asymmetry factor, position of the center point, distortion);

– linking the obtained model to the geodetic coordinate system of ground reference points of photography centers;

– on the basis of certain coordinates and parameters the construction of a polygonal model of the terrain surface is carried out.

The model obtained in this way is used to generate orthophoto plans.

The method of working with the program is as follows:

– uploading the received photos to the software environment;

– linking photography centers and downloading data to the selected coordinate system;

– determination of a point model of the Earth's surface;

– marking reference points on photographs and loading the coordinates of reference network points (in the presence of a terrestrial reference network);

– generation and optimization of a polygonal model of the Earth's surface.

Figure 9–12 shows screenshots of the program windows, which illustrate the process of processing aerial photography of EC plantations in the experimental field of NULES of Ukraine.

A computer equipped with a dual-core processor (Intel Pentium G4620i) with 8 GB of RAM was used to process these materials.

Data processing was carried out within 15 minutes from the moment of uploading photos to receiving an orthophoto plan and in the format of BMP – digital terrain model

Figure 9 shows the process of creating a project, consisting of blocks (chunk 1) – the processed parts of the project with their photos, model parameters and coordinate system, etc.

The position of the selected image is shown in the display window of the model (Fig. 11) in a three-dimensional coordinate system. Pictures that did not find enough common points will still be displayed with spheres / balls and marked NA (not aligned) in the photo list.

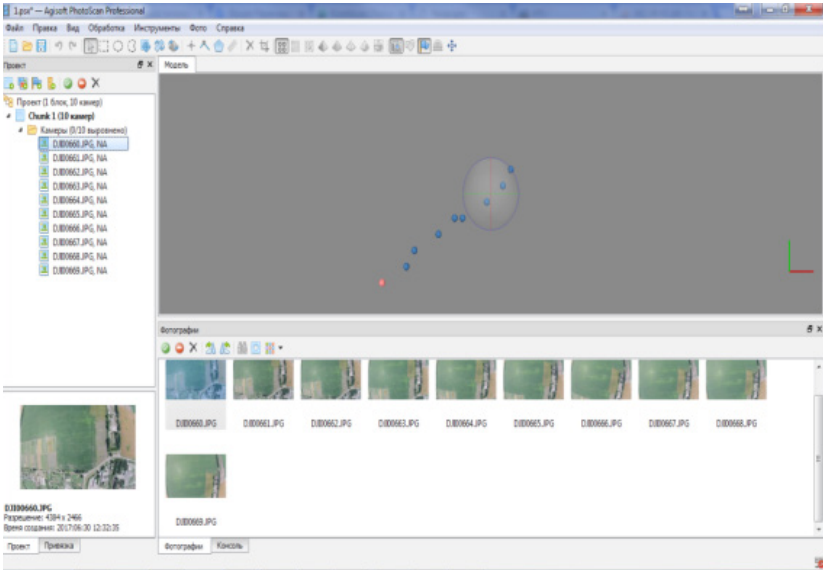

Figure 9. Uploading images from the UAV to Photo Scan

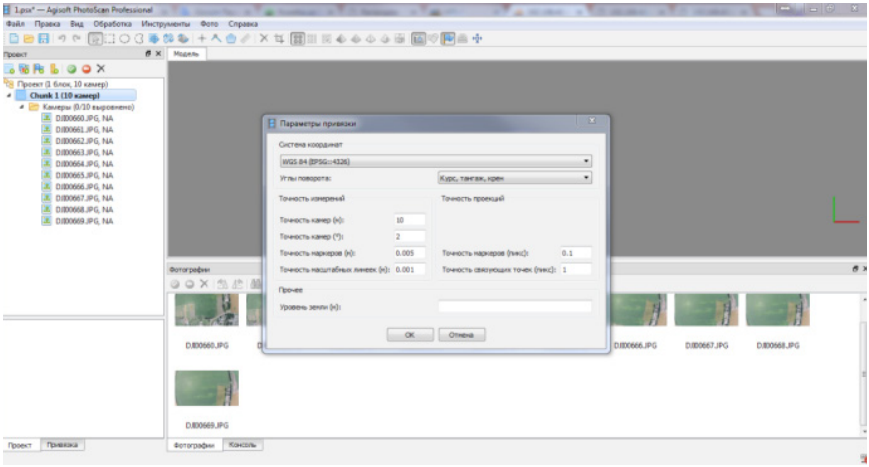

Figure 10. Choice of coordinate system

Figure 10 shows how the coordinate system is selected.

Construction of the terrain model is carried out by selecting the appropriate item in the processing menu “Bild Tiled Model”. The digital model of the area in the form of an orthophoto plan of the area is shown in (Fig. 12).

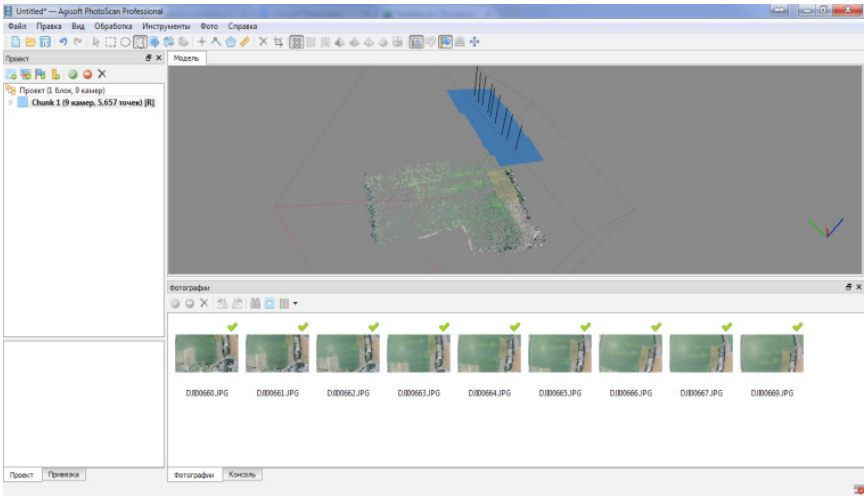

Figure 11. The result of the command “Align Photos”

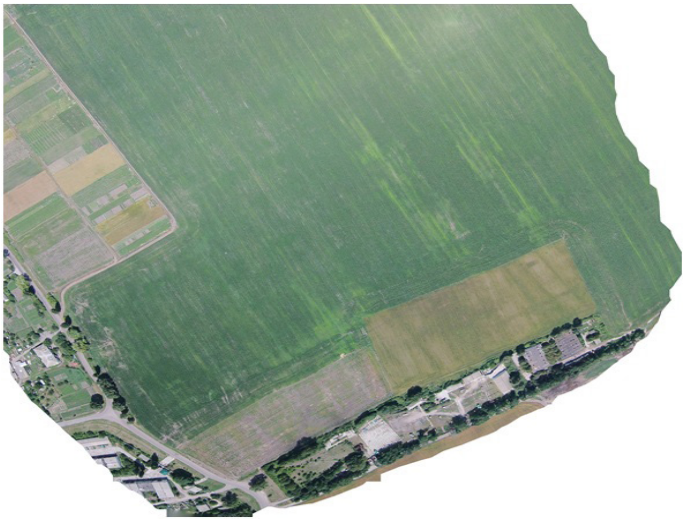

Figure 12. Orthophoto plan of private fields (3.3 ha)

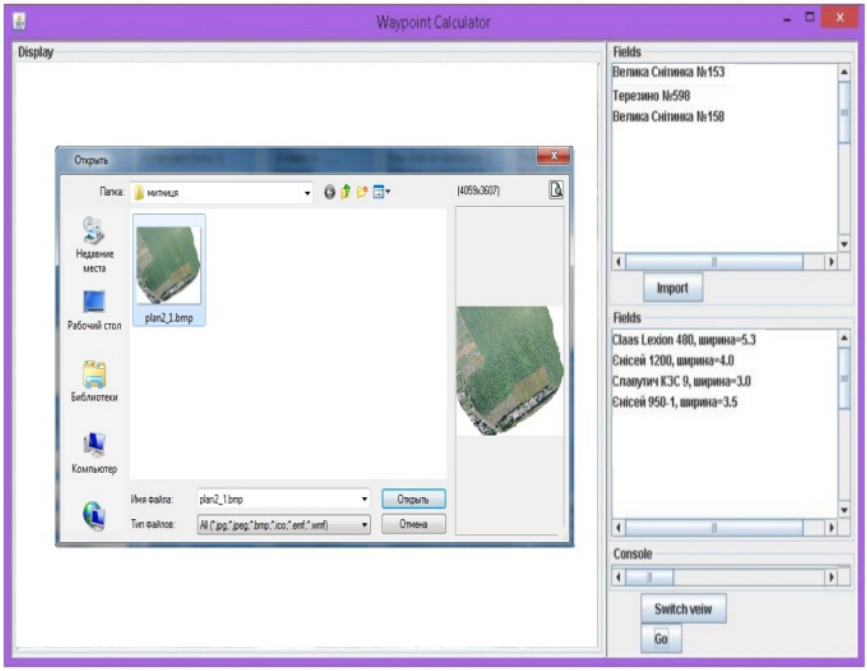

Figure 13. Launch the program and download the orthophoto plan to the software environment

Starting the program begins with downloading a file in BMP format in the software environment PhotoScan orthophoto plan, by clicking "Open Photo" (Fig. 13).

After uploading the image, the META window will display the service parameters required to generate the blocks used for image analysis. According to the results of the program, a necessary condition for the correct geographical location of the blocks is the operator's input of the coordinates of the starting point and scaling parameters, which must be transferred from the PhotoScan program when creating an orthophoto plan file. The software starts after clicking the "Scan" button.

When the block analysis is completed, the program notifies you with the text message "Image analysis is complete!", After which the "map" button will be available in the main program window and an interactive map. htm file will be created with visualization of software results using Google Maps.

The interface and the block of laying the optimal routes of the software are shown in (Fig. 14).

According to the results of the program, the trajectories of the BZK are formed in the form of coordinates of points (Fig. 15).

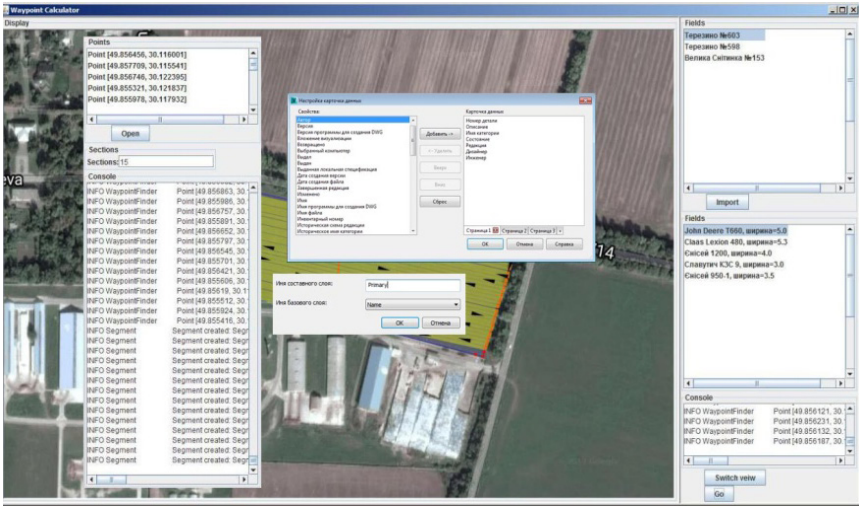

Figure 14. Working window of software for laying optimal routes BZK

Figure 15. Visualization of the results of the software of laying the optimal routes BZK

The obtained data on the optimal routes in.shp/kml format are entered into the software environment of the EFARM parallel driving system (Fig. 16).

Figure 16. EFARM parallel driving system

Based on the use of the proposed software for laying the optimal routes of AHC and parallel driving system EFARM provides: parallel driving on the line AB, curve AB, perimeter-line AB, perimeter-curve AB; entering

the coordinates of the fields using GPS; entering the coordinates of the field manually by selecting points on the map; import fields in.shp /.kml format; export fields in.kml format; measuring the area of the field and perimeter; keeping records of economic activity; adding harvest history; soil mapping and obstacle display; search for fields using a filter.

The practical application of such a navigation system provides: optimization of agricultural machinery; saving all types of costs and increases the efficiency of EC collection; possibility to work at night and in conditions of limited visibility; storage of notes and images with reference to a certain point in the field; automatic storage of all data and reports; parallel driving of any quantity of AHC.

In addition, using this software provides an opportunity to quantify the yield, the feasibility of travel of the harvesting and impassable area with obstacles that should be avoided within a particular section of the field when building optimal routes.

Development of methodical bases of the organization of speed control of movement of unmanned combines

To determine the average speed of ACH based on the use of Land damage expert software, a field yield map is formed, which is divided into squares with a relative from 0 to 1 yield (Fig. 17).

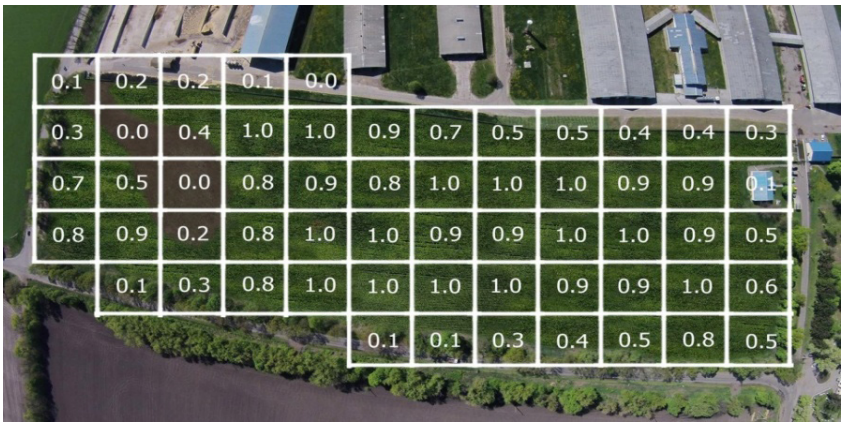

Figure 17. Forecasting the yield of each section of the field based on the prediction of the neural network

Each section of the field has its own distribution of field yields (Fig. 18).

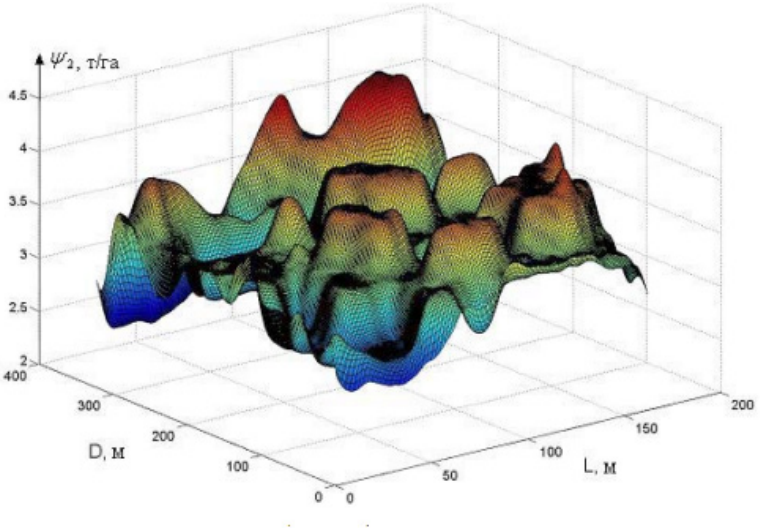

Figure 18. Yield of yield distribution of each section of the field

Taking into account the surface of the yield distribution, a yield map is drawn up (Fig. 19).

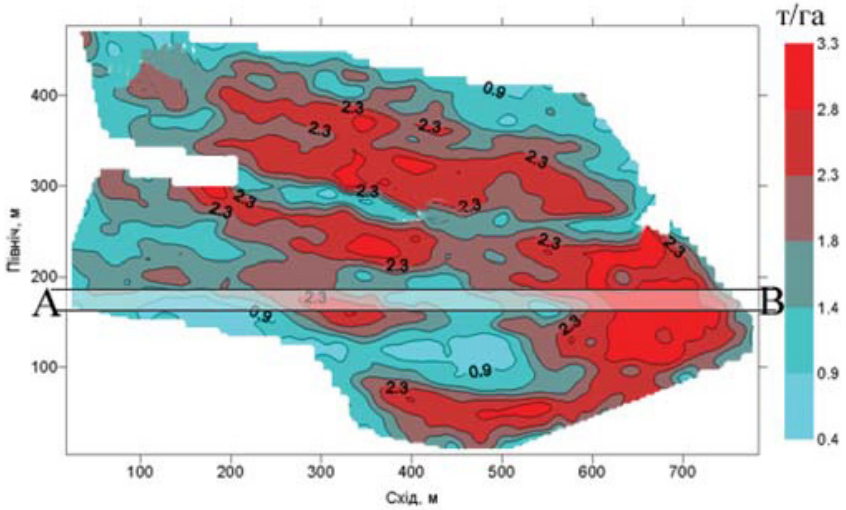

Figure 19. Cartogram of field yields

From (Fig. 19) shows that the yield on one of the passes ACH (illuminated strip AB) in the field area varies from 9 to 33 kg / ha of winter wheat. In such cases it is difficult to provide uniform (in the range of rational operating modes) loading of working systems of ACH.

Significant changes in the intensity of grain heap flow (especially peak loads) negatively affect fuel consumption, quality of harvesting, wear of machine parts and components and reliability of the combine in general, as well as drive systems due to significant power disturbances on the working bodies.

That is, significant fluctuations in crop yields in the direction of movement of the harvesting machine have a negative impact on the work of BZK, if you do not change the kinematic and technological modes of operation. It is possible to level similar phenomena by application of systems of automatic regulation of speed of BC which is defined as follows.

Let the parameters of this field be known: the shape is rectangular, the length D is 325 m, the width L is 162 m.

In accordance with this technique, the direction of the y-axis of the rectangular coordinate system is set and the number of passes k is found for which the selected prototype ACH will process the entire field

$$k = \text{int}\left(\frac{L}{B}\right) = \text{int}\left(\frac{162}{6}\right) = 27, \tag{7}$$

where B – is the width of the reaper BC

On the basis of data on field productivity in the course of BZK movement we will receive a sample of values of productivity in function $\varphi_2(y)$.

Determine the average yield of this field M_h as a mathematical expectation of the function $\varphi_2(y)$

$$M_h = 0{,}35\ kg / m^2. \tag{8}$$

The average speed of BC is determined by the expression

$$V_0 = \frac{Q_h}{BM_h(1+\varepsilon)} = \frac{9}{6 \cdot 0{,}35 \cdot 2{,}5} = 1{,}71\ m / c. \tag{9}$$

where Q_h – BZK productivity.

Based on this, a cartogram of the speed of the BZK in the field is formed (Fig. 20).

Thus, with the help of the developed methodical apparatus the organization of speed control of movement of unmanned combines is provided.

Analysis of previous research has shown that at present there are unresolved issues regarding the construction of decision support systems for the management of harvesting equipment in real time, taking into account the conditions of a dynamic and partially defined external environment. In order to eliminate deviations between the planned and actual performance of technological units, it is necessary to solve the problem of operational management and re-planning of works. The procedure for solving this problem consists of the same points as the procedure for solving the planning problem, differing only in the initial data.

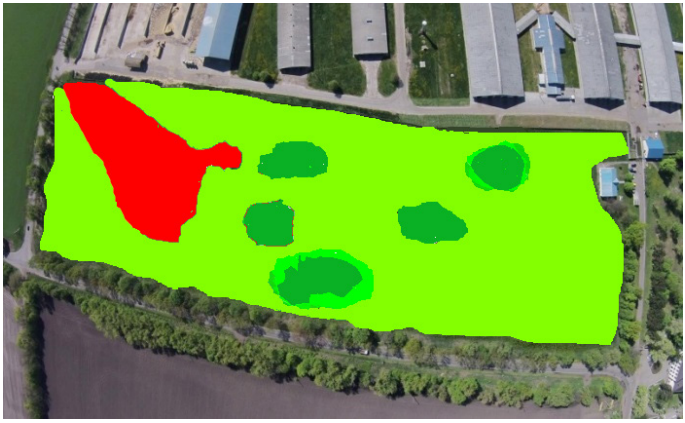

Figure 20. Map of the speed of BZT: – nominal speed; – recommended speed; – 0.4–0.1 nominal speed; – 0.9–0.5 rated speed

The subsystem of operational management of EC assembly processes is built on the basis of a hybrid intelligent support and decision-making system (IS DMS), the main components of which include: knowledge base, simulation unit ACH, monitoring, planning, control and management subsystems, training module and interface. During the development of the knowledge base and ISC system integration of models and algorithms and production rules based on classical methods of modeling and optimization of systems and methods of artificial intelligence, which provides effective solutions to planning, control and operational management of collection and processing of various types of organic raw materials.

A necessary condition for effective management of the harvesting campaign is constant control of the technological process of harvesting EC. Deviation from the work plan in most cases occurs due to a malfunction of technical means or in adverse weather conditions. But there are situations

when the deviation of the "plan-fact" is influenced by other factors, resulting in possible failure of the plan, and vice versa. Failure to implement the plan may be due to reduced work intensity or the user's errors in entering initial data into the system, which reduces the adequacy of the model to the real process. The increase in targets may be due to increased speed of technological operations, which may lead to additional losses of biomass or reduce its quality. Also at the stage of implementation of the intelligent system in the process of assembly work there is a need to complete the system in order to obtain more adequate solutions.

The practical application of ISK has reduced the length of harvesting routes and the total cost of the harvesting campaign by 12–15% due to the rapid determination of energy crops, harvesting planning and implementation of compromise-optimal routes of harvesting equipment. Based on this, the company's profit when applying ISK increased by more than 12%. In addition, as the results of the practical application of ISC show, the time spent on making informed decisions is significantly reduced by the system processing large amounts of information.

Thus, on the basis of the analysis of EC harvesting processes the methodical bases of construction of intelligent control system of unmanned combine harvesters of energy crops for biogas plants are developed, the functional structure of ISK by EC harvesting process for conditions of industrial production of biomethane is substantiated.

Conclusion

1. A method for the synthesis of optimal routes of ACH movement has been developed, using which, on the basis of data obtained from UAVs, the following is provided: the minimum path of BK movement, bypassing stationary obstacles and areas without biomass.

2. The problem of synthesis of the optimal trajectory of ACH in given conditions is solved by the method of dynamic programming with the generalized criterion of optimality according to the nonlinear scheme of compromises taking into account the bypass of sites without biomass, due to which fuel consumption is minimized by more than 12%.

3. Developed models and algorithms are the basis for the organization of the ISC, in a complex dynamic environment characterized by constant uncertainty and variability of many factors.

4. Developed guidelines for optimal planning and control of unmanned aerial vehicles based on the use of UAVs, as well as the structure of algorithms (modules), the use of which provides effective solutions to the planning, control and operational management of ACH.

References:

1. *Защелкин К. В.* Реализация комбинированного способа навигации автономного мобильного робота / К. В. Защелкин, В. В. Калиниченко, Н. О. Ульченка // Электротехнические и компьютерные системы, 2013.– № 9(85).– С. 102–109.
2. *Адамів О. П.* Моделі та інтелектуальні засоби адаптивного керування автономним мобільним роботом [Текст] дис. … канд. техн. наук: захищена 12.12.2007 / Адамів Олег Петрович.– Одеса, 2007.– 124 с.
3. *Fahimi F.* Autonomous Robots. Modeling, Path Planning and Control / F. Fahimi – New York: Springer, 2009.– 348 p.
4. *Hachour O.* Pathplanning of Autonomous Mobile robot / O. Hachour // International Journal of Systems Applications, Engineering and Development.2009.– Issue 4.– P. 178–190.
5. *Lumelsky V.* Sensing, intelligence motion / V. Lumelsky – New Jersey: Wiley-Interscience, 2006.– 456 p.
6. *Song H.* Research on Path Planning for the Mobile Intelligent Robot / H. Song, L. Hu // World Congresson Computer Science and Information Engineering.2009.– No. 1.– P. 121–144.
7. *Siegwart R.* Introduction to Autonomous Mobile Robots / R. Siegwart, I. Ourbakhsh. – Boston: MIT Press, 2004.– 336 p.
8. *Jian Y.* Comparison of Optimal Solutions to Realtime Path Planning for a Mobile Vehicle / Y. Jian, Q. Zhihua, W. Jing, C. Kevin // IEEE Transactions on Systems, Man and Cybernetics. Part A: System and Humans.2010.– Vol. 40.– P. 721–725.
9. *Meyer A. K. P., Ehimen E. A., Holm-Nielsen J. B.* Future European biogas: Animal manure, straw and grass potentials for a sustainable European biogas production. Biomass and Bioenergy. 2017. URL: https://doi.org/10.1016/j.biombioe. 2017.05.013
10. *Schröder P., Beckers B., Daniels S., Gnädinger F., Maestri E., Marmiroli N., Mench M., Millan R., Obermeier M. M., Oustriere N., Persson T., Poschenrieder C., Rineau F., Rutkowska B., Schmid T., Szulc W., Wit-*

ters N., Sæbø A. Intensify production, transform biomass to energy and novel goods and protect soils in Europe – A vision how to mobilize marginal lands Science of the Total Environment. – Vol. 616–617. 2018. – P. 1101–1123.

11. *Laasasenaho K., Lensub A., Rintalac J.* Planning land use for biogas energy crop production: The potential of cutaway peat production lands. Biomass and Bioenergy. – Vol. 85. 2016. – P. 355–362.
12. *Ciccolia R., Sperandei M., Petrazzuolo F., Broglia M., Chiarini L., Correnti A., Farneti A., Pignatelli V., Tabacchioni S.* Anaerobic digestion of the above ground biomass of Jerusalem Artichoke in a pilot plant: Impact of the preservation method on the biogas yield and microbial community. Biomass and Bioenergy. – Vol. 108. 2018. – P. 190–197.
13. *Sahoo K., Mani S., Das L., Bettinger P.* GIS-based assessment of sustainable crop residues for optimal siting of biogas plants Biomass and Bioenergy. – Vol. 110. 2018. – P. 63–74.
14. *Höhn J., Lehtonen E., Rasi S., Rintala J.* A Geographical Information System (GIS) based methodology for determination of potential biomasses and sites for biogas plants in southern Finland. Applied Energy – Vol. 113. 2014. – P. 1–10.
15. *Burg V., Bowman G., Erni M., Lemm R., Thees O.* Analyzing the potential of domestic biomass resources for the energy transition in Switzerland. Biomass and Bioenergy, – Vol. 111. 2018. – P. 60–69.
16. *Gunchenko Y.A.* Using UAV for unmanned agricultural harvesting equipment route planning and harvest volume measuring // Gunchenko Y.A., Shvorov S.A., Zagrebnyuk V.I., Kumysh V.U., Lenkov E.S. // 2018// 2017 IEEE4th International Conference on Actual Problems of Unmanned Aerial Vehicles Developments, APUAVD2017 – Proceedings URL: https://www.scopus.com/authid/detail.uri?authorId=57193057973
17. *Mezhuyev Vitaliy, Gunchenko Yurii, Shvorov Sergey, Chyrchenko Dmitry*. A Method for Planning the Routes of Harvesting Equipment using Unmanned Aerial Vehicles. 2020. Intelligent Automation And Soft Computing, 2020 Copyright © 2020, TSI® Press – Vol. 26. – No. 1. – P. 119–130. URL: https://doi.org/10.31209/2019.100000133

Yurii Gunchenko, Doc.Tech.Science, prof., Head of the Computer science and technologies department, Odesa National University, 2 Dvoryanska str., Odesa Ukraine

E-mail: gunchenko@onu.edu.ua.
ORCID: http://orcid.org/0000-0003-4423-8267

Sergey Shvorov, Martynenko Department of Automation and Robotic Systems, National University of Life and Environmental Sciences of Ukraine, Kyiv, Ukraine
E-mail: sosdok@nubip.edu.ua.
ORCID: https://orcid.org/0000-0003-3358-1297

Taras Davidenko, Martynenko Department of Automation and Robotic Systems, National University of Life and Environmental Sciences of Ukraine, Kyiv, Ukraine
E-mail: davidenkotaras009@gmail.com.
ORCID: https://orcid.org/0000-0003-0277-6892

Anna Yukhimenko, Martynenko Department of Automation and Robotic Systems. National University of Life and Environmental Sciences of Ukraine, Kyiv, Ukraine
E-mail: 12345777anna123456@gmail.com.
ORCID: https://orcid.org/0000-0003-0638-3420

Dmytro Slutskyi, post-graduate student of the Technical Cybernetics and Information Technologies Department, Odesa National Maritime University. Mechnikova str, 34 Odessa, Ukraine
ORCID: https://orcid.org/0000-0003-3734-9460

Larysa Martynovych, post-graduate student of the Computer science and technologies department, Odesa National University, 2 Dvoryanska str., Odesa, Ukraine
E-mail: larysa.yaroslavna@gmail.com
ORCID: https://orcid.org/0000-0001-7351-1467

MATHEMATICAL MODEL OF POLYMER MELTING FLOW IN CHANNELS OF COEXTRUSION EQUIPMENT

Tetiana Tereshchenko, Valentina Kozlovskaya,
Iryna Buchynska, Nataliia Shtefan

Abstract. The article presents a mathematical model of the polymer melt flow. Model of the process of forming a multi-layer structure by the method of coextrusion. The developed mathematical model allows to calculate the process parameters at each section of the coextrusion dies. The calculated parameters of technological and design parameters for each layer of the multi-layer structure were obtained.

Keywords: mathematical model, coextrusion dies, polymer, melt flow.

Introduction and statement of the problem

The main task of creating a model for the operation of a coextrusion dies is to develop a consistent and connected in all parameters mathematical representation of the operation of the dies and to calculate the main technological and design parameters.

Main part

The main characteristics of the coextrusion dies for processing secondary polymer materials into multi-layer products: pressure distribution at the exit from each channel of the dies, the uniformity of which determines the thickness variation of each layer and the quality of the finished product as a whole; specific consumption of polymer melt through a predetermined section at the outlet of the distribution channel; difference in thickness of the formed polymer layer [1, 2, 3, 4].

We simplify the connection diagram through stages. At the first stage, we determine the resistance of each section of the conical part of the distribution channel. At the second one, we determine the resistance at each section of the pipe, considering the fact that the material flow is split into two ones: one flow continues to move through the pipe, the second flow moves in the conical part of the channel.

We determine the resistance in the sections of the conical part of the distribution channel. In a channel with a flat section, sections of characteristic geometry are connected in series. Therefore, the equivalent resistance of the conical part takes the following form:
for $i = 1$ section

$$R_e^1 = \sqrt[n]{(R_1^1)^n + (R_2^1)^n + ... + (R_j^1)^n + ... + (R_i^1)^n} \tag{1}$$

for i-th section

$$R_e^1 = \sqrt[n]{(R_1^i)^n + (R_2^i)^n + ... + (R_j^i)^n + ... + (R_i^i)^n} \tag{2}$$

for $i = k$ section

$$R_e^k = \sqrt[n]{(R_1^k)^n + (R_2^k)^n + ... + (R_j^k)^n + ... + (R_i^k)^n} \tag{3}$$

The general connection diagram of the resistances, considering the obtained dependences, is simplified. We calculate the resistance at each section of the pipe. We simplify the design scheme sequentially, starting from the point of confluence of material flows in the pipe. In this case, the resistance is defined as equivalent for the three sections. Two sections are connected in series, and the third one in parallel with these two sections.

Considering the calculation formulas for the serial and parallel connection of the sections, the expressions for calculating the resistance for the i-th pipe section take the following form:
for $i = k - 1$ section

$$R_{ek-1} = \frac{R_e^{k-2} \cdot \sqrt[n]{(R_{k-1})^n + (R_{ek})^n}}{R_e^{k-2} \cdot \sqrt[n]{(R_{k-1})^n + (R_{ek})^n}} = \\ = \frac{R_e^{k-2} \cdot \sqrt[n]{(R_{k-1})^n + \left(\frac{R_e^{k-1} \cdot \sqrt[n]{(R_k)^n + (R_e^k)^n}}{R_e^{k-1} + \sqrt[n]{(R_k)^n + (R_e^k)^n}} \right)}}{R_e^{k-2} + \sqrt[n]{(R_{k-1})^n + \left(\frac{R_e^{k-1} \cdot \sqrt[n]{(R_k)^n + (R_e^k)^n}}{R_e^{k-1} + \sqrt[n]{(R_k)^n + (R_e^k)^n}} \right)}}. \tag{4}$$

for i-th section

$$R_{ei} = \frac{R_e^{i-1} \cdot \sqrt[n]{(R_i)^n + (R_{ei+1})^n}}{R_e^{i-1} \cdot \sqrt[n]{(R_i)^n + (R_{ei+1})^n}} = \tag{5}$$

$$= \frac{R_e^{i-1} \cdot \sqrt[n]{(R_i)^n + \left(\frac{R_e^i \cdot \sqrt[n]{(R_{i+1})^n + (R_{ei+1})^n}}{R_e^i + \sqrt[n]{(R_{i+1})^n + (R_{ei+1})^n}} \right)}}{R_e^{i-1} + \sqrt[n]{(R_i)^n + \left(\frac{R_e^i \cdot \sqrt[n]{(R_{i+1})^n + (R_{ei+1})^n}}{R_e^i + \sqrt[n]{(R_{i+1})^n + (R_{ei+1})^n}} \right)}}.$$

Sequentially transforming and simplifying the connection diagram of the resistances of the distributor sections, we derive an expression for calculating the equivalent channel resistance. The resulting expression allows you to determine the total back pressure ΔP_Σ in the channel as follows:

$$\Delta P_\Sigma = 2 \cdot \mu \cdot \left(R_{e1} \cdot Q_{\frac{1}{2}} \right)^n \tag{6}$$

Substituting the obtained dependences into expression (6), we have the following final formula for calculating the pressure in the distribution channel:

$$\Delta P_\Sigma = 2 \cdot (\alpha_0 + \alpha_1 \cdot \gamma + \alpha_2 \cdot T) \cdot e^{-b(T-T_0)} \cdot \gamma^{(b_0 + b_1 \cdot \gamma + b_2 \cdot T)} \times$$
$$\times \left(\sqrt[n]{(R_1)^n + \left(\frac{R_e^1 \cdot \sqrt[n]{(R_2)^n + \left(\frac{R_e^2 \cdot \sqrt[n]{(R_3)^n + (R_{e4})^n}}{R_e^2 + \sqrt[n]{(R_3)^n + (R_{e4})^n}} \right)}}{R_e^1 + \sqrt[n]{(R_2)^n + \left(\frac{R_e^2 \cdot \sqrt[n]{(R_3)^n + (R_{e4})^n}}{R_e^2 + \sqrt[n]{(R_3)^n + (R_{e4})^n}} \right)}} \right) \cdot Q_{\frac{1}{2}}} \right)^n \tag{7}$$

Further, having expressions for calculating the resistance of each section of the channel, the total consumption of material and the total pressure in the channel, we determine the distribution of material flows over the sections of the channel. Let's consider the distribution point of the total flow of the polymer melt onto the flow in the pipe and the flow in the conical part of the channel. Equivalent resistance of the distribution channel at this point is R_e^1. Material consumption through resistance R_1 is equal to $Q_1 = Q_1/2$, pressure in section is P_1. The material consumption equation is the following:

$$Q_1 = Q_2 + Q_e^1 \Rightarrow Q_2 = Q_1 - Q_e^1 \tag{8}$$

The pressure at the considered point for the conical section is as follows:

$$P_e^1 = (P_e^1 \cdot Q_e^1)^n \cdot \mu \tag{9}$$

The pressure at the considered point for the pipe is as follows:

$$P_{e3} + P_2 = \left(\sqrt[n]{(R_2)^n + (R_{e3})^n} \cdot Q_2 \right)^n \cdot \mu \tag{10}$$

Considering that, after mathematical transformations, we obtain following expressions for calculating the flows of the polymer melt at the exit from the considered point:

$$Q_e^1 = Q_1 \cdot \frac{\sqrt[n]{(R_2)^n + (R_{e3})^n}}{R_e^1 + \sqrt[n]{(R_2)^n + (R_{e3})^n}} \tag{11}$$

$$Q_e^1 = Q_1 \cdot \frac{R_e^1}{R_e^1 + \sqrt[n]{(R_2)^n + (R_{e3})^n}} \tag{12}$$

Substituting expression (11) into expression (9) and expression (12) into expression (10), we calculate the pressure drop in each section under consideration:

$$P_e^1 = \left(Q_1 \cdot \frac{R_e^1 \cdot \sqrt[n]{(R_2)^n + (R_{e3})^n}}{R_e^1 + \sqrt[n]{(R_2)^n + (R_{e3})^n}} \right)^n \cdot \mu \tag{13}$$

$$P_2 = \left(Q_1 \cdot \frac{R_2 \cdot R_e^1}{R_e^1 + \sqrt[n]{(R_2)^n + (R_{e3})^n}} \right)^n \cdot \mu \tag{14}$$

We pass to the next point of distribution of polymer melt flows. Similarly, we determine the melt flows and pressure at each section of the channel.

For the i-th point of distribution of the polymer melt in the channel, we calculate the flow rate through the sections under consideration and the pressure drop in the sections:
for pipe section:

$$Q_i = Q_{i-1} \cdot \frac{R_e^{i-1}}{R_e^{i-1} + \sqrt[n]{(R_i)^n + (R_{ei+1})^n}}, \tag{15}$$

$$P_i = \left(Q_{i-1} \cdot \frac{R_i \cdot R_e^{i-1}}{R_e^{i-1} + \sqrt[n]{(R_i)^n + (R_{ei+1})^n}} \right)^n \cdot \mu, \tag{16}$$

for conical section:

$$Q_e^i = Q_i \cdot \frac{\sqrt[n]{(R_{i+1})^n + (R_{ei+2})^n}}{R_e^i + \sqrt[n]{(R_{i+1})^n + (R_{ei+2})^n}}, \tag{17}$$

$$P_e^i = \left(Q_i \cdot \frac{P_e^i \cdot \sqrt[n]{(R_{i+1})^n + (R_{ei+2})^n}}{P_e^i + \sqrt[n]{(R_{i+1})^n + (R_{ei+2})^n}} \right)^n \cdot \mu, \tag{18}$$

For the last of the considered points of distribution of the polymer melt in the channel, we determine the flow rate through the sections under consideration and the pressure drop in the sections:
for pipe section:

$$Q_k = Q_{k-1} \cdot \frac{R_e^{k-1}}{R_e^{k-1} + \sqrt[n]{(R_k)^n + (R_e^k)^n}}, \tag{19}$$

$$P_k = \left(Q_{k-1} \cdot \frac{R_k \cdot R_e^{k-1}}{R_e^{k-1} + \sqrt[n]{(R_k)^n + (R_e^k)^n}} \right)^n \cdot \mu, \tag{20}$$

for conical section:

$$Q_e^k = Q_k, \tag{21}$$

$$P_e^k = (Q_k \cdot P_e^k)^n \cdot \mu. \tag{22}$$

The essence of mathematical modeling of the coextrusion dies operation in the process of creating a multi-layer polymer structure consists in sequential passage in the algorithm along each of the four distribution channels (from the point of injection of the polymer melt into the pipe to the exit from the conical channel) [7, 8, 9]. At the same time, the main characteristics of the process of forming layers are calculated with the accumulation of the result, and the pressure value and thickness difference of each formed layer are estimated [10, 11, 12].

The Euler method was used as a method for implementing the mathematical model of the coextrusion dies in the process of creating a multilayer structure. The coordinates of the modeled section of the distribution channel of the coextrusion dies are counted through fixed, set intervals of the channel length and height (Fig. 1). Each of the sections under consideration is a section of simple geometry: a section of a pipe and spiral grooves is a pipe channel, a section of a conical part is a slotted channel. The nature of the flow of the polymer melt in the areas under consideration is assumed to be the same as in the areas of simple geometry. Calculated events in the model are considered to have occurred at the end of this interval [13, 14, 15].

As a result of modeling the process of creating a multilayer polymer structure, the values of pressure and shear rate were obtained in sections of the pipe and the conical part of the distribution channel.

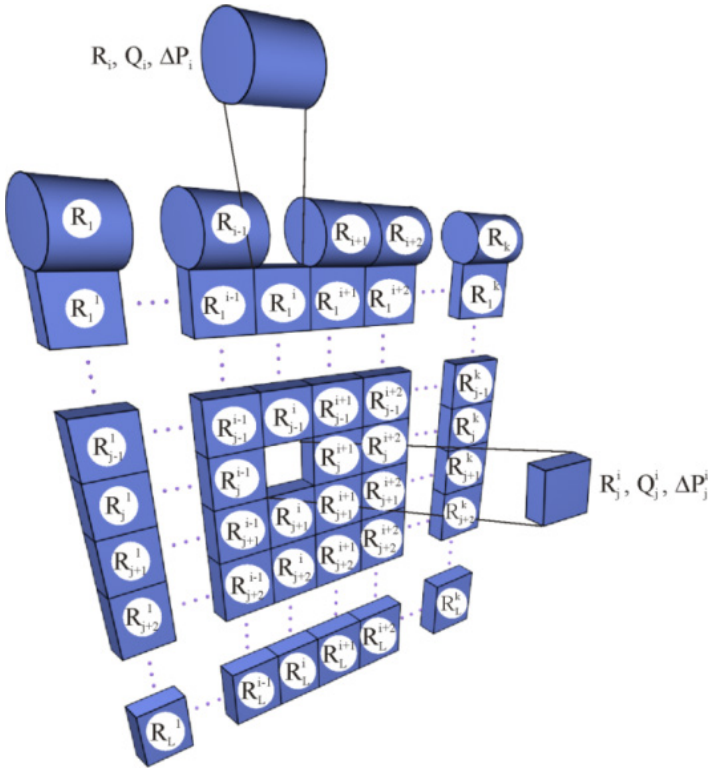

Figure 1. Drawing demonstrating the division of the distribution channel into sections

The chart of the distribution of shear rates along the length of the pipe for each distribution channel of the coextrusion dies is shown in (Fig. 2).

The pipe shear rate plots correspond to the pipe pressure plots. A decrease in the shear rate in the channels of the primary polymer in the 160–180˚ section leads to a decrease in the melt flow rate. This leads to an increase in the residence time of the melt in the channel and the formation of stagnant zones. But since the period of time of the onset of destruction of the primary polymer is several times longer than the period of time of destruction of the secondary, this character of the shear rate curve does not affect the stability of the process. In the channels of the recycled polymer material, this problem is solved due to the presence of spiral grooves.

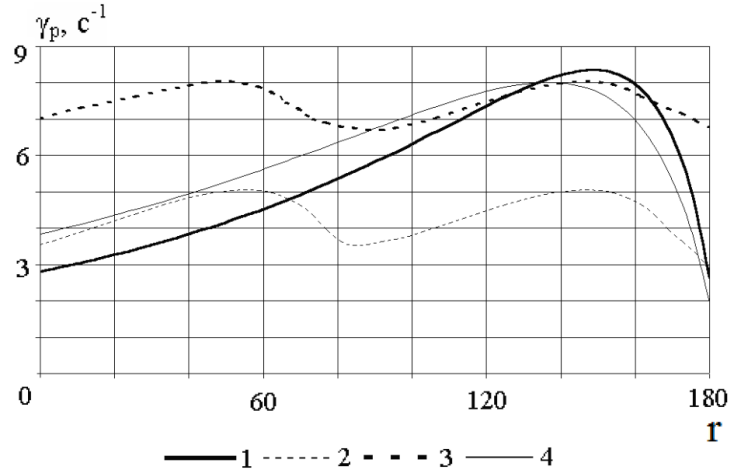

Figure 2. Chart of the distribution of shear rates in a pipe: (1-outer layer, 2-first middle layer (industrial recycled polymers), 3-second middle layer (household recycled polymers), 4-inner layer)

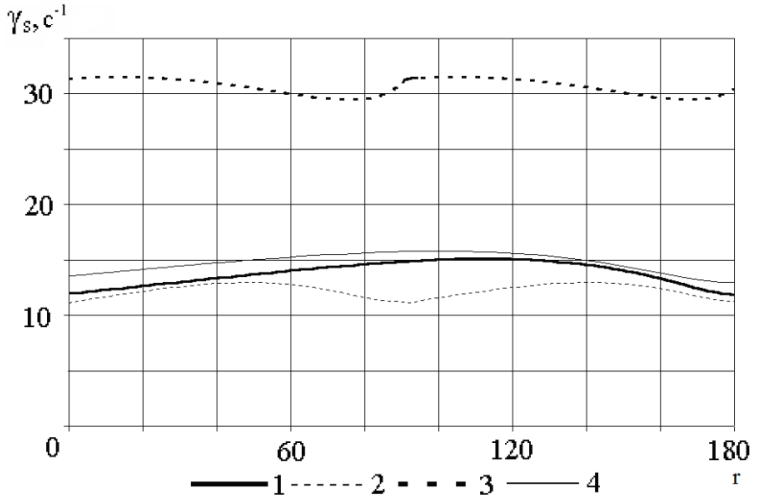

Figure 3. Chart of the distribution of shear rates in a conical section: (1-outer layer, 2-first middle layer (industrial recycled polymers), 3-second middle layer (household recycled polymers), 4-inner layer)

The chart of the distribution of shear rates in the conical part of the channel for each distribution channel of the coextrusion dies is shown in (Fig. 3).

The chart shows that the shear rate along the channels of the proposed coextrusion dies is in the range of 11.0–32.0 s^{-1}. Low shear deformations indicate that the processing of polymeric materials is carried out at a stable viscosity of the melt of the polymeric material (both primary and secondary). This is due to the fact that the viscosity of the polymer at low shear rates depends little on the level of shear deformations (the initial portion of the rheological characteristic is straight-line).

The pressure and shear rate obtained as a result of modeling make it possible to calculate the value of the maximum linear velocity of the melt flow in the channel sections and to plot the linear velocity diagrams. The shape of the plots of the maximum linear melt flow rate corresponds to the shape of the plots of shear rates in the conical part of the channel. As a result of modeling, it can be concluded that the presence of spiral grooves gives a deviation in the flow rates of 18–21%, while the primary polymer channel forms a layer with a deviation of the melt flow rates of 22–27%.

The obtained results of modeling the process of creating a multi-layer structure make it possible to calculate the total pressure created by each distribution channel and the difference in thickness of each of the formed layers of the structure. The calculation is carried out for the range of total productivity ΣQ = 20 – 40kg/h (Table 1).

Table 1. – Data summary on the pressure and thickness in die channels

Layer number	**Thickness, ΔQ,%**	**Pressure P, MPa**		**ΔP, MPa**
		ΣQ = 20kg/h	**ΣQ = 40kg/h**	
1	27	5,337	8,089	2,752
2	21	4,299	5,792	1,493
3	18	6,113	7,578	1,465
4	22	4,531	6,868	2,337

The increase in pressure ΔP with a change in the total productivity ΣQ is nonlinear for different dies channels. To determine the operating range of the productivity of this coextrusion dies, the dependence of the pressure in the distribution channels on the total productivity was obtained by the simulation method.

The pressure working range in the distribution channel is $P = 3.0–10.0$ MPa. The results of modeling the process of creating a multi-layer structure show that with such a pressure range in the channel, the total productivity of the dies is $\sum Q = 10 – 58$ kg/h. This range allows you to process a wide range of finished products.

The thickness of the formed layer and the pressure in the distribution channel depend on the geometric parameters of the channel. The gap h has the greatest influence. The chart of the influence of the geometry of the gap on the thickness difference and pressure for each layer, obtained by mathematical modeling, is shown in (Fig. 4).

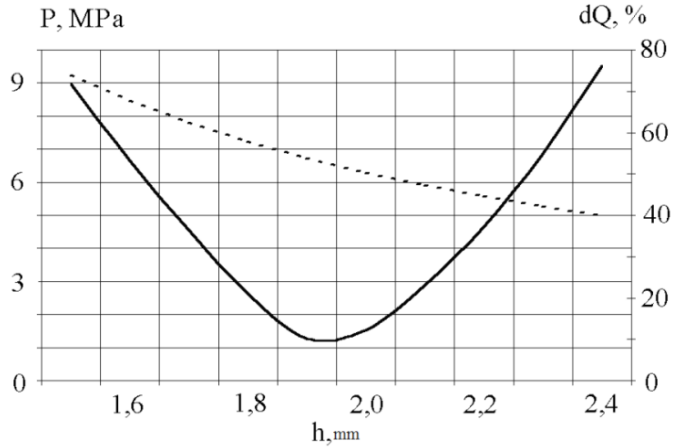

Figure 4. Pressure P (- - - -) and thickness dQ (——) of the outer layer on the gap

Similar dependences were obtained for the inner layer of the primary polymer and two middle layers of the secondary polymer. Analyzing the data obtained as a result of modeling, it can be concluded that the pressure in the distribution channel increases inversely with a decrease in the shaping gap. The difference in thickness of the layer has the optimal value of the forming gap.

Analysis of the results obtained allows us to determine the minimum and maximum value of the forming gap, which provides the required thickness variation of the layer and pressure in the distribution channel. The quality of the finished product is ensured under the condition that the thickness difference of the layer does not exceed 40%. Table 2 shows the values of the forming gap and pressure for each distribution channel.

Table 2. – Data summary on the pressure in die channels

Layer number	h, mm		Pressure P, MPa	
	min	max	max	min
1	0,95	1,17	7,093	5,126
2	1,45	1,75	5,489	4,232
3	1,67	2,21	8,054	5,675
4	1,16	1,57	6,882	3,951

Conclusion

1. For the purpose of rational design of the coextrusion dies, a method has been developed for calculating the pressure and productivity in the sections of the distribution channels, considering the mutual influence of polymer melt flows by applying the principle of electrophysical analogies.

2. Based on the results of mathematical modeling, the values of pressure, shear rates and linear velocities of melt flows in the sections of the distribution channels of the coextrusion dies were obtained for analyzing the shaping capabilities of the channels and determining the thickness difference of each layer.

3. The range of the total productivity of the coextrusion head and the temperature ranges of melts of polymer materials for each layer of the multilayer structure, considering the pressure, were determined by the method of mathematical modeling. The influence of the size of the forming gap on the values of pressure and thickness difference in the distribution channels was evaluated in order to rationalize the design of the coextrusion dies. The analysis of the results obtained made it possible to determine the minimum and maximum values of the forming gap, which provides a thickness in layers of no more than 40% in the operating pressure range.

References:

1. Rauwendaal C. Polymer extrusion. Munich, Germany: Hauser Cnarduer, 2001.
2. Раувендаль К., Экструзия полимеров. – Санкт-Петербург., Россия: Профессия, 2008.
3. Дядичев В. В. Переработка отходов полимерных материалов методом соэкструзии. – Луганск, Украина: Изд-во ВНУ им. В. Даля, 2003.

4. Дядичев В. В., Переработка отходов полимерных материалов методом соэкструзии. Луганск, Украина: Изд-во ВНУ им. В. Даля, 2003.
5. Тагер А. А. Физико-химия полимеров. – Москва, Россия: Научный мир, 2007.
6. Janeschitz-Kregl H. Polymer Melt Rheology and Flow Birefrringence. – Berlin, Germany: Springer, 1993.
7. Дядичев В. В. "Соэкструзионная переработка вторичных поименых материалов (теория, технология, оборудование)", дис. докт. наук, ВНУ им.В.Даля, – Луганск, 2003.
8. Дядичев В. В., Терещенко Т. М., Муххамед А. Ф. Аль-Фаури. "Математическая модель течения вторичного полимерного материала в формующем канале соэкструзионной головки", на Международной научно-методической конференции "Проблемы математического моделирования", – Днепропетровск, 2005. – С. 57–58.
9. Терещенко Т. М. "Разработка формующего оборудования для переработки вторичных полимерных материалов методом соэкструзии", Вестник ВНУ им. В. Даля, – № 10(92). 2005. – С. 211–215.
10. Michaeli W. Extrusion dies for plastics and rubber: design and engineering computations. – Munich, Germany: Hanser Publishers, 1992.
11. Steller R. T. "Theoretical Model for Flow of Polymer Melts in the Screw Channel", Polym. Eng. Sci., – Vol. 30. – No. 7. 2009. – P. 400–407.
12. Дядичев В. В., Терещенко Т. М. "Обработка давлением вторичных полимерных материалов с использованием специального оборудования", на Международной научно-практической конференции "Научные исследования – теория и эксперимент 2005", Полтава, 2005. – С. 20–23.
13. Леваничев В. В., Терещенко Т. М., Гапонов А. В. "Математическая модель процесса течения полимера в кольцевых распределительных каналах экструзионных головок", Ресурсозберігаючі технології виробництва та обробки тиском матеріалів у машинобудуванні, 2009. – С. 229–238.
14. Дядичев В. В., Леваничев В. В., Терещенко Т. М. "Методика описания реологии расплава полимера в широком диапазоне скоростей сдвига", Ресурсосберігаючі технології виробництва та обробки матеріалів у машинобудуванні, 2003. – С. 68–72.
15. Кузніченко С. Д., Терещенко Т. М., Коваленко Л. Б. "Використання математичного моделювання в процесах переробки вторинних

полімерів", Вісник КрНУ імені Михайла Остроградського, № 5(100). 2016. – С. 87–91.
16. Леваничев В. "Модель течения расплава полимера", Восточно-Европейский журнал передовых технологий, – Т. 4. – № 7(64). 2013. – С. 39–41.
17. Леваничев В. "Анализ полной реологической модели течения расплава полимера", Восточно-европейский журнал передовых технологий, – Т. 2. – № 6(74). 2015. – С. 11–16.
18. Levanichev V. "Study of multi-layer flow in coextrusion processes", TEKA Commission of motorization and power industry in agriculture, – Vol. 14. – Issue 1. 2014. – P. 144–153.

Tetiana Tereshchenko, PhD, Associate Professor, Dept. of Information Technologies, Odessa State Environmental University, 15 Lvivska Str, Odesa Ukraine
E-mail: tereshchenko.odessa@gmail.com
ORCID: https://orcid.org/0000-0001-7691-6996

Valentina Kozlovskaya, PhD, Associate Professor, Dept. of Information Technologies, Odessa State Environmental University, 15 Lvivska Str, Odesa Ukraine
E-mail: vkozlovskaya20@gmail.com,
ORCID: https://orcid.org/0000-0003-0353-5281

Iryna Buchynska, Assistent, Dept. of Information Technologies, Odessa State Environmental University, 15 Lvivska Str, Odessa Ukraine
E-mail: buchinskayaira@gmail.com
ORCID: https://orcid.org/0000-0002-0393-2781

Nataliia Shtefan, assistant, Dept. of Information Technologies, Odessa State Environmental University, 15 Lvivska Str, Odesa Ukraine
E-mail: amalon.7@gmail.com
ORCID: https://orcid.org/0000-0001-6301-6534

MATHEMATICAL MODEL OF THE PHASE DYNAMICS OF INTRAVENTRICULAR PRESSURE TAKING INTO ACCOUNT THE MAIN FACTORS OF THE MYOCARDIAL CONTRACTIVE FUNCTION

Olena Kirik, Alla Yakovleva, Irina Shubenkova

Abstract. An approach to mathematical modeling of the pumping function of the heart myocardium is proposed. Analysis of the model confirms the possibility of displaying with its help the fundamental physiological properties of the heart, which provide blood circulation in the human body. The model is a theoretical basis for optimizing the processes of correction of the patient's functional state; therefore, it can be useful for specialists in the field of theoretical and practical cardiology.

Keywords: mathematical modeling of cardiac activity; nonlinear dynamic system; intraventricular pressure; myocardial pumping function; systemic blood flow.

Introduction and statement of the problem

Due to the high prevalence and high mortality, coronary heart disease occupies an important place in clinical medicine. One of the main consequences of this disease is the suppression of the pumping function of the heart, followed by a violation of the systemic circulation.

Specialists in the field of theoretical and practical cardiology have always studied the contractile activity of the myocardium and its pumping function, and this problem occupies a leading place in modern research. But mathematical modeling and methods of systems analysis are becoming increasingly important in this area [1–7]. However, despite the large number of works devoted to this topic, interest in models that combine the achievements of theory with practice remains high.

The purpose of this work is to investigate the extent to which the mathematical model allows to reproduce the basic integral characteristics of the heart to assess the functional state according to the measurements of intraventricular pressure and its assessment by non-invasive method.

Known models reflect two approaches to the study of heart function: the representation of the heart as a pump or muscle [8, 9].

It is the dynamic processes that determine the formation of intraventricular pressure throughout the cardiac cycle, most fully reflect the functional characteristics of the heart, and their mathematical representation, have sufficiently informative parameters that are suitable for assessing the degree of cardiac dysfunction in the clinic.

The proposed approach is based on the representation of cardiac function as a nonlinear dynamic system that formalizes the activity of the ventricles of the heart according to the phase structure of the cardiac cycle.

Description of the mathematical model and its biophysical interpretation

Consider second-order differential equations:

$$\ddot{p} + \alpha_i (p - p_c - p_{0i})^2 \dot{p} - b_i \dot{p} + c_i (p - p_c) = 0 \tag{1}$$

where – $p : [0, \infty] \to R$; $\alpha_i, b_i, c_i, p_{0i}, p_c$ certain constants; $i = 1,2$

After replacing the variables we obtain the Lennar equation, which describes the dynamics of systems with one degree of freedom in the presence of linear reducing force and nonlinear attenuation:

$$\ddot{x} + \alpha_i (x - p_{0i})^2 \dot{x} - b_i \dot{x} + c_i x = 0, \quad i = 1,2 \tag{2}$$

One of the partial cases of such equations is the van der Paul equation, which generates relaxation oscillations [10]. A characteristic feature of such equations is the existence of a stable limit cycle on which trajectories emerge from any initial conditions. Subsequently, the value of is interpreted as blood pressure in the left ventricle.

The differential equation describing the change in was chosen for the following reasons: first, it is one of the simplest equations of dynamics, the solution of which is characterized by alternating fast and slow motion, and secondly, it is an equation of the 2nd order that allows further on the basis of Newton's second law to give a physical interpretation of the constants of this equation.

We present each of equations (2) as a system of two first-order equations:

$$\begin{aligned} &\dot{x} + \frac{\alpha_i}{3} (x - p_{0i})^3 - b_i x - c_i y = 0, \\ &\dot{y} = -x, \quad i = 1,2. \end{aligned} \tag{3}$$

The equation of isocline $\dot{x} = 0$ for system (3) will look like

$$y = \frac{1}{c_i}\left[\frac{\alpha_i}{3}(x - p_{0i})^3 - b_i x\right], \quad i = 1,2. \tag{4}$$

The motion of the phase point $(x(t), y(t)$ according to system (3) at $i = 1$ or $i = 2$ is described in [10]. Consider a motion that differs from (4) in that from will pass according to system (3) first *at* = 1, then at $i = 2$ and then again at $i = 1$. In this case, at certain points in time there will be switching on the variable y. The phase portrait for this movement is shown in (Fig. 1). Isoclines are represented by solid lines for $i = 1$ and $i = 2$.

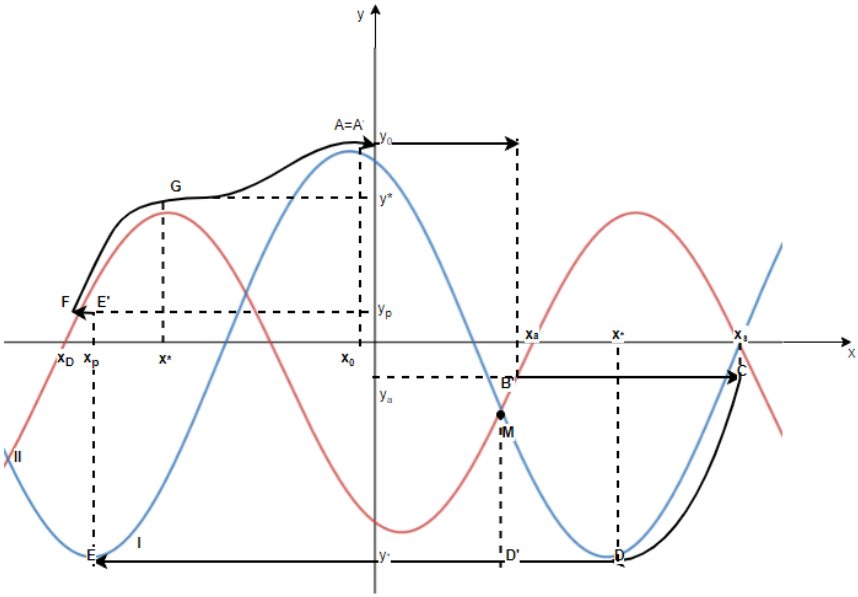

Figure 1. Phase portrait of the phase point cyclic motion

From point *A* to point *D* (Fig. 1) the phase point moves according to system (3) at $i = 1$. In this case, from point *A* to point *C* – the phase of rapid motion. At point *B* there is a pulse switch to point *B*', the growth rate slows down. At the point *C* *x* acquires the maximum value. Then begins a period of slow decrease *x*, and from point *D* to point *D′*– a rapid decrease. At the point *D′* there is a transition to the system (1) at $i = 2$, which moves to the point *G*.

At first, the movement remains fast. After the pulse correction at point *E* to point *E′* there will be a deceleration of the rate of descent *x*. At the point *F* *x*

becomes minimal, and a slow increase in x begins. At the point F x becomes minimal, and a slow increase in x begins. At the point G there is a transition to the system (3) at $i = 1$, which generates a small area of fast and again slow growth x. The phase point again turns into $A' = A$. The cycle is over.

The trajectory $x(t)$ during motion, which is described above, is shown in (Fig. 2).

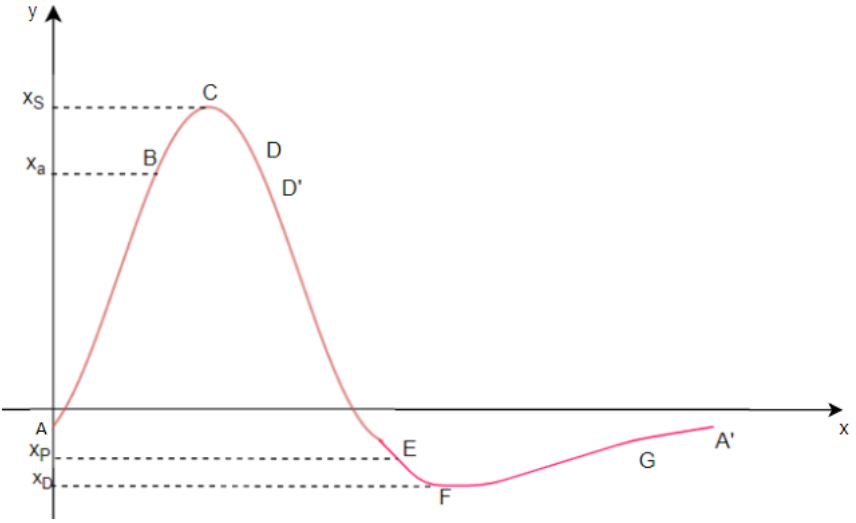

Figure 2. Curve of intraventricular pressure change

The alternation of areas of fast and slow growth indicates an analogy of the qualitative behavior of the trajectory of the system (3) and the curve of change in intraventricular pressure, which is characteristic of the left ventricle of the human heart.

In (Fig. 2) the phase of systole corresponds to the movement of the phase point $(x(t), y(t))$ according to system (3) at $i = 1$, diastole – at $i = 2$.

Systole begins at point A and ends at point D. The movement of the phase point from A to B corresponds to the phase of the isometric voltage. During the isometric contraction that occurs when the valves are closed, the intracardiac pressure increases rapidly (Fig. 2). When it reaches a pressure slightly higher than in the aorta p_D, the aortic valve opens. At this point, the release of blood from the heart begins. During the opening of the valve, the rate of growth of intraventricular pressure slows down. At point D, the pressure reaches its maximum value $x_s + p_c$. At the point corresponding to point D, ventricular systole ends and an intermediate

interfacial state begins, which corresponds to the closing time of the aortic valve. This interval corresponds to the segment *DD*' in (Fig. 1). We assume that the point *D'* has a coordinate on the abscissa axis equal to the abscissa of the point *M* – the point of intersection of isoclines I and II. At the moment corresponding to the point *D*', the motion will occur according to system (3) at $i = 2$.

The *D*'*E* section corresponds to the isometric relaxation phase. At point *E*, the pressure in the left ventricle becomes slightly lower than the pressure in the atrium, the mitral valve opens. At this point, a new pulse correction occurs from point *E* to point *E'*. This correction slows down the rate of intraventricular pressure.

The filling period corresponds to the movement in sections *E'F* and *FG*, point *F* – the minimum value of pressure $x_D + p_c$, section *GA*' – atrial systole, the movement already occurs according to system (3) at $i = 1$. At point *A* the cardiac cycle ends.

Qualitative features of the phase portrait of the system (3) can be taken as the basis for a mathematical description of the heartbeat.

Consider the physiological interpretation of equation (2).

The diameter of the ventricle $l(t)$ at time t will be called the diameter of a sphere of minimum size, containing a volume equal to the ventricle. The value of $l(t)$ varies according to the following law [11]:

$$\ddot{l} = k_1(H - H_0),$$

where $H(t)$ is the voltage at time t, k_1, H_0 are constants.

According to Laplace's law

$$p - p_c = \frac{H - H_0}{l_c},$$

where l_c is the average value of $l(t)$ during the cardiac cycle T. There is a dependence $\ddot{l} = -kx$, $k = k_1 * l_c$, because pressure and voltage as forces are directed in different directions. Formula (4) allows us to interpret law (2). Differentiating the equation twice

$$\dddot{l} + \int_0^t (-k)\frac{\alpha_i}{3}(x - p_{0i})^3 dr - b_i\dot{l} + c_i(l + l_c) = 0, \quad i = 1,2 \tag{5}$$

and substituting $\ddot{l}$ by formula (3), we obtain equation (2).

Note that

$$\frac{\alpha_i}{3}\int_0^t (-k)(x - p_{0i})^3 dr \approx -k\int_0^t \alpha_i p_{0i}^2 x dr = \alpha_i p_{0i}^2 \dot{l}, \tag{6}$$

Consider the interpretation of the coefficients of equation (2) a_i, b_i, c_i, p_{0i} taking into account (4) and (5). Multiply equation (5) by m, where m is the mass of the shock volume of blood. This will allow us to interpret the terms of equation (5) as forces under the influence of which there is a contraction and relaxation of the heart. We have

$$m\ddot{l} + \int_0^t (-k)\frac{1}{3}ma_i(x - p_{0i})^3 dr - mb_i\dot{l} + mc_i(l - l_c) = 0 \qquad (7)$$

From formula (6) it follows that the second term of equation (7) describes the force of viscous friction, which during systole prevents the penetration of blood into the aorta. This force is the result of two factors. One of them is related to the aortic pressure (back pressure) and is characterized by the coefficient p_{01}, and the other, which corresponds to the coefficient a_1, prevents stretching of the aorta. During diastole, the first factor, characterized by the coefficient p_{02}, is associated with the venous pressure that fills the ventricle, and the second, which corresponds to the coefficient a_2, prevents the stretching of the heart muscle. Note that $p_{01} > 0$, $p_{02} < 0$, $a_i < 0$, $i = 1,2$.

Let us analyze the force described by the third term $mb_i\dot{l}$ of equation (7). With constant motion, when the system oscillates, its energy must remain unchanged. In this case, part of the energy is dissipated by friction, so the system must continuously replenish energy from a source of external force to maintain undamped oscillations. Such a force must be proportional to i [12]. The role of the coefficient of proportionality is played by the constant $b_i > 0$, $i = 1,2$. Thus, the third term of the equation is a force that increases the contractile activity of the myocardium and ensures the rhythm of its work. This force is formed by a whole block of controlling factors.

The fourth term $mc_i(l - l_c)$ of equation (7) describes a law similar to Hooke's law for mechanical systems, where the coefficient $c_i > 0$, $i = 1,2$, and characterizes the stiffness of the myocardium. In the systole phase, the model interprets this law as Frank-Starling's law, according to which the force of heart contraction is proportional to the length of stretching of the heart muscle. The coefficient characterizes the sensitivity of the Starling mechanism.

Justification of the physiology of the model

To substantiate the physiological nature of the model, all constants of the model are fixed, except for one, and it is proved that a change in an

unfixed constant corresponds to one of the factors affecting contractile activity and adequately reflects changes in the body.

1. Let us study the influence of the constant b_i on contractile activity.

Consider the systole phase. We fix all the coefficients except b_i. We assume that the largest ejection by volume occurs in the *CD* section. Let us find the travel time *T* of the path *CD*. From (Fig. 1)

$$T = \frac{y_\alpha - y_*}{x_c}, \quad x_c = \frac{x_* + x_0}{2},$$

where x_c is the average pressure at the *CD* section. Find x_* and y_*. To do this, we use formula (7) for $i = 1$. Differentiating the function $y(x)$ and equating the derivative to zero, we obtain

$$x_* = p_{01} + \sqrt{\frac{b_1}{\alpha_1}} \tag{8}$$

Substituting x_* in (7), we obtain

$$y_* = \frac{b_1}{c_1} + \left(\frac{2}{3}\sqrt{\frac{b_1}{\alpha_1}} + p_{01} \right);$$

$y_a = y(x_s)$ from formula (7), therefore

$$A = y_\alpha - y_* = \frac{1}{c_1}\left[\frac{\alpha_1}{3}(x_s - p_{01})^3 - b_i x_s + \frac{2b_1\sqrt{b_1}}{3\sqrt{a_1}} + b_1 p_{01} \right].$$

We decompose the function $y(x)$ into a Taylor series in the neighborhood of the point x_*, taking into account that

$$y'_x(x_*) = 0,$$

$$y''_x(x_*) = \frac{1}{c_1} \cdot \left[2\alpha_1 (x - p_{01}) \right]\Big|_{x=x_*} = \frac{2\sqrt{\alpha_1 b_1}}{c_1},$$

$$y''_x(x_*) = \frac{2\alpha_1}{c_1} \ldots .$$

Skipping the intermediate calculations, we get

$$\Delta \approx \frac{\alpha_1}{3_{c_1}}\left(x_s - p_{01} - \sqrt{\frac{b_1}{\alpha_1}} \right)^2 \left(x_s - p_{01} + 2\sqrt{\frac{b_1}{\alpha_1}} \right). \tag{9}$$

Determine $\sqrt{b_1} = z$. Let us investigate the function $\Delta(z)$ to the extremum. To do this, we use the necessary condition $\Delta'_z = 0$. From formula (9) we obtain

$$-\frac{6}{\sqrt{a_1}}\left(x_s - p_{01} - \frac{z}{\sqrt{a_1}}\right)\frac{z}{\sqrt{a_1}} = 0.$$

The function $\Delta(z)$ has two extremum points $z_1 = (x_s - p_{01})\sqrt{a_1}$ and $z_2 = 0$. From the form of a cubic parabola (8) it follows that at point z_1 the function $\Delta(z)$ reaches a minimum, and at point z_2 – a maximum. In the interval $[0, z_1]$ the function $\Delta(z)$ decreases. Let's mark

$$b_1^0 = \frac{a_1}{3}\frac{(x_s - p_{01})^3}{x_s}.$$

On the interval $\left[\sqrt{b_1^0}, z_1\right]$ there is

$$T(z) = \Delta(z)\cdot f_1(z), \text{ where } f_1(z) = \frac{2}{p_{01} + x_s + \frac{z}{\sqrt{a_1}}}.$$

It follows that $T(z)$ decreases with increasing z in the interval $[0, z_1]$, because $T(z)$ is a decreasing function.

Thus, the ejection period T comes with an increase in b_1 on the interval $\left[b_{01}, (x_s - p_{01})^2 a_1\right]$.

On the interval $\left[0, b_1^0\right]$, the value y_a should be considered equal to zero. From this it is easy to see that with an increase in b_1 in the indicated interval, the value of T increases. The graph of dependence $T(b_1)$ is shown in (Fig. 3).

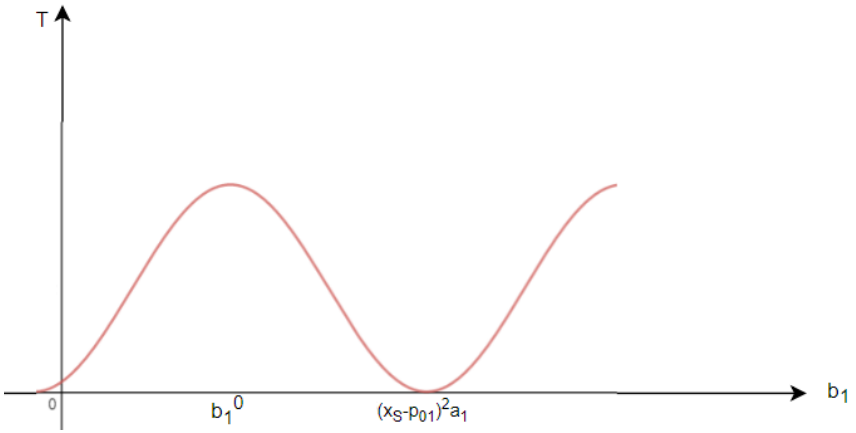

Figure 3. The curve of the dependence of the duration for the cardiac cycle

Note that $b_1 = 0$ – the minimum value of b_1, corresponds to the case in which there is no energy inflow. The case $b_1 = (x_s - p_{01})^2 a_1$ corresponds to a situation in which the ejection period is zero. Thus, the admissible values of b_1 can lie only in the interval $\left[0, (x_s - p_{01})^2 a_1\right]$.

The entire period of systole T_s, which corresponds to the movement from point A to point $D(D')$, also comes with an increase in b_1. Let's demonstrate this.

Divide the entire period of systole into two intervals, T' and та T $(T' + T = T_s)$. On the interval T' there is a fast movement from point A to point C, on the interval T – a slow movement from point C to point D. Note that the interval T' is small compared to the interval T, and therefore, when studying the dependence of the period of the entire systole on different parameters, it would be enough to stop at the interval T. As we know, $T(b_1)$ is a falling function. But it turns out that T' also comes with an increase in b_1. Indeed, the rate of change of the x coordinate during the movement of the phase point (x, y) in sections AB and $B'C$ is equal to the difference between the y coordinate and the value of the cubic parabola (1) at the point x. As b_1 increases, the difference between the maximum and minimum values of the parabola (1) will grow, since

$$y_{max} = \frac{b_1}{c_1}\left[\frac{2}{3}\sqrt{\frac{b_1}{a_1}} - p_{01}\right],$$

$$y_{min} = y_* = -\frac{b_1}{c_1}\left[\frac{2}{3}\sqrt{\frac{b_1}{a_1}} + p_{01}\right].$$

From here

$$y_{max} - y_{min} = \frac{4}{3}\frac{b_1}{c_1}\sqrt{\frac{b_1}{a_1}}.$$

This increase leads to an increase in speed. This increases the path, because the abscissa of the point A, at which systole begins, is equal to $-\sqrt{\frac{b_1}{a_1}} + p_{01}$ and, thus, decreases. As can be seen from the formulas, the speed increases faster than the path. Therefore, the value of T' decreases with increasing b_1.

Similar considerations can be made when studying the period of diastole T_d.

In summary, we can conclude that as the coefficients b_1 and b_2 increase, the duration of the cardiac cycle $T_s + T_d$ decreases, so the heart rate increases.

Let us now consider the dependence of the shock volume V on the magnitude of the activating factors. Let us first estimate the work A spent on the ejection of blood into the aorta, as well as the movement of the point $\left(x(t), y(t)\right)$ in the area of CD. From formula (3) the value of $y(t)$ can be interpreted as the rate of change of diameter l. According to the model, the maximum modulus of change l is equal to $|y_*|$, and the minimum $-|y_a|$. Hence, estimating the kinetic energy of motion, we conclude that the work is proportional to $y_*^2 - y_a^2$, i.e. $A \sim y_*^2 - y_a^*$.

From formula (3) it follows that the average force under the influence of which changes l,

$$x_c = \frac{x_* + x_s}{2} \tag{11}$$

From here, the shock volume can be roughly represented as

$$V = k_v V_0,\ V_0 = \frac{y_*^2 - y_a^2}{x_* + x_s}, \tag{12}$$

where k_v is the coefficient of proportionality.

Using the previously accepted notation, you can write:

$$V_0 = \frac{\Delta}{f_1}\left(-y_* - y_a\right) = \frac{a_1}{3c_1}\Delta_1\left(-y_* - y_a\right)^* \frac{x_s - p_{01} + 2\sqrt{\frac{b_1}{a_1}}}{f_1}$$

where $\Delta_1 = \left(x_S - p_{01} - \sqrt{\frac{b_1}{a_1}}\right)^2$.

Next, we show that the function $V\left(b_1\right)$ first increases, reaches a certain maximum, and then tends to decrease.

Consider the function

$$\frac{x_s - p_{01} + 2\sqrt{\frac{b_1}{a_1}}}{f_1} = 2 - \frac{x_s + 3p_{01}}{p_{01} + x_s + \sqrt{\frac{b_1}{a_1}}}.$$

It is obvious that it grows with the growth of b_1. Therefore, to study the nature of the dependence $V\left(b_1\right)$, it is sufficient to investigate the function $\Delta_1\left(-y_* - y_a\right)$.

Consider first the function

$$f_2 = c_1\Delta_1{}^*\left(-y_a\right) = \left(x_s - p_{01} - \sqrt{\frac{b_1}{a_1}}\right)^2\left[-\frac{a_1}{3}\left(x_s - p_{01}\right)^3 + b_1 x_s\right] \tag{13}$$

Let's replace the variables $z=\sqrt{b_1}$ and examine the dependence $f_2(z)$. From the formula (13) it is seen that the function $f_2(z)$ is a parabola of the fourth degree, which can have three local extrema – one maximum and two minimums. We find them from the equation $f_2'(z)=0$. Minimum points:

$$z_{min}^{+}=(x_s-p_{01})\sqrt{a_1}$$

$$z_{min}^{-}=\frac{\sqrt{a_1}(x_s-p_{01})}{4}\left(1-\sqrt{\frac{11x_s-8p_{01}}{3x_s}}\right),$$

wherein $z_{min}^{+}>z_{min}^{-}$.

The maximum point will be $z_{max}=\frac{\sqrt{a_1}(x_s-p_{01})}{2}\left(1-\sqrt{\frac{11x_s-8p_{01}}{3x_s}}\right)$.

So, $f_2(z)$ increases on the interval $\left[z_{min}^{-},z_{max}\right]$.

Note that y_a cannot be a positive value because it contradicts the physics of the process. Therefore, for $z\le\sqrt{b_1^o}$ we should assume that $f_2(z)=0$. Hence $f_2(z)$ increases in the interval $\left[0,z_{max}\right]$.

Consider now the function

$$f_3=c_1\Delta^{*}(-y_{*})=\left(x_s-p_{01}-\sqrt{\frac{b_1}{a_1}}\right)b_1\left(\frac{2}{3}\sqrt{\frac{b_1}{a_1}}+p_{01}\right).$$

As the last factor grows with increasing b_1, it is enough to investigate the function $f_4=\left(x_s-p_{01}-\sqrt{\frac{b_1}{a_1}}\right)^2 b_1$. The function $f_4(z)\left(z=\sqrt{b_1}\right)$ has two local minima: at points 0 and $\sqrt{a_1}(x_s-p_{01})$ and a maximum at point $z^{max}=\frac{(x_s-p_{01})\sqrt{a_1}}{2}$. This me ans that f_4 increases in the interval $\left[0,z^{max}\right]$.

It follows that the function f_3 increases on the interval $\left[0,z\right]$, where $z\ge z^{max}$.

Let us now consider on which interval can grow the function

$$\Delta_2{}^{*}(-y_{*}-y_a)=\frac{1}{c_1}(f_2+f_3).$$

In the case of $\sqrt{\frac{11x_s-8p_{01}}{3x_s}}\le 1$ $\quad z_{max}\le z^{max}\le z$, therefore, the function under study increases in the interval $\left[0,z_{max}\right]$. Otherwise $z_{min}^{-}\le 0$ and the function increases on the interval $\left[0,\min\left\{z,z_{max}\right\}\right]$.

Thus, the existence of such an interval is shown, the change of admissible values of b_1, on which the shock volume V increases with increasing b_1. Let the inequality hold

$$b_1^o \le \min\left\{z_{max},\ z^{max}\right\} = b_1^*. \tag{14}$$

It will be valid at a certain ratio between x_s and p_{01}. We will assume that relation (14) characterizes the state of the functioning myocardium in the norm.

In the interval $\left[b_1^o, b_1^*\right]$ $T\left(b_1\right)$ decreases, and $V\left(b_1\right)$ increases with increasing b_1. These dependences show that the proposed model reflects the Boudich effect, because with increasing heart rate decreases $T\left(b_1\right)$, which necessarily entails an increase in b_1. As b_1 grows, $V\left(b_1\right)$ grows and the contraction force (proportional to x_c) increases. The dependence $V\left(b_1\right)$ is shown in (Fig. 4).

The systole period was considered in the study of stroke volume V. Since the same volume (during stationary work of the heart) must be received during diastole, it is possible to obtain certain ratios between the coefficients that characterize systole and diastole.

2. Let us investigate the dependence of the impact volume V on the stiffness coefficient c_i , $i = 1,2$

The relationship between diastolic filling v and pressure p in the ventricular cavity is described by equation [2]

$$p = \frac{1}{c_2}\left(v - u\right) \ , \quad v \ge u$$

where u is the unstressed volume of the ventricle; c_2 – its diastolic distension.

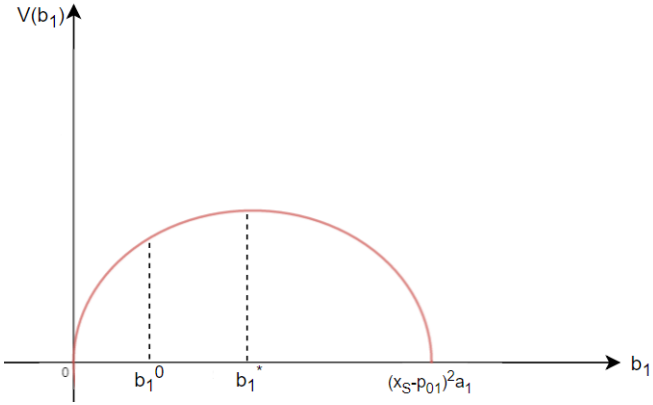

Figure 4. Dependence of impact volume on the magnitude of activating factors

According to the definition of the stiffness coefficient $c = \frac{1}{c_2}$. From formula (12) it is seen that at constant p with decreasing c_2, and hence with increasing c, the volume of blood entering the ventricle during diastole decreases. In steady state, the same volume will be displaced during systole. In the proposed model, this pattern is preserved.

Previously, the dependence of V on c at constant pressure was studied. Let us now consider this dependence provided that the work expended on displacement remains constant.

Let's examine the phase of systole. The same considerations can be applied to diastole.

Suppose that at certain parameters of the model a certain amount of work A_c is expended on the emission of blood. With increasing c_1 there is a decrease in work. We will compensate for this decrease by increasing b_1. This can be done in the case when the initial $b_1 \le z^2_{max}$.

With decreasing c_1, the opposite picture is observed. However, at certain values of c_1 such compensation is impossible. In this case we will use b_1 for which the maximum work is reached. The dependence of $V(c_1)$ and $A(c_1)$ has the form shown in (Fig. 5 and Fig. 6).

Cases $c_1 < c_1^1$ and $c_1 > c_1^2$ are pathological. As mentioned earlier, as c_1 decreases, b_1 should decrease, which leads to a decrease in x_* (Fig. 1). The case $x_* = x_a$ a corresponds to $c_1 = c_1^1$. Recall that when $x_* > x_a$ the valve closes when $x_* = x$. At $x_* < x_a$ the aortic valve will be closed at $x = x_a$ In this case, $y_a = 0$, x_s may not be reached, the point y_*, which previously corresponded to x_*, now corresponds to the point x_a and is equal to the value of the parabola I at the point x_a. It follows that as $c_1 < c_1^1$ decreases, $|y_*|$ decreases, reaching zero, and the shock volume decreases (see formula (12)). The case of such a small stiffness coefficient c_1 can be called the case of "plasticine heart". It is characterizes by a rapid decrease in the ejection period and the inability to achieve the required maximum systolic pressure.

Consider now the case $c_1 > c_1^2$. When c_1 increases, x_* increases (due to b_1 increase), which leads (see item 1) to a decrease in the emission period T. The work expended on the emission in this period T cannot reach the value A_0. This reduces the impact volume. The case of large c_1 can be called the case of a "stone heart".

The case when c_1 is within $c_1^1 < c_1 < c_1^2$, corresponds to normal heart function. In this case, V decreases relatively slowly with increasing c_1 within these limits.

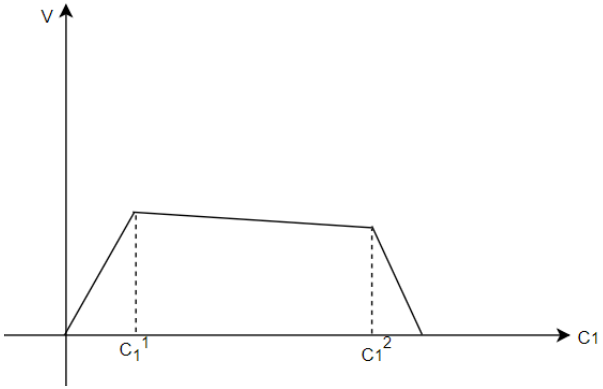

Figure 5. Dependence of impact volume on stiffness coefficient

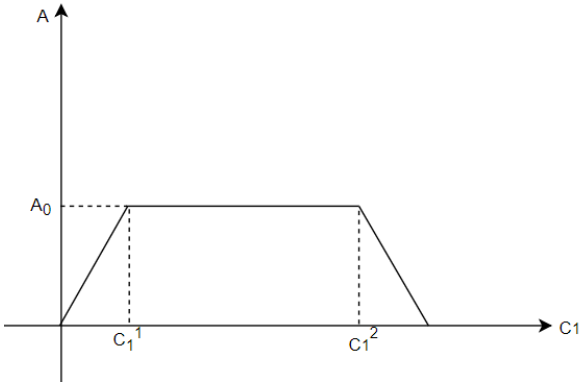

Figure 6. Dependence of the work spent on blood ejection on the coefficient of rigidity

Consider how the volumetric velocity W depends on c_1:

$$W = \frac{V}{T + T' + T_D} = \frac{V}{T} \cdot \frac{T}{T + T' + T_D}. \tag{15}$$

From item 1 it follows that

$$\frac{V}{T} = \frac{A}{x_c T} = \frac{A}{x_c \dfrac{y_a - y_*}{x_c}} \sim |y_a| + |y_*|. \tag{16}$$

Let us consider the behavior of $\dfrac{V}{T}$ with an increase in c_1. As before, to compensate for the reduced work, the parameter b_1 must be increased. By the definition of y_a and y_* it follows that in this case $|y_a|$ and $|y_*|$, and

therefore $\frac{V}{T}$. In this case, T will decrease. It follows from formula (15) that at large T, W increases with increasing c_1. On further growth, the first factor in (15) is bounded, and the second tends to zero.

This indicates the presence of a certain optimal c_1 in the interval of normal heart function.

Note the compensatory properties of changes in x_a and x_s. With a change in x_a, the difference $x_s - x_a$ becomes larger, which leads to the fact that the case of "plasticine heart" occurs at lower c_1. With an increase in x_s with other fixed parameters, the stroke volume increases, since the path from C to D increases. The case of a "stone heart" will occur at large c_1.

3. It is known that with an increase in mean arterial pressure after the end of transient processes, in order for the stroke volume to remain unchanged, the heart must do a lot of work [13]. This indicates that with constant work of the heart, the stroke volume decreases. This phenomenon is called the Anrep phenomenon, the model reflects this phenomenon.

4. As noted in paragraph 1, the coefficients $a_i\,(i=1,2)$ characterize a force of the "friction force" type, that is, a force that prevents the movement of blood, therefore, with its increase, certain physiological parameters should worsen. This is illustrated by the example of changes in the space velocity W.

Conclusion

In the proposed model of the dynamics of internal ventricular pressure, the main factors and forces that affect the contractile activity of the heart are concentrated. This approach correlates with the work of Ziman [14], which is an example of a geometric approach to modeling using differential equations.

The use of mathematical modeling and systems approach in physiology is in good agreement with the main goal of physiology as a science. Within the framework of this work, it is the definition of general principles of functioning and quantitative description of the pumping function of the heart as a theoretical basis for optimizing the functional state and the processes of its correction.

References:

1. *Хаютин В.М.*Физиология сердечного выброса.– Київ, Україна: Наук. думка, 1970.
2. Теоретические исследования физиологических систем. Математическое моделирование / Под общ. ред. Н.М. Амосова. – Київ, Україна: Наук. думка, 1977.
3. *Лищук В.А., Мосткова Е.В.* Система закономерностей сердца. Клин. физиология кровообращения,– № 1.2006. – С. 16–21.
4. *Баум О.В., Волошин В.И., Попов Л.А.* «Биофизические модели электрической активности сердца» Биофизика, – Т. 51. – № 6. 2006. – С. 1069–1086.
5. *Quarteroni A., Lassila T., Rossi S., Ruiz-Baier R.* Integrated Heart – Coupling multiscale and multiphysics models for the simulation of the cardiac function. Computer Methods in Applied Mechanics and Engineering. – Vol. 314. 2017. – P. 345–407. Doi: 10.1016/j.cma.2016.05.031
1. *Cardona K., Gómez J., Ferrero J., Saiz J., Rajamani S., Belardinelli L.,* et al. Simulation study of the electrophysiological mechanisms for heart failure phenotype. Computing in Cardiology, 2011. IEEE, – P. 461–464.
2. *Gomez J.F., Cardona K., Martinez L., Saiz J., Trenor B.* Electrophysiological and structural remodeling in heart failur e modulate arrhythmogenesis 1D Simulation Study. PLoS ONE9(9): e106602, 2014. URL: https://doi.org/10.1371/journal.pone.0106602
3. *Карпман В.Л., Парин В.В.* Руководство по физиологии: сердечный выброс. Физиология кровообращения. Физиология сердца.– Ленинград: Наука, 1980.
4. *Arabia M., Franconi C., Guerrisi M.* et al. Anew automatically controlled electric TAH, Trans. Amer. Soc. Artif. Jnt Organs.– 26.1980.– P. 60–65.
5. *Эрроусмит Д., Плейс К.* Обыкновенные дифференциальные уравнения.– Москва: Мир, 1986.
6. Биомеханика сердечной мышцы / Под общ. ред. Г.Р. Иваницкого.– Москва: Наука, 1981.
7. *Ландау Л.Д., Лифшиц Е.М.* Механика.– Москва: Наука, 1965.
8. Физиология кровообращения. Физиология сердца. Сер. Руководство по физиологии.– Ленинград: Наука, 1980.
9. *Zeeman E.C.* Population dynamics from game theory, in: Z. Nitecki, C. Robinson (Eds.), Global Theory of Dynamical Systems. Lecture Notes in Mathematics, – Vol. 819. Springer N.Y., 1980. – P. 471–497.

Olena Kirik, PhD, Senior researcher, Institute for Applied Systems Analysis at Igor Sikorsky Kyiv Polytechnic Institute, 37 Peremohy ave., Kyiv, Ukraine
E-mail: okirik@ukr.net.
ORCID: http://orcid.org/0000-0001-9688-8822

Alla Yakovleva, PhD, Associate professor, Institute for Applied Systems Analysis at Igor Sikorsky Kyiv Polytechnic Institute, 37 Peremohy ave., Kyiv, Ukraine
E-mail: aliakovleva@ukr.net
ORCID: http://orcid.org/0000-0003-3794-0015

Irina Shubenkova, PhD, Associate professor, Institute for Applied Systems Analysis at Igor Sikorsky Kyiv Polytechnic Institute, 37 Peremohy ave., Kyiv, Ukraine
E-mail: shubenkova1959@gmail.com.
ORCID: http://orcid.org/0000-0002-7433-2070

METHOD FOR3D IMAGING OF OBJECTS WITH RANDOM MOTION COMPONENTS IN InISAR

Hennadii Bratchenko, Marin Milković,
Hennadii Smahliuk, Iryna Seniva

Abstract. Method for three-dimensional (3D) imaging of objects with random motion components in interferometric inverse synthetic aperture radar (InISAR) is proposed. This method includes some known steps for 2D imaging of targets with regular and random components of spatial motion in ISAR. Introduction of two additional antennas for 3D InISAR imaging in proposed method is used to separate two orthogonal random phase components. These components can be used for prediction of phase dependencies for all spatial elements of target and 3D imaging of whole object not only its some of strong bright points.

Keywords: interferometric inverse synthetic aperture radar, 3D imaging, target, random components of spatial motion, bright point, phase dependence, prediction.

Introduction and statement of the problem

One of the requirements to perspective radars is the capability of the recognition of objects (targets). For the realization of such capability, it should be measuring of various radar target characteristics, the choice of informative and robust features, and teaching the recognition device (RD). After those preparatory steps, the RD is possible to decide on the class (or type) of the observed object [1, 2, 3].

The recognition features that are associated with the form of the target are most informative. Known examples of such features are the high range resolution profile (HRRP) which is a one-dimensional target image, a two-dimensional (2D) radar image (RI) that is obtained by processing of complex HRRP's sequence in the inverse synthetic aperture radar (ISAR) and three-dimensional (3D) RI that can be restored by using at least two complex 2D RI in an interferometric ISAR (InISAR) [4, 5, 6]. Unlike traditional single-channel ISAR, additional receiving channels with antennas separated in space allow performing interferometric

measurements of the coordinates of some bright points (scatterers) on the target [4, 5, 6, 7].

Random components of the target rotational motion lead to the defocusing of 2D ISAR images if we use only adaptation to the random component of the radial motion of the target. This situation takes place with a sufficiently long time of the target observation at long ranges, when the influence of the random components of yaw, roll and pitch of the target cannot be neglected. For relatively short observation intervals is possible ISAR imaging of partial 2D images with a decreased cross-range resolution. In [8], a 2D image restoration method based on measuring the laws of phase variation for several bright points (BPs) on a target was proposed. This method can also be applied in several receiving channels of an InISAR. This makes it possible to restore the 3D RI of the target for several BPs with the biggest radar cross-sections. The use of the interferometric method directly for partial images doesn't provide sufficient accuracy of measuring the BP (or scatterer) coordinates. In [9], the possibility of estimating the vector and the plane of the target rotation for calculating the scale and orientation of the projection of the 2D ISAR image with respect to the line-of-sight (LoS) is considered. However, in the case of a random change in the modulus and orientation of the rotation vector, it is necessary to make an estimate at each discrete moment of observation. For the development of the ISAR restoration method [8], it is possible, according to the measuring phase laws and coordinates of BPs, the separation of the random phase laws into two orthogonal components. One of them corresponds to the rotation of the target in the horizontal plane, and the other – in the vertical plane. These components can be used to predict the phase law of an arbitrary point on the object, which will allow restoring the 3D coordinates of a larger number of BPs on the target.

The goal of the investigation is to develop an improved method for restoring a 3D radar image of a target with a random component of spatial motion based on the separation of motion components in horizontal and vertical planes.

Mathematical model

Vector of the echo signal complex envelope at the output of linear section of the receiver can be calculated as follows [2]

$$X(t)=\sum_{i=1}^{I} A_i\left(r^0\right) S_i U\left(t-2\rho_i^T r^0/c\right) e^{-j\frac{4p}{\lambda}\rho_i^T r^0}, \qquad (1)$$

where $A_i\left(r^0\right)$ is the polarization scattering matrix of *i*-th scatterer; S_i is the polarization vector of incident wave; I is the number of illuminated local scattereres; r^0 is the unit vector of the incident wave (or direction of LoS); $U(t)$ is the complex envelope of signal at the output of optimal processing device; ρ_i is the radius vector of the *i*-th scatterer phase centre; «^{T}» **is the symbol of transposition;** c is the speed of light.

The equation $\frac{4\pi}{\lambda} p_i^T r^0$ in exponent of (1) is a phase of the echo signal of *i*-th scatterer. Object's movement leads to different changes of scatterers spatial position relatively the radar while the observation is in progress. In this case, considering the rotation matrix given small angles of yaw ψ, roll γ, pitch θ, and elevation ε of the target being observed at the azimuth β ratio, the phase multiplier entering expression (1) for the *i*-th scatterer with $p_i = \left(x_i^{'} \quad y_i^{'} \quad z_i^{'}\right)^T$ can be approximately computed, given that the right-hand Cartesian coordinate system has an origin at the centre of the object's rotation $\left(x_f^{'}, y_f^{'}, z_f^{'}\right)$, as follows [8]:

In this case, for the right-hand Cartesian coordinate system with an origin at the centre of the object's rotation $\left(x_f^{'}, y_f^{'}, z_f^{'}\right)$, considering the rotation matrix given small angles of yaw ψ, roll γ, pitch θ, and elevation ε of the target being observed at the azimuth β, the phase multiplier in expression (1) for the *i*-th scatterer with r, is

$$\begin{aligned} p_i^T r^0 \approx & \left(x_i^{'} - x_f^{'}\right)\left(\cos\beta - y\sin\beta\right) + \\ & + \left(z_i^{'} - z_f^{'}\right)\left(y\cos\beta + \sin\beta\right) + \\ & + \left(y_i^{'} - y_f^{'}\right)\left(g\sin\beta - q\cos\beta + \varepsilon\right). \end{aligned} \tag{2}$$

Consider a mathematical model of the phase law of the echo signal from BP_1 with $\rho_1 = \left(x_1 \quad y_1 \quad z_1\right)^T$, which are counted relatively coordinate system with the origin at the reference point $O\left(x_f^{'}, y_f^{'}, z_f^{'}\right)$. The reference point can be selected on the target, for example, using the dominant scatterer algorithm (DSA) [10]. The O_x axis coincides with the line of sight, the O_z axis lies in the horizontal plane and the O_y axis lies in the vertical plane (Fig. 1). The phase law of the echo signal of BP_1 for the receiving-transmitting antenna *B* in time from (2) takes the form

$$\varphi_1(t) = x_1 \frac{4\pi}{\lambda} + y_1\varphi_y(t) + z_1\varphi_z(t), \tag{3}$$

where λ is the radar wavelength;

$\varphi_y(t)$ and $\varphi_z(t)$ are the phase laws of the components for point with coordinates $y = 1$ m and $z = 1$ m due to the rotation of the target with an angular velocity directed along the axis O_z and O_y, respectively, divided by 1 m.

The first term in (3) is the constant component of the phase. Its value depends on the x_1 coordinate, which is usually measured using a broadband signal by numbered sample along the Lo *S*. The ambiguity of the phase measurement allows us to consider this component as a random variable. This component of the phase, however, does not influence on the ISAR imaging process.

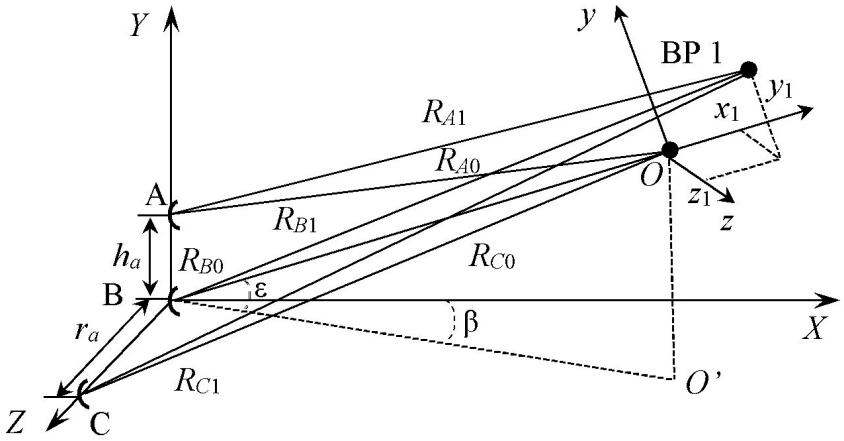

Figure1. Interferometric ISAR with L-shape arrangement of three antennas A, B, and C

Suppose that as a result of applying the method described in [8], the phase laws of the form (3) for several BP_s are obtained. For two arbitrarily selected BPs, whose coordinates are measured by the interferometric ISAR with L-shape arrangement of three antennas (Fig. 1), a system of linear equations can be constructed

$$\begin{cases} \varphi_1(t_i) = y_1\varphi_y(t_i) + z_1\varphi_z(t_i); \\ \varphi_2(t_i) = y_2\varphi_y(t_i) + z_2\varphi_z(t_i), \end{cases} \tag{4}$$

where t_i is the i-th moment of time at the interval of target observation, $i = 1, 2, \ldots, N$, since the image is restored in the range resolution element by N discrete complex samples of the echo signal;

$\varphi_1(t_i)$ and $\varphi_2(t_i)$ are phase laws for BP 1 and BP 2, respectively;

y_1, z_1 and y_2, z_2 are the coordinates of BP_1 and BP_2, respectively, obtained by the interferometric method;

$\varphi_y(t_i)$ and $\varphi_z(t_i)$ in the system of equations (4) for the i-th moment of observation, the targets are unknown. They can be found as a result of solving the system of equations (4). For example, using the Cramer's Rule, we obtain

$$\varphi_y(t_i) = \frac{1}{D}\begin{vmatrix} \varphi_1(t_i) & z_1 \\ \varphi_2(t_i) & z_2 \end{vmatrix} \text{ and } \varphi_z(t_i) = \frac{1}{D}\begin{vmatrix} y_1 & \varphi_1(t_i) \\ y_2 & \varphi_2(t_i) \end{vmatrix}, \quad (5)$$

where $D = \begin{vmatrix} y_1 & z_1 \\ y_2 & z_2 \end{vmatrix}$ is the determinant of the system matrix. The solution of the system of equations (4) allows us to find the values of the functions $\varphi_y(t_i)$ and $\varphi_z(t_i)$ at discrete moments of observation, which follow with a pulse repetition interval. The dependencies obtained are further proposed to be used to predict the phase law of an arbitrary *BP* in a given volume of space. This will allow using the results of measurements in InISAR for 3D imaging. The resolution depends on the nature of the target movement. In the case of a regular movement of the target in the horizontal plane, the additional random component of the movement in the vertical plane is used to resolve the BP_s in height.

The algorithm for restoring a three-dimensional RI of a target, which has regular and random components of spatial motion components, must include the following steps:

1. Estimation of the phase laws for not less than two the most powerful and isolated scatterers on the set of partial complex ISAR images sequentially restored by the method described in [8].

2. Restoration of two-dimensional complex ISAR images in each of the three channels using these laws [8].

3. Measurement of height and cross-range for the two most powerful BPs on ISAR images by the interferometric method (Fig. 1) [7, 11]

$$y_1 = \frac{\lambda(\varphi_{A1} - \varphi_{B1})}{2\pi}\frac{(R_{A1} + R_{B1})}{2h_a \cos\varepsilon},$$

$$z_1 = \frac{\lambda(\varphi_{C1} - \varphi_{B1})}{2\pi}\frac{(R_{C1} + R_{B1})}{2r_a \cos\beta},$$

where y_1, z_1 are the coordinates of BP_1 at the moment of time i =1 at the interval of target observation;

$\varphi_{A1}, \varphi_{B1}, \varphi_{C1}$ are the phases measured for BP 1 on complex ISAR images with use A, B, and C antennas respectively;
ε and β are elevation and azimuth angels respectively.

4. Calculation of the phase laws $\varphi_y(t)$ and $\varphi_z(t)$ according to the equations (4), (5).

5. Design of the expected phase laws for elementary cells in the picture plane (yO_z) and then application of these laws to the 3D image restoration.

The implementation of step 5 of the 3D RI restoration algorithm can be performed in different ways. The first option involves focusing of individuals scatterers in the parallelepiped in which the target to be. To do this, a set of HRRPs is selected separately in each cell in the picture plane (yO_z) in each resolved cell along the line of sight O_x. In such sets of the HRRPs, the expected phase laws for the corresponding cells are linear. Such the algorithm implementation has disadvantages: high computational costs (the need to perform a Fourier transform for each cell in a certain volume); not taking into account the orthogonality of individual components for cells with the same y coordinate. The second option involves orthogonality property consideration. In this embodiment, the random component of the phase law in the plane xO_y is used to pre-compensate this phase component for all BPs with coordinate y_1 by multiplying the signal samples in the corresponding distance resolution cell by the phase coefficient $e^{-jy_1\varphi_y(t)}$. The component of phase $\varphi_z(t)$ is used to select the HRRPs, which will correspond to the linear phase law for a set of cells with the same coordinate y_1. We can use this set of HRRPs for all other values of the y coordinate, which reduces computational costs. Evidently, by eliminating the influence of the random phase component due to the target rotation in the vertical plane, we achieve fulfilling the condition of orthogonality of the reflected signals for BPs with the different z coordinates at the same y_1 coordinate. Thus, individual BPs with the coordinate y_1 in the xO_z plane are focused simultaneously. The advantage of this variant of the algorithm step 5 implementation is the reduction of computational costs and influence of residuals of defocused BP_s, especially if several BPs in the range resolution cell have close values of the y coordinate. At the same time, the disadvantage of this implementation is not taking into account the possible impact of residuals due to poor focusing of the BPs with a big difference coordinate y from the selected coordinate y_1. To reduce the influence of such BPs we plan to use the CLEAN algorithm [9, 12, 13]. Sequential removal of the influence of signals of individual BPs, especially the most powerful ones, after their focusing

using such an iterative algorithm, will permit to improve the focusing of BPs with a smaller cross-section. Therefore, the next sixth step of the 3D InISAR imaging algorithm may be an additional refinement of the y and z coordinates by the interferometric method for each of the BPs based on the results of phase measuring after the multichannel CLEAN procedure. Additional application of such a procedure will require an increase in computational costs, but provides better focusing of two-dimensional ISAR images, and increases the accuracy of measuring the spatial coordinates of the BPs in the final three-dimensional InISAR image.

To confirm the fundamental possibility of separating the phase laws in the vertical and horizontal planes, the simulation was carried out.

The simulation

The simulation was carried out using a point model of an object consisting of five isotropic BPs as in [7]. The object's model had a cube shape with a 16 m edge. On the surface of the cube there were two point scatterers on the front face (*BP* 1 and *BP* 4), two on the back (*BP* 2 and *BP* 3) and one in the geometric centre (*BP* 5) (Fig. 2 a).

The initial parameters of target observation are range of the object to radar 110 km, the height 8 km, the azimuth $\beta = 0$ °. The target flight direction is parallel to axis O_rZ (Fig. 1), the speed of flight is 750 km/h, and the observation time is $T_{obs} = 8s$. For simulation of random spatial components of target moving in the yaw, roll and pitch rotation matrices were added harmonic dependencies $\gamma(t) = A_\gamma \sin(\omega t + \psi_\gamma)$ where $A_\gamma = 0.1^o$, $\omega = 2\pi/T_{obs}$ and $\psi_\gamma = \pi/3$ for the roll, $\psi_\gamma = 1$ for the yaw and $\psi_\gamma = 0.5$ for the pitch angles. During the observation, 1024 complex high range resolution profiles (HRRPs) were taken. The second antenna A height was chosen $h_a = 1.75$ m. The third antenna C was put on $r_a = 3$ m from the first one in horizontal plane (Fig. 1). Radar parameters are the wavelength 3 cm, the chirp probing pulse with rectangular envelope (pulse width is 13.65 μs, frequency deviation is 150 MHz); the signal-to-noise ratio 100 dB for one HRRP.

The signal processing includes a matched filtration. Also, we use the Hamming filters for obtaining as HRRPs as cross-range profiles. The ISAR images of the three antennas are restored with a fast Fourier transform to store the phase information of each BP. The dominant scatterer algorithm (DSA) of Steinberg [10] using to eliminate the influence of random initial

phases of HRRPs and focus ISAR images in all channels. After that procedure, the LoS is directed to this reference point.

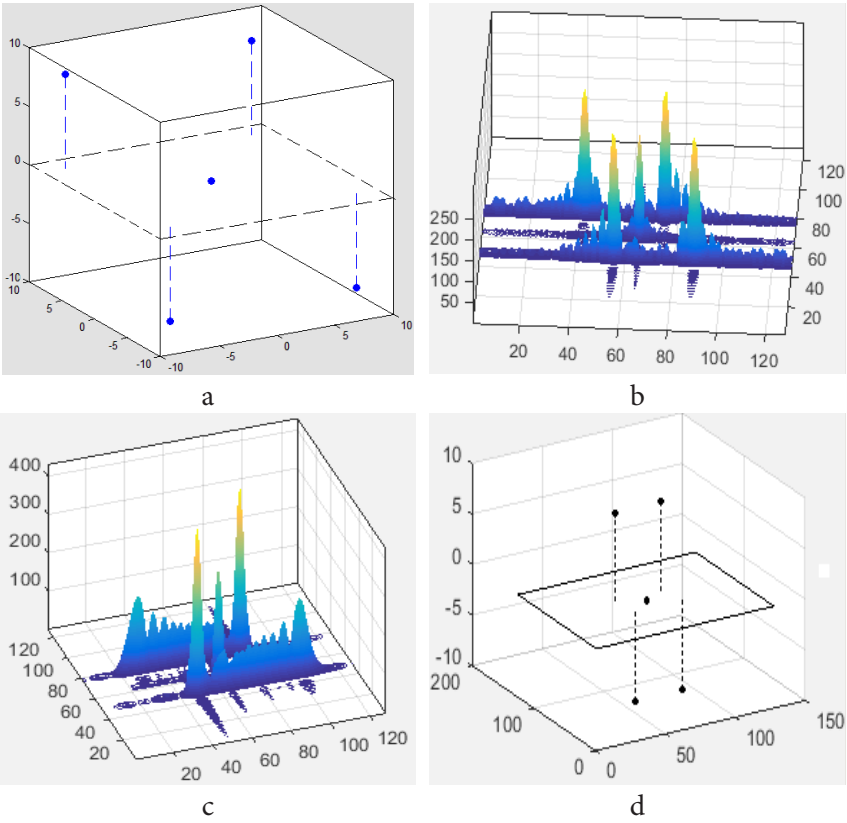

Figure 2. Simulation results of restoration 3D RI in InISAR with L-shape arrangement of three antennas: a – target model, b – ISAR image restored by using method of [8], c – ISAR image restored by using all set of HRRPs, d – 3D InISAR image

As a result of simulation by the method described in [8], we restored two complex 2D ISAR images of the object consisting of five *BPs* (Fig. 2 b and 2 c). The unwrapped phase dependencies (taking into account the ambiguity of their measurement) by a sequence of 896 partial 2D images for four *BPs* are used to select 512 HRRPs with a phase law close to linear for restoring image in (Fig. 2 b). Examples of the measured phase dependencies for *BP* 1 and *BP* 4 are shown in (Fig. 3 and Fig. 4). In (Fig. 2 c), for comparison with (Fig. 2 b), we can see more unfocused the 2D ISAR image

obtained using the whole set of 1024 HRRPs. DSA selects the *BP* 5 in the object's centre as the reference scatterer. For the ISAR image in (Fig. 2 b), the peaks are better focused, but their cross-range coordinates have significant errors. The use of interferometric measurements allows you partly to correct the cross-range errors and measure the heights of the BPs relative to the line of sight (Fig. 2 d). The measurement results are presented in table 1. The numbering of O_x and O_z axes in (Fig. 2 b, c, d) correspond the number of 0.5 m cells. The dimensionless units on the vertical axis in (Fig. 2 b), c correspond to the amplitude of echo signals of scatterers.

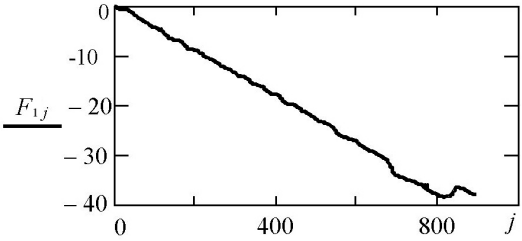

Figure 3. Example of the measured phase dependence for *BP* 1

The sequence of solutions of the system of equations (4) for BP 1 and BP 4 gives dependencies (Fig. 5) and (Fig. 6). In (Fig. 5), the dotted line shows the dependence of the object roll in the scale. It is similar to the phase dependence due to the rotational motion of the target in the vertical plane.

Table 1. – Results of measuring coordinates of bright points

Coordinates	Number of the bright point			
	1	2	3	4
y, m	–7.367	7.381	7.368	–7.382
z, m	–7.424	–8.478	7.283	8.465

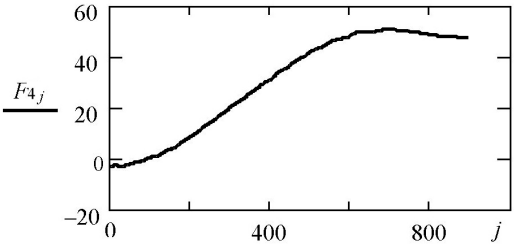

Figure 4. Example of the measured phase dependence for *BP* 4

The obtained dependencies (Fig. 5, Fig. 6) we can use to predict the phase laws of other BPs with given coordinates in the picture plane xO_y.

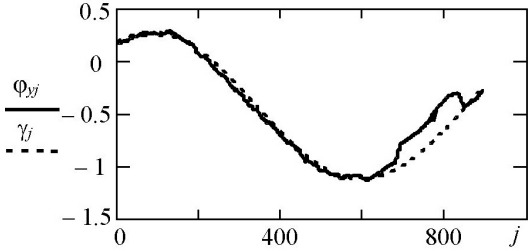

Figure 5. Relative phase law (solid line) and scaled dependence of the roll angle of the target (dashed line) in the vertical plane

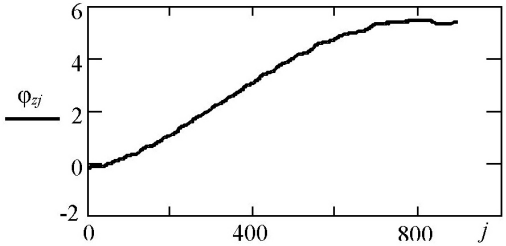

Figure 6. Relative phase law in the horizontal plane

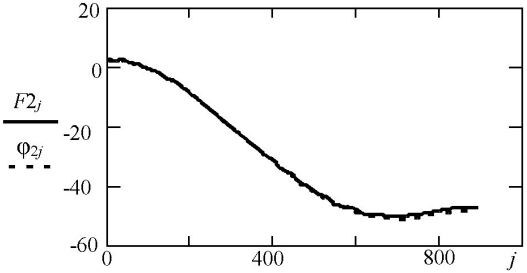

Figure 7. Measured (solid line) and restored (dashed line) phase dependencies for *BP* 2

For example, the reconstructed dependencies for BP 2 and BP 3 (dashed line) in comparison with the results of direct measurement (solid line) are presented (Fig. 7 and Fig. 8). Their good match confirms the possibility of predicting the phase law for BP with given coordinates. Such laws can be used to restore 3D ISAR images.

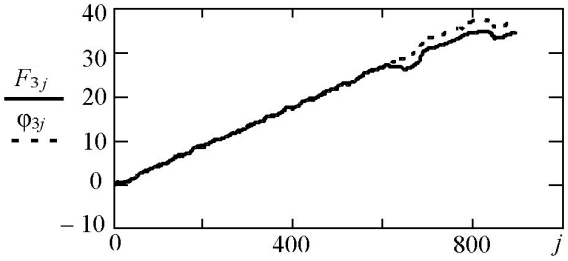

Figure 8. Measured (solid line) and restored (dashed line) phase dependencies for *BP* 3

Conclusion

Method for 3D imaging of objects with random motion components in InISAR is proposed. The novelty of this method is a separation of two orthogonal random phase components in vertical and horizontal planes. The possibility of separation is illustrated by the results of the simulation. These components can be used for prediction of phase dependencies for all spatial elements of target and 3D imaging of whole object not only its some of the strong bright points. Further study of the capabilities of the method will include simulation of the 3D imaging of objects of more complex shape for more complex observation conditions (lower signal-to-noise ratio, random nature of target movement in a turbulent atmosphere).

References:

1. *Горелик А. Л., Барабаш Ю. Л., Кривошеев О. В., Эпштейн С. С.,* Селекция и распознавание на основе локационной информации; Под. Ред. А. Л. Горелика. – Москва: Радио и связь, 1990.
2. *Ширман Я. Д., Горшков С. А., Лещенко С. П., Братченко Г. Д., Орленко В. М.* Методы радиолокационного распознавания и их моделирование, Зарубежная радиоэлектроника. Успехи современной радио-электроники. – № 11. 1996. – С. 3–63.
3. *Yakov D. Shirman Sergey A. Gorshkov Sergey P.* Leshchenko, Valeriy M. Orlenko Sergey Yu. Sedyshev, and Oleg I. Sukharevskiy, Computer simulation of aerial target radar scattering, recognition, detection, and tracking, Yakov D. Shirman Editor, – Boston London: Artech House, 2002.

4. *Xu X., Narayanan R. M.* Three dimensional interferometric ISAR imaging for target scattering diagnosis and modeling, IEEE Trans. Image Process., – Vol. 10. – No. 7. – Jul. 2001. – P. 1094–1102.
5. *Wang G., Xia X., Chen V. C.* Three-dimensional ISAR imaging of maneuvering target using three receivers, IEEE Trans. Image Process., – Vol. 10. – No. 3. – Mar. 2001. – P. 436–447.
6. *Martorella M., Stagliano D., Salvetti F. and Battisti N.* 3D interferometric ISAR imaging of noncooperative targets, IEEE Trans. Aerosp. Electron. Syst., 50, 2014. – P. 3102–3114.
7. *Smaglyuk H. H., Bratchenko H. D.* DSc, Grygoriev D. V. and Plotnik A. I. "3D position measurement simulation of air target's scatterrers in interferometric ISAR", Збірник наукових праць Одеської державної академії технічного регулювання та якості. – Вип. 2(11), 2017. – С. 58–64. DOI: https://doi.org/10.32684/2412-5288-2017-2-11-58-64.
8. *Skachkov V. V., Bratchenko H. D., Milkovic M., Tkachuk O. V., Smahliuk H. H. and Grygoryev D. V.* Adaptive methods for measuring coordinates and radar imaging. – Varazdin: University North, 2018.
9. *Salvetti F.* Multi-channel techniques for 3D ISAR (Doctoral thesis). University of Adelaide, School of Electrical and Electronic Engineering, Adelaide, South Australia. 2015.
10. *Steinberg B. D.* "Microwave imaging of aircraft", Proceedings of the IEEE, – Vol. 76(12). – January, 1989. – P. 1578–1592.
11. *Братченко Г. Д., Смаглюк Г. Г., Сеніва І. С., і Орел Д. І.,* "Вимірювання просторового положення блискучих точок цілі в інтерферометричній РЛС з ІСА за умов скошеного спостереження", Збірник наукових праць Одеської державної академії технічного регулювання та якості, вип. – 2(15), 2019. – С. 57–66. DOI: https://doi.org/10.32684/2412-5288-2019-2-15-57-66.
12. *Martorella M., Salvetti F., Stagliano D.* "3D target reconstruction by means of 2D-ISAR imaging and interferometry", in: Proceedings of the Radar Conference (RADAR), 2013 IEEE, 2013. – P. 1–6.
13. *Salvetti F., Gray D., Martorella M.* "Joint use of two-dimensional tomography and ISAR imaging for three-dimensional image formation of non-cooperative targets", in: EUSAR2014; Proceedings of the tenth European Conference on Synthetic Aperture Radar; Proceedings of. VDE, 2014. – P. 1–4.

Hennadii Bratchenko, Doc.Tech.Science, prof., Dept. of Standartization, Sertification and Educational Assessment, Odesa State Academy of Technical Regulation and Quality, 15 Kuznechna str., Odesa, Ukraine
E-mail: bratchenkohd@gmail.com.
ORCID: http://orcid.org/0000-0002-0314-8188

Marin Milković, PhD, prof., rector, University North, Trg dr. Zarko Dolinar 1, Koprivnica, Republic of Croatia
E-mail: mmilkovic@unin.hr

Hennadii Smahliuk,Senior Lecturer, Dept. of Electronics and Microsystems Technology, Odesa State Academy of Technical Regulation and Quality, Odesa, Ukraine
E-mail: madcat-a@yandex.ua
ORCID: https://orcid.org/0000-0003-1104-3703

Iryna Seniva, graduate student, Dept. of Standartization, Sertification and Educational Assessment, Odesa state academy of technical regulation and quality, Odesa, Ukraine
E-mail: iren10590@gmail.com

TELECOMMUNICATION TECHNOLOGIES OF TECHNICAL DIAGNOSTICS OF THE UNIFIED NATIONAL SYNCHRONOUS INFORMATION SYSTEM

Valerii Koval, Vitaliy Lysenko, Mykhaylo Klymash,
Oleksandr Samkov, Oleksandr Osinskiy, Dmytro Kalian

Abstract. A transmission of synchronization signals by using modern telecommunication technologies is a promising area that provides the necessary accuracy, information security, and quality assurance. Despite an active development of asynchronous telecommunication networks (IP networks), it is effective to decide on the transmission of synchronization information through these networks based on the precision time protocol, PTP, which allows the time scale to be distributed with an accuracy of a few microseconds. In this paper we presented the results of scientific research, which confirmed a possibility of transmission and technical diagnosis of the parameters of synchronization signals in the country using existing IP networks.

Keywords: telecommunication technologies; synchronous information; IP network; PTP protocol; signal of accurate time

Introduction and statement of the problem

Modern infocommunication technologies are characterized by intensive use of the reference values of time and frequency scale to ensure synchronous operation of high-tech systems in telecommunications, metrology, defense, cybersecurity, and in many sectors of the economy [1–4]. High-precision measurements of time and frequency is an important part of ensuring a unity of the measurements in the state, on which high-quality operation of the digital telecommunications, military facilities, synchronization of technological processes in science and economy, and people awereness depend.

The existence of its own system of high-quality and efficient synchronization and information support of economic sectors is, to a certain extent, a sign of a high level of the state development. Despite the fact that currently the state service of State Service of Uniform Time and Standard

Frequencies [5], while forming and maintaining the national time scale at the level of the best national scales in the world, practically does not perform the function of transmitting synchronization signals through the information channels. As a result, the problems of using modern telecommunication technologies are the burning issues of today that update scientific research to solve this problem.

Ways of transmitting synchronization information

The State Service of Uniform Time and Standard Frequencies, including the State Enterprise "Ukrmetrteststandard", only partially transmits the reference time and frequency signals to the consumers and performs the function of time scale.

Technical means of the Service do not form a unified system and cannot meet the requirements of all consumers, that induces them to use synchronization information of the other states (for example, from the satellite navigation systems GNSS), which poses a threat to national security and increases the risks of losing the unity of time and frequency measurements within the state. It is known that the main disadvantages of such satellite systems are the dependence of signal quality on non-stationary characteristics of the open medium of radio signal propagation, absence of protection against intentional distortion of synchronization information, etc. [4, 5].

Effective transfer of information about uniform precise time, reference frequencies, precise timestamps (synchronization information) to the objects in need is possible through the creation of a unified national synchronous information system (UNSIS) [4, 5]. Implementation of the proposed idea will create the conditions for information security of the critical infrastructure of the country, as well as the applied results of a dual use will be received for the state institutions, such as the Armed Forces of Ukraine, State Enterprise Derzhspetszviazok (The State Service of Special Communications and Information Protection of Ukraine), and State Enterprise "Ukrmetrteststandard".

In general, a set of large systems or their subsystems and separate dedicated objects, primarily high-tech government information systems, can be the consumers of synchronization information. The national facilities requiring synchronization information are telecommunication networks, digital television, integrated electric power systems, metrology, billing, air and railway transport, oil and gas pipelines, agricultural, environmental

and other sectors of the economy. Also, it should be noted the importance of obtaining reference signals of the precise time by special services, which solve the problems of the national cybersecurity of the state and the need to introduce a unified (Kyiv) accounting and reporting time.

There are different distribution mechanisms and protocols which are used to transfer synchronization information to the consumers from the state frequency and time standards or precise time service that support the coordinated national scale. The protocols intended for remote transmission of timestamps in digital code are the protocol of IRIG family and the Network Time Protocol (NTP), which is developed for a widespread use in the computer networks with IP protocol. Additionally, the ToD (Time of Day) protocol has found its application in metrology. To implement the ToD protocol, an asynchronous interface of RS-232 type is used that transmits NMEA messages with a time scale information supplemented by an analog pulse signal with a frequency of 1 Hz (or 1 pps), which accurately records the timing of scale transition through a zero value of seconds. Also, a modern protocol has been developed for transmitting a timestamp over existing IP networks. This protocol is defined in the IEEE-1588 international standard as the Precision Time Protocol (PTP). The analysis results of technical characteristics and application features of these protocols are given in (Table 1).

Table 1. – Technical characteristics and application features of protocols

Protocol	**Accuracy provided**	**The need for a separate network**	**Application features**
IRIG-B	10 μs – 1 ms	yes	–
ToD	0.1–10 μs	yes	At a distance of up to 10 m
NTP	1–100 ms	no (UDP/IP network)	Depends on a network
PTP (IEEE-1588–2008)	0.1–10 μs	no (UDP/ IP network or Ethernet)	Does not depend on a network *

** for a network that supports PTP in accordance with the requirements of the standard*

Based on the data given above, we can conclude that the PTP protocol is the only one that can provide a microsecond accuracy and does not require a development of a dedicated network. Experimental studies and the

global practice of implementing PTP protocol on existing networks in different industries led to the intensification of its standardization in various sectors of the economy [4, 5]. Implementation of PTP protocol is largely due to the active transition of telecommunication operators to the use of packet switching technologies in the networks. It is worth noting that in such networks, the PTP protocol can be applied with some deterioration in performance, even without its support by other network equipment.

Analysis of the use cases of technical means of the UNSIS telecommunications of Ukraine

An important problem of creating the UNSIS of Ukraine is the justification of the technical means chosen to organize the transmition of synchronization information, that is, the means of telecommunication [4]. There are three ways to solve this problem: 1) to create your own separate digital transport synchronization network; 2) to rent UNSIS as a separate one imposed on information networks, primarily on primary and secondary ones; 3) to transmit the synchronization information along with other useful information in their transport environment, and then select it in the synchronization nodes in one way or another. It can be argued that currently the most developed networks are the synchronization networks of information infrastructures, including telecommunications, where an extensive theoretical and practical experience of their development and operation has been accumulated [3, 4].

In order to reduce the costs of developing the UNSIS of Ukraine, as one of the stages, it can be proposed to develop separate but interconnected synchronization networks of telecommunication operators of different departments and sectors of the economy of Ukraine, or individual large synchronization facilities. A large number of industry-specific synchronization networks with different types of primary sources and synchronization devices from the technical side can significantly reduce the quality of synchronization information and they are not economically feasible, so the number of such networks should be limited. In essence, a developemnt of other, separate but interconnected synchronization networks, such as regional, departmental, or private ones, is an alternative to the project concept of the UNSIS of Ukraine. Such establishment may have the following disadvantages. Firstly, the UNSIS of Ukraine will have a status of the national one, and not just telecommunication and other operators. In addition, today a

number of synchronization facilities, not only in the field of telecommunications and informatization, require synchronization information as a comprehensive product [5]. The UNSIS should become a queueing system for domestic consumers of synchronization information with further involvement of partners from other countries and continents. Secondly, a fragmentation and refinement of synchronization networks, even specific local telecommunication networks, to the "personal business" of the operators/owners, which is currently observed in the industry, will complicate a number of interaction procedures. In the future, this situation can not only cause deterioration in performance of synchronization infrastructures, their failure or partial loss of synchronization, but it can also lead to a complete failure of synchronization of all or some telecommunication networks in the country and, as a result, to emergency situations.

Separate, but interconnected synchronization networks of telecommunication operators can be considered as separate components of the UNSIS of Ukraine. The choice of synchronization method of the national digital communication network is a responsibility of the national administrations. Right now, the UNSIS of Ukraine, which would overtake all synchronization facilities of Ukraine (railway transport, oil and gas pipelines, electric power industry, space and defense facilities, etc.), can be developed only under the state programs of Ukraine. Here we can distinguish three strategies for implementing the UNSIS project of Ukraine [4]:

- to offer the UNSIS of Ukraine for all consumers of synchronization information. Such centralized management (let's say, at the level of the Cabinet of Ministers) can reduce technical and economic costs, but it requires significant capital investment at the initial stage (permissible construction steps);
- to offer separate synchronization networks for different consumers of synchronization information of Ukraine;
- to offer a digital transport network (primary) and partially a network of synchronization information services (secondary) of the Derzhspetszviazok (The State Service of Special Communications and Information Protection of Ukraine) as a set of innovative means. The indicated synchronization networks need to be reconstructed and expanded, and there need to be developed a dedicated network of the UNSIS of Ukraine in order to provide consumers of all sectors of the economy of Ukraine with the necessary synchronization signals. First of all, it is necessary to ensure

the transmission of information about the precise time, and then move on to the transmission of synchronization signals of the unified Kyiv accounting and reporting time to consumers throughout Ukraine and update the existing synchronization equipment, including the one of the domestic manufacturers, which is much cheaper than the imported.

Technical Diagnosis of Telecommunications of the UNSIS of Ukraine

In the conditions of operation of the digital means of telecommunications of the UNSIS of Ukraine changes in the parameters of synchronization signals occur, the reasons for which are both technical features of their functioning, and the influence of external destabilizing factors. This leads to the fact that theoretical calculations, models and developed systems in some cases are not compliant with the real processes that occur in the geographically dispersed network objects. Therefore, at different stages of the lifecycle of the UNSIS of Ukraine, one of the most important tasks is to determine a technical condition of the digital means and the network in general, that is, technical diagnostics. A measurement of the synchronization signals' parameters, which are transmitted to different sections of the UNSIS of Ukraine, are integral to the processes of monitoring the technical condition with a given accuracy. The tasks performed by the automated system of technical diagnostics (ASTD) include the tasks of collecting and analyzing the received information and identification of existing problems. It is worth noting that detection of the problem areas and nodes is impossible without obtaining reliable and up-to-date information on the quantitative and qualitative characteristics of the synchronization signals of the UNSIS of Ukraine. Therefore, the formation of high quality synchronization signals with a given accuracy and reliability is impossible without the use of technical diagnostic system.

We found that it takes quite a long time to conduct automatic measurements of time intervals (wandering the phase of synchronization signals) with simultaneous measurements of several synchronization signals, accumulation and storage, archiving of the results and joint statistical processing using a specialized server ASTD [4].

To implement the automated system of technical diagnostics of the process of quality control of synchronization signals, it is necessary to meet a

number of requirements. The main requirement is the need to develop organizational and technical measures to ensure implementation of the simultaneous multi-channel measurements of monitored synchronization signals at the geographically dispersed objects, algorithmic processing and visual presentation of control results in real time in a format convenient for the operator. Improvement of the efficiency in the implementation of these requirements can be achieved through the use of IP technologies, both for transmiting synchronization signals and for moving the measurement data.

The tasks of ensuring simultaneous measurement of the parameters of the monitored synchronization signals of the UNSIS of Ukraine determine the structure of the ASTD (Fig. 1), in which an IP network is used to transmit data of the monitoring results. In order to expand system functionality, a method of multichannel control of time intervals of synchronization signals is proposed [7–9], the technical implementation of which is ASTD with geographically distributed control units of synchronization signals (CUSS) (Fig. 1).

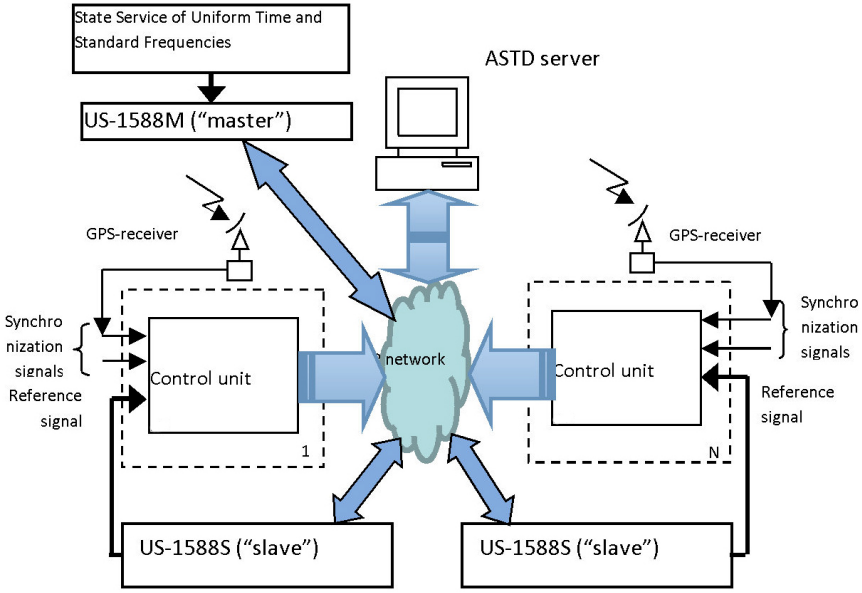

Figure 1. The structure of the automated system of technical diagnostics

The proposed method of monitoring is based on the use of multi-channel geographically distributed over objects, control units (hardware) that perform continuous measurements (days, weeks) of several synchronization signals.

The monitoring results are processed and transmitted over the IP network to the ASTD server. The server performs additional processing of measurement results, including statistical, and generates data in a format convenient for the operator. Based on the generated up-to-date data in the centralized point of ASTD, an informed decision is made to involve the methods of theory of statistical decisions and necessary control actions are formed.

The synchronization signals' control unit (Fig. 1) includes a precision reference signal generator with an automatic frequency control system and the corresponding control sections. The precision reference signal generator is based on the principle of phase-locked loop frequency of a crystal oscillator with deviation control and adaptive digital phase discriminator [10]. The generator of the reference signal, directly or due to the process of automatic frequency control from external sources, generates reference (standard) time stamps, in relation to which the deviation of the time intervals of the monitored synchronization signals is measured in the control sections.

The measurement results of time interval deviation are periodically (with a period of one second) transmitted over the IP network via Ethernet to the ASTD server. It is possible to service the UCS through the serial interface RS-232 using the Telnet protocol.

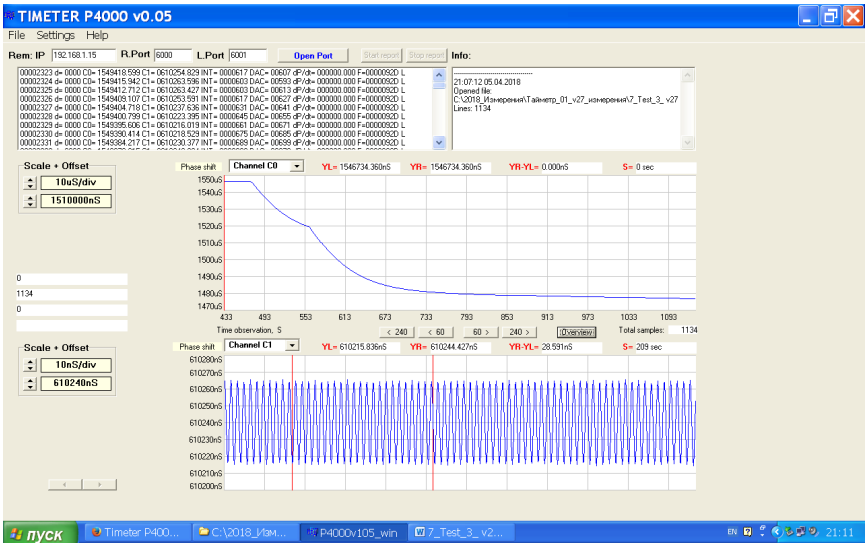

Figure 2. Visualization of the monitoring results of two synchronization signals in real time

Developed in the Embarcadero RAD Studio XE22012 environment, the P4000 win XP software provides the ability to simultaneously visualize the results of real-time monitoring of four synchronization signals generated by the UCS. As an example, (Fig. 2) shows photographs of the browser with graphs and control data of two synchronization signals (Channel C0 and Channel C1), given in the publication [11].

Experimental studies results of the precise timestamps transmission over the IP networks

Let us analyze the research results of PTP protocol on the possibility of its implementation in the intelligent power systems [4]. Since the base standard of PTP protocol contains a wide range of permissible installations and settings, the specialists optimize a configuration of the protocol depending on the characteristics of the industry networks where this protocol will be implemented, which increases the characteristics or simplifies implementation of the protocol.

Experimental studies of the information system for transmitting the precise timestamps over the existing IP networks were carried out using a set of US-1588 equipment of domestic production ("Information Service Technologies Ltd", Kyiv) and a laboratory sample of a quality control device for generating synchronization signals, which includes a blocks of primary transducers (BPT) «TIMETER» [4]. The US-1588 is intended for transmitting the precise timestamps over the data transmission networks using the packet switching based on TCP/IP or UDP/IP protocols at a speed of 10/100 Mbit/s that are compliant with the requirements of IEEE-1588 standard [4]. The most common example of these packet networks where the US-1588 equipment can be used, is the local 10/100 Mbit/s Ethernet network or the IPv4-based network.

The experimental studies of the information system for transmitting the precise timestamps, which consists of the digital information transmission system based on the US-1588M and US-1588S equipment that provides digital transmission of synchronization information over the corporate IP network of the NUBiP of Ukraine. The measured parameters are characteristics of the TIE synchronization signals determined in accordance with the International Recommendations ITU-TG.810 and G.8262 [4]. The experimental studies of the set of US-1588 equipment of domestic production showed a compliance of its main characteristics with

the requirements of the "energy" profile of PTP protocol when transmitting the precise timestamps over the existing corporate IP-network of the NUBiP of Ukraine [4]. It is worth noting that the contribution of the synchronizing device US-1588M ("master") to the deviation of time interval is no more than 50 ns at a rate not exceeding 200 ns. The parameters of the set of US-1588 equipment allow to ensure instability of the transmitted timestamps at the level of 300 ns (range).

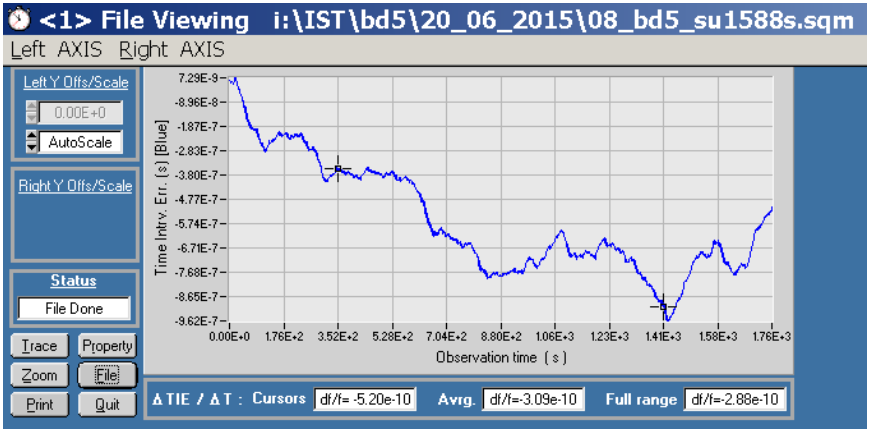

Figure 3. The measurement results of the TIE of output signal of the information system of the precise timestamps transmission over the corporate IP-network of the NUBiP

(Fig. 3) shows the measurement results of the TIE of output signal of information system of the precise timestamps transmission over the corporate IP-network of the NUBiP of Ukraine. Taking into account the measurement results, it can be stated that the maximum deviation does not exceed one microsecond.

Conclusion

Implementation of the proposed idea as a set of innovative means that will work as part of the unified national synchronous information system of Ukraine from the national standard source, is a great alternative to foreign satellite navigation systems. The system will allow to ensure information survivability and increase reliability by diversifying digital transmission of synchronization signals.

The solution of this problem at the state level will create the conditions, firstly, to increase information security of the users, and, secondly, to increase competitiveness in the market through the cost-effective integrated service delivery to both government agencies and corporate consumers.

It is important that the implementation of the proposed idea will create conditions for information security of critical infrastructure of the country. Also, we will receive the applied results of a dual use for the state institutions, such as the Armed Forces of Ukraine, State Enterprise Derzhspetszviazok (The State Service of Special Communications and Information Protection of Ukraine), State Enterprise "Ukrmetrteststandard", etc. The proposed set of innovative means will not only provide high-quality reference signals of the uniform time, but also create the conditions for effective synchronous information support of other infrastructure facilities of the country with the lowest costs, and will have the applied dual-use results for the Armed Forces of Ukraine, due to thedevelopment of a unified national synchronous information system of Ukraine, that is a modern autonomous ground-based system, independent of foreign time and frequency services.

References:

1. *Брени С.* Синхронизация цифровых сетей связи. Пер. с англ. – Москва, Россия: Мир, 2003.
2. *Рыжков А. В.* , Частота и время в инфокоммуникациях XXI века. – Москва, Россия: МАС, 2006.
3. *Борщ В. І., Коршун Є. І. , Туманов Ю. Г. , та Чумак О. М.* Синхронізація й синхронізація в телекомунікаційних системах. Київ, Україна: Наукова думка, 2004.
4. *Коваль В. В., Кальян Д. О., та Самков О. В.* Автоматизована система передачі синхросигналів з використанням IP-мереж: монографія. – Київ, Україна: НУБіП України, 2016.
5. *Velychko O. M., Kalian D. O., Koval V. V., and Samkov O. V.* Terminal devices for synchro-information systems with adaptive properties for IoT, in Proc. International Conf. AICT-2017, – Lviv, Ukraine, 2017. – P. 22–25.
6. *Коваль В. В., Дорогобед В. В., Козирська Т. О. , та Циб В. М.* Информационная система многоканального мониторинга сигналов синхронизации цифровых телекоммуникаций, на IV Всеукр.

наук.-практ. конф. Проблеми технічного регулювання та якості, – Одеса, 2014. – С. 100–104.
7. *Koval V. V., Kalian D. O., Tepliuk V. M. , Shkliarevskii I. I. and Khudyntsev M. M.* Multichannel Clock Signal Monitoring System for Infocommunication Networks, in Proc. International Conf. Modern problems of Radio Engineering, Telecommunications and Computer Science (TCSET'2016), – Lviv-Slavske, Ukraine, 2016. – P. 618–620.
8. *Коваль В. В., Комащенко А. В., Самков О. В., та Худинцев М. М.* Система многоканального мониторинга тактовых синхросигналов телекоммуникационных сетей, на Восьмій міжнародній нак.-практ. конф, Інфокомунікації – сучасність та майбутнє, – Одеса, 2018. – С. 88–91.
9. *Коваль В. В., Лисенко В. П., та Худинцев М. М.* Автоматизований багатоканальний моніторинг сигналів міток точного часу інтегрованих систем електропостачання, на нак.-практ. конф. Кібербезпека енергетики, – Одеса, 2019. – С. 34–37.
10. *Коваль В. В., Кальян Д. О. ,* та В. В. Коваль, Адаптивний цифровий фазовий дискримінатор, МПК (2016.01) H 03 D13/00, H 03 D3/04 (2006.1). Патент на винахід України № 113473, Січень 25, 2017.
11. *Dmytro Kalian, Nadiia Kazakova, Boris Kravchenko, Valerii Koval* Automated system for Monitoring Synchronizing precise time signals at SMART-GRID power plants, Projectowanie, badania, i eksploatacja. Tom 1.– Wydawnictwo naukowe Akademii techniczno-humanistycznej w Bielsku-Bialey. Bielsku-Bialey, Poland. 2019. – P. 155–160. [Online]. Available: URL: http://www.engineerxxi.ath.eu/book/designing-researches-and-exploitation-2019-vol-1/. Accessed on: November 10, 2020.

Valerii Koval, Doc.Tech.Science, prof., Dept. of Automation and Robotic Systems named by I. I. Martynenko, National University of Life and Environmental Sciences of Ukraine, 11 Heroyiv Oborony Str, Kyiv Ukraine.
E-mail: v.koval@nubip.edu.ua.
ORCID: http://orcid.org/0000-0003-0911-2538

Vitaliy Lysenko, Doc.Tech.Science, prof., Head of the Automation and Robotic Systems named by I. I. Martynenko, National University of Life and Environmental Sciences of Ukraine, 11 Heroyiv Oborony Str, Kyiv Ukraine.
E-mail: vlysenko@nubip.edu.ua.
ORCID: https://orcid.org/0000-0002-5659-6806

Mykhaylo Klymash, Doc.Tech.Science, prof., Head of the Telecommunication, Lviv Polytechnic National University, 2 Profesorska Str., Lviv Ukraine
E-mail: samkov@ied.org.ua.
ORCID: http://orcid.org/0000-0002-1166-4182

Oleksandr Samkov, Doc.Tech.Science, head's assistant, Deputy Director for Scientific and Technical Work Institute of Electrodynamics of the National Academy of Sciences of Ukraine, 56 Peremohy ave., Kyiv Ukraine
E-mail: samkov@ied.org.ua.
ORCID: http://orcid.org/0000-0003-2790-8564

Oleksandr Osinskiy, National Academy of Sciences of Ukraine, 54 Volodymyrska Str, Kyiv Ukraine
E-mail: osinskiy@usnan.org.ua.

Dmytro Kalian, Postgraduate student National University of Life and Environmental Sciences of Ukraine, 11 Heroyiv Oborony Str, Kyiv Ukraine
E-mail: dmytro.kalian@gmail.com.
ORCID: http://orcid.org/0000–0003–2016–2253

TOWARD THE METHODOLOGY FOR CONSIDERING MENTALITY PROPERTIES IN EGOVERNMENT PROBLEMS

Alexander Makarenko

Abstract. A general framework for eGovernment is considered. The results of system analysis of different components of eGovernment are proposed. Also the background for considering and modeling of human properties of individuals is described. It is proposed also the models for considering spreading and development of eGovernment in the society. The approach allows forecasting the dynamics of opinion formation, and leading to modeling of the behavior of eGovernment participants. Our approach is based on the attempt to utilize the principles of associative memory from neural networks. Also the models with internal mental structures structure of individuals are considered and results of computer experiments are discussed. Different kinds of opinion evolution are discussed including punctuated equilibrium. Indexes for power distribution in eGovernment are proposed. Further research problems just as recommendations for practical implementations are proposed.

Keywords: eGovernment, opinion formation, associative memory, reputation, mental patterns, participants, evolutionary approaches, cybersecurity.

Introduction

Recently eGovernment became more and more common technologies for society tasks and for society transformations. But practical experience in eGovernment using is far ahead of theoretical foundations of eGovernment. Before in the series of papers [1–4] we had proposed outline of the problems of eGovernment. For example we had considered the eGovernment from the point of view of system analysis [1]; some presumable methodologies for eGovernment considering [2, 3]; sustainability of society and of eGovernment [4]; general models of large social systems [5, 6]. But for deep understanding of eGovernment and moreover for practical implementation of eGovernment systems more elaborated concepts, models and methodologies should be developed.

Thus in given paper we propose some approach for accounting mental properties of eGovernment participants, the ways of transformations and the number of related properties, including investigation of system elasticity, calculating power indexes, supply the security of the system etc.

The structure of the paper is next. At section 1 we propose the general scheme of eGovernment droving from the point of view proposed by author concepts. Some detalization of such concepts is proposed at section 2. Section 3 devotes for considering transformations in society and of eGovernment subsystem.

General framework

Government is the society part. So it should be considered in the general frames accepted for considering society and social systems. Usually in general problems of large social systems three 'pillars' had been considered (Fig. 1).

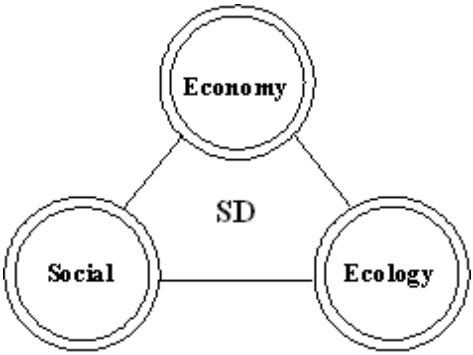

Figure 1. Three 'pillars' of social systems

All such components (and restrictions on corresponding recourses) also should be considered in eGovernment problems. Remark that scientific community agrees that 'ecology' and 'economy' 'pillars' have more or less developed models. But 'social' 'pillar' has less adequate models. So in discussion of general framework for eGovernment we will concentrates on the methodologies for 'social' aspects. At first stage we will accept that the models for 'ecological' and 'economical' components will supply the forecasts for 'social' components environment. (This is only the approximation because 'social' pillar has impact on other). Following approach from [5, 6] we suppose at the first approximation that he social part of eGovernment

consists from N individuals with bonds between them. The individual posses own dynamics of some parameters of social type.

We suppose that the 'Social' part of government also has the 'technical' part. 'Technical' part includes interfaces between *participants of eGovernment and administrative (electronic and* classical) part. For example 'technical' part may include communication lines, computers, analytical and security centres personal interfaces etc. Administration may include top-level leaders, decision-making departments, data collection and processing departments, press centres and many others. Thus at first approximation the eGovernment system may be represented by schemes on the figures 2 a, 2 b. Figures 2 a corresponds to traditional arrangement of government. But the figure 2 b display the origin some new aspects of government which include the 'electronic' government.

The essentially new elements are individuals with access to servers (S) through communications lines and separate departments for decision-making.

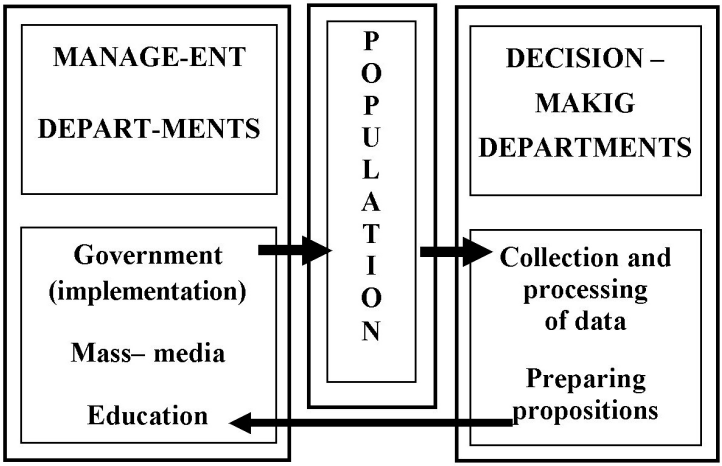

Figure 2 a. Simple scheme of 'classical' government

Of course such pictures are oversimplified. So it is possible to pose more detailed scheme which can help to understand the structure and role of eGovernment in social system. Remark that evidently hierarchical nature of considered social systems. Such pictures may also help to pose the tasks of investigation and design of eGovernment systems of different level and scales.

Of course such presumable schemes also are some approximations for real system. For example because a lack of place we doesn't show explicitly infrastructures, organizations, forms and industry, cities and villages, social networks and many others. But just such schemes allows for stress some components and aspects of eGovernment. Such pictures illustrate the different presumable scales of eGovernment systems; non-homogeneous character of systems especially of population; hierarchy in systems; interrelations and interactions between subsystems. Probably such pictures may help in classifications and ranking of eGovernment projects and necessary cost evaluation. For example the scales of projects may expand from local to the country or international level.

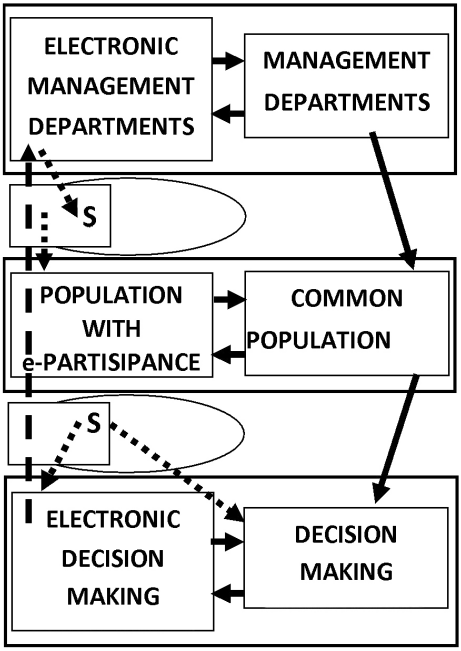

Figure 2 b. Scheme with 'classical' and 'electronic' governent

It had been stressed by many researchers including author [1–4] that the eGovernment development require the searching of optimal ways for design and financing of eGovernment. Recently it is impossible with applications of mathematical models and approaches. The models are necessary as for global problems (for example for sustainable development) as for searching more local regional commercial projects and solutions.

Of course a lot of mathematical models exist for different components of remarked above pillars of system (it may be the goals of separate papers). So here we will concentrate on the aspects most closely related to eGovernment especially to the less formalized (just theoretically).

Namely below we will consider the components related with 'population' and 'government' blocks from figures 2. Remark that usually any of components of eGovernment include as 'classical' as 'new' component ('new' means related to 'electronic' part of eGovernment). The share of 'new' components may be evaluated by some formal procedures and indexes. The fracture F (%) of population which use the interfaces (external and through PC) of eGovernment may serves as one of the simple examples. The fracture FG (%) of government departments involved in eGovernment may serves as second example. The part of power in given social system transferred to population through eGovernment is the third example. But just the task of such blocks modelling is very complex (but possible in principle for all pillars and components). For describing one presumable approach for general modelling here we will concentrate mainly on human – related tasks.

Short description of associative of associative memory approach for some social problems

First of all we stress some problems related to population participants at eGovernment: 1) formation of public opinion on some issue by electronic system; 2) voting on some question through eGovernment; 3) expanding of eGovernment system; 4) evaluation of power distribution between population and administration. Below we propose for illustration the development of methodology the first problem. Remark that in this paper we intend only to illustrate the background of methodology on the base of simplest examples.

A General ideas

We present here briefly the core idea of the approach and the rough draft of the model that we are going to develop in the research. The proposed model does not pretend to be full and is intended only to demonstrate the basic ideas presented here.

As the first example we consider the simplified problem when all individual are involved in eGovernment system. Lets all individuals pose personal opinion through electronic networks and received some revised

information through networks. Remark that the type and volume of information is different. The first is the case of fully open process when all individuals know the opinion of all involved participants. The second case is the backward distribution for all participants only the integral results (for example average opinion – say the percents of supporting individuals or the power of support of some issue).

In order to make easier understanding of the method and to simplify the initial formulas, we consider the idealized society. The opinion development consists of discrete steps, at which the actual exchange of opinion take place. Within each step we identify the sub steps, which describe the dynamic bidding and asking or decision-making processes for every individual. The society consists of N homogeneous participants (in future developments the homogeneous assumption obviously should be removed).

With every participant we associate the state variable $s_i \in S = \{0, \pm 1, \pm 2, \ldots, \pm M_i\}$, where s_i represents the number of shares that participant i is planning to strength (if $s_i > 0$) or to weak (if $s_i < 0$) opinion, and M_i is the maximum allowed volume, which represents the power of opinion of participant i_{is} able to accept.

With every pair of participants i and j we associate the variable $c_{ij} \in R$ – the integral value of reputation that participant j has from the point of view of participant i. This value measures the degree of how well informed; participant j is in the eyes of the participant i. The large positive values of c_{ij} mean that, in the opinion of participant i, participant j is an informed (news, insider) participant, the values close to zero can mean that the participant j is an uninformed (noise, nice) or liquidity participant, while the negative values mean that the participant j is either insider who work against the information he has in order to hide himself, or a participant who is likely to be wrong in his judgment. The reputation variables c_{ij} form a matrix

$$C = \{c_{ij}\}_{i,j=1,\ldots,N} \tag{1}$$

that we call the matrix of reputation. The approach c_{ij} valuation will be discussed later at the end of this section.

As one of the basic characteristics of the system we introduce the concept of a vector field of influence

$$F = \{f_i\}_{i=1,\ldots,N} : f_i = \sum_j c_{ij} \frac{s_j}{M_j}, \; c_{ii} = 0 \tag{2}$$

where f_i means the integral influence of opinions of all other participants on i participant. The intuition behind this formula is the following. The ratio s_j / M_j represents the opinion intentions of participant j at the current step. It shows the number of opinion participant j is planning to support or reject as a percentage of what his actual power is. The product $c_{ij} \times s_j / M_j$ is the information about intentions of participant j filtered through the matrix of reputation. Thus, the sum (2) represents all the available to participant i information about the actions of other participants, and since it is filtered through the matrix of reputation, it is meaningful and trustworthy to him. We would like to note here, that all the other information, participant i might have, is already incorporated in his initial intensions s_i.

Obviously, the best strategy for rational individual will be to adjust his own initial intentions to the filtered information about others. Speaking formally, we say that every participant is associated with the information utility function, which he is trying to maximize during the decision-making process. It is done by correlating the decision of individual i with the corresponding value of the field of influence f_i.

Thus, we may formulate the evolution equation describing the opinion dynamics (of course it is the simplest possible example of dynamics):

$$s_i(t+1) = \begin{cases} s_i + 1, & \text{if } f_i(t) > 0 \text{ and } s_i(t) < M_i, \\ s_i - 1, & \text{if } f_i(t) < 0 \text{ and } s_i(t) > -M_i, \\ s_i & \text{otherwise.} \end{cases} \quad (3)$$

The initial conditions for this dynamic equation are the intentions of each individual to support opinion at the beginning of the opinion forming step. They are formed under the influence of the sources outside the system, and represent the participant's forecast of how well the particular opinion distribution will be doing.

Given the initial conditions for s_i and known values of influence matrix, we may calculate the dynamics of the opinion patterns. Such dynamics is expected to be beneficial for each participant, since it leads to the maximal utilization of the filtered, and therefore useful, information available to him.

Obviously, the system consists of protagonists with different and frequently antagonistic goals. Thus, the actions beneficial for a particular participant do not necessarily benefit the others. Moreover, each participant acts from his own interests and generally, if somebody wins, someone loses. However, all these egoistic individuals comprise the system we con-

sider. Therefore, from the system point of view the question is, whether the defined above dynamics of every participant leads to a meaningful evolution of the whole system, or is this just a disordered, chaotic motion? The answer can be found using the analogy with the physical systems.

As the variable summarizing the evolution of the system, we introduce the concept of 'energy' E, which characterizes the impact all the participants have had on each other in making their supporting/rejection decisions:

$$E = -\sum_i f_i s_i$$

Thus, at any given point in time, 'energy' E characterizes the state of the society. Naturally, we are interested in the evolution of the opinion patterns leading to a state that has the property of stability. By analogy with the physical systems, we will call the state of the system stable if the 'energy' E has a local minimum in this point. As we will see, the system will tend to minimize its energy during the evolution process. To show this, we will first formulate and prove the following statement.

Statement 1. Under the law of evolution (3) the system evolves to a local minimum of energy E.

After energy reaches the local minimum, due to (A_1) any change of the state of the system will increase the energy, which is impossible because of (A_2). Thus, $s_i(t+1) = s_i(t)\ \forall i$, and the system will retain its stable state until some external forces are applied. Such stable state can be thought as equilibrium, at which opinion pattern takes place. It simply means that all the participants have reached their decisions having maximized their own information utility functions. Since we are assuming that all the external information the participants might have is represented by their initial intentions, evolution occurs. Thus, maximization of individuals' information utility functions leads to the minimum of energy of the system and, therefore, to its coordinated movement during the decision-making step.

The next evolution step begins with the new initial conditions, which contain the new information participants have been able to obtain.

The reputation matrix in the described above model remains invariable during the supporting/rejection or decision-making steps. Obviously, it should change at each evolution step, since participants analyze their own performance as well as the performance of other participants and society as a whole. Therefore, each individual might assign different coefficients to the corresponding elements of the matrix of reputation, which will be enforced at the next evolution step.

Thus, the reputation matrix plays one of the major roles in the proposed model, and the applicability of the model depends, to a great extent, on the correctness and accuracy of the reputation coefficients. The numeric values for the entries of the matrix of reputation are not readily available. However, one of the advantages of the given approach is that it uses already proved and experimentally tested algorithms for the identification of the matrix C via the prior observations of the opinion patterns. This algorithm has the form of the well-known rule from the pattern recognition theory of associative memory models [7]. Its brief idea can be outlined as follows.

Suppose we have recorded information about opinion patterns Z_k, $k = 1,\ldots,K$, where $Z_k = \{s_i\}$ at the time moment k, K is the number of observations, $i = 1,\ldots,N$, N – number of participants. Then the matrix of reputation C can be evaluated as

$$C = \{c_{ij}\},\ c_{ij} = \sum_k \frac{s_{ik}}{M_i} \times \frac{s_{jk}}{M_j},\ c_{ii} = 0 \tag{4}$$

Of course such model correspond more to the case of opinion formation in parliaments, administrative councils, and cyberspace networks. But a lot of improvements of model can be proposed. Here we describe some of most evident.

Anyway more realistic is situation that only F(%) of population is involved in egovernance processes. Then the frames of the model are the same but for all population only opinions of Ne e-participants are known. This allows further developments. At first the opinion of this Ne participants serves as the information for other part on society by mass-media, social relations etc. Such information serves also as some kind of social questionnaires (with the same difficulties and problems). As such the date of e-participants opinion may serve as the database for other models and approaches. At second the changes in reputations $C = \{c_{ij}\}$ can be introduced. Such changes in reputations may have different reasons – internal and external. Internal changes have internal process of evolution as the source. External changes may have the mass-media influence, straggle of political parties, and education system as the main reasons. Remark that special dynamical equations may be derived for evolution of $C = \{c_{ij}\}$ during time flow [7].

Presumable variety of matrix of reputation properties may follow to a lot of different effects (which we cannot describe here because the lack of space). We only remark here the possibility of periodic solutions for slightly non-symmetrical matrix of reputation and chaotic behaviour of public opinion in the case of sufficiently non-symmetric reputation matrix. Also

the abrupt transition between quasi-stable stats of opinion during time in case of non-constant matrix of reputation $C = \{c_{ij}\}$.

B. Accounting the internal structures of eGovernment participants

The next step in development of proposed models is to account the internal structure of participants (we named such participants as 'intellectual').

Let us consider the idealized market as the collection of *N* intellectual participants. We will consider the process with discrete time steps. Each participant should to do decision (change of state) at each time step in dependence of all participants' states.

Participant's state is described by the variable $S_i(t) \in S = \{0, \pm 1, \pm 2, \ldots, \pm M_i\}$, which corresponds to the amount of the recourse (opinion, information, materials and so on), which may be gain (if $S_i(t) < 0$) or collect (if $S_i(t) > 0$) by i individual (participant). Here M_i is the maximal volume of its resource (its potential). Interaction of individuals in organization is described by influence matrix $C = \{c_{ij}\}$, $j = 1, \ldots, N$, $c_{ij} \in [0,1]$ where c_{ij} – influence coefficient of j individual on i. The influence matrix C may reflect the authority power in organization. In simplest model we take $C_{ij} = 0$, $i = 1, \ldots, N$.

So the collection $Q^R(t) = \left(\{S_l^R(t)\}, \{C_{lj}^R\}\right)$, $i, j = 1, \ldots, N$ represents the real state at moment t. Let us consider also $Q^i(t) = \left(\{S_l^i(t)\}, \{C_{lj}^i\}\right)$, $i, j, l = 1, \ldots, N$ as ideal pattern of situation from the i participant point of view. Then we can calculate the difference between real and ideal patterns of situation:

$$D_i(t) = \left\| Q^i(t) - Q^R(t) \right\| \tag{5}$$

We suppose that the dynamics of i participant depends on the difference $D_i(t)$ and on the mean influence field by other participants. We accept the influence field $G(t) = \{g_i(t)\}$, $i = 1, \ldots, N$ as:

$$g_i(t) = \sum_{j=1}^{N} C_{ij}^R \frac{S_j^R(t)}{M_j} \tag{6}$$

The term $\frac{S_j^R(t)}{M_j}$ in (6) corresponds to the activity of j participant at the moment t. The term $C_{ij}^R \frac{S_j^R(t)}{M_j}$ corresponds to activity with reputation accounting. In general case the dynamical law for participant takes the form (*F* some law for participant's reaction, named frequently activation function):

$$S_i^R(t+1) = F(v_i(t)) \tag{7}$$

where the argument $v_i(t)$ may takes the form:

a) Multiplicative

$$v_i(t) = \alpha(D_i(t))g_i(t) \tag{8}$$

where for example $\alpha(D_i(t)) = e^{-kD_i(t)}$. In simplest evident variant we may take:

$$D_i(t) = \sum_{j=1}^{N} \left| S_j^i(t) - S_j^R(t) \right| \tag{9}$$

b) additive $v_i(t) = g_i(t) + f_i(D_i(t))$, where $f_i(D_i(t))$ – some influence function. The simplest example is:

$$f(D_i(t)) = \sum_{j=1}^{N} C_{ij}^R \frac{(S_j^R S_j^i)}{M_j} \tag{10}$$

In this model vector $v_i(t)$ represent the understanding by i participant on the tendencies in system: If $v_i(t) > 0$, then the tendency is to increase the recourse, if $v_i(t) \approx 0$, then the stability is the main tendency, if $v_i(t) < 0$, then the tendency is to reduce the resources.

One of the most usable forms of activation function *F* in such type models are:

$$S_i^R(t+1) = \begin{cases} S_i^R(t) + 1 & \text{if } v_i(t) > \dfrac{\|G(t)\| \left| S_i^R \right|}{M_i} \text{ and } S_i^R(t) < M_i, \\ S_i^R(t) - 1 & \text{if } v_i(t) > \dfrac{\|G(t)\| \left| S_i^R \right|}{M_i} \text{ and } S_i^R(t) > -M_i, \\ 0 & \text{otherwise,} \end{cases} \tag{11}$$

$$\text{where } \|G(t)\| = \frac{\sqrt{\sum_{i=1}^{N} g_i^2(t)}}{N} \tag{12}$$

Remark that very interesting development of proposed models consist in introduction time dependence of connections by some dynamical laws. The models described here correspond to the constant bonds.

Research tasks and problems to be solved

Proposed approach allows developing the software and trying to understand some properties of society and particularly eGovernment. Here

we describe some examples of computer experiments with the models (5)–(12) which accounting the internal structure of participants and non-constant in time reputation of participants (Fig. 3).

The horizontal axe corresponds to the steps of evolution of opinion formation. The vertical axe represents the intentions of different participants. The left picture correspond to stabilization of intentions of participants. The right-side picture corresponds to the case of society with changeable reputations during evolution.

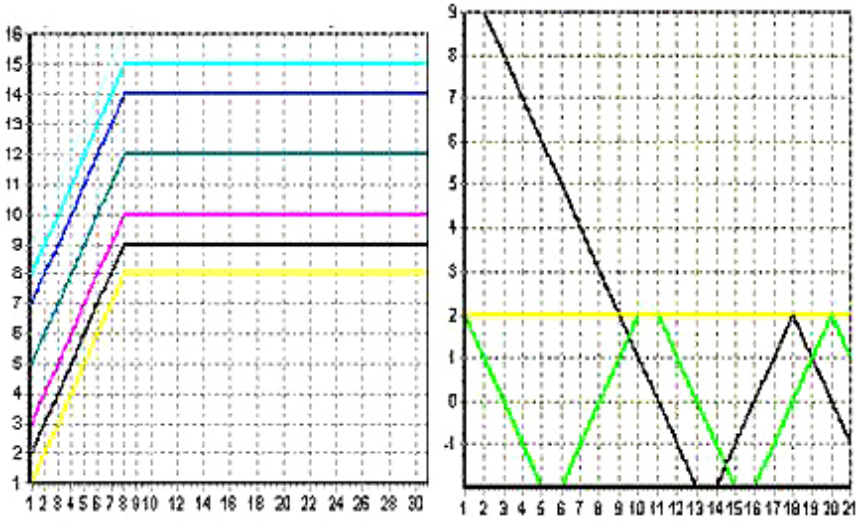

Figure 3. Example of opinion formation modeling

The right picture illustrates the possibilities of oscillations of the opinion. The oscillations are intrinsic for society with asymmetrical reputation of participants. Moreover the society with mostly asymmetrically informed participants may have chaotic behavior. Other very interesting phenomenon is the possibilities of sudden changes of stable opinion patterns in the case of variable reputation of participants. It may correspond to real phenomena in the society. Also it may correlate with phenomena of punctuated equilibrium in biology.

Of course till now our computational investigations are model with artificial date and further investigations will be interesting. But just now some prospective issues may be discussed.

First of all proposed internal representation may be considered as some correlate to ontology of participant. Also it may be interesting for

considering classical problem of reputation. At second the approach reminiscent usual multi-agent approach. The description of participant remember participant with special representation of the internal and external worlds by network structure. Also the prospective feature in the approach is the associative memory in proposed models. Remark that recently we had found the possibility of multi-valued solution existing in case of individuals which can anticipate the future [8].

Conclusions

Thus in proposed paper we consider the approach for system analysis and modeling which implement some properties of real society and eGovernment. The main distinctive features are the accounting of internal properties of participants. As the authors envisage, the modeling principles, described in section 3 can lead to the formulation and solution of the following problems:

Development of models of opinion patterns for the specific real problems.

Investigation of the control and security problems of eGovernment on the base of proposed approach.

Introducing and investigation different indexes of eGovernment operating, especially of power of e-participants community.

Numerical simulation of specific local eGovernment problems.

Analysis of the eGovernment spreading in society on the base of proposed methodology.

Forming proposition for building general tasks computing systems of investigation and managing eGovernment with accounting all aspects remarked above.

Proposed approach allows re-formulate the problems of cyber security of networks and more generally security of society.

References:

1. *Makarenko A.* System Analysis, Foresees and Management of E-Services Impacts on Informational Societies. Proc. 4th Eastern Europ. eGov Days, Prague, Czech Republic. 2006. – 6 p.
2. *Makarenko A.* Toward the building some methodic of understanding and improvement of e-Government Proc. 6th Eastern Europ. eGov Days, Prague, Czech Republic 2008. – 5 p.

3. *Makarenko A., Goldengorin B., Krushinskiy D., Smelianec N.* Modeling of Large-Scale crowd's traffic for e_Government and decision-making. Proc. 5th Eastern Europ. eGov Days, Prague, Czech Republic. 2007. – 5 p.
4. *Makarenko A., Samorodov E., Klestova Z.* Sustainable Development and eGovernment. Sustainability of What, Why and How. Proc. 8th Eastern Europ. eGov Days, Prague, Czech Republic. 2010. – 5 p.
5. *Makarenko A.* New Neuronet Models of Global Socio-Economical Processes. In 'Gaming / Simulation for Policy Development and Organisational Change' (J. Geurts, C. Joldersma, E. Roelofs eds), Tillburg Univ. Press. 1998. – P. 133–138.
6. *Makarenko A.* Sustainable Development and Risk Evaluation: Challenges and Possible new Methodologies, In. Risk Science and Sustainability: Science for Reduction of Risk and Sustainable Development of Society, eds. T. Beer, A. Izmail- Zade, Kluwer A.P., Dordrecht. 2003. – P. 87–100.
7. *Haykin S.* Neural Networks: Comprehensive Fundations.– N.Y.: MacMillan. 1994. – 697 p.
8. *Makarenko A.* Anticipatory participants, scenarios approach in decision- making and some quantum – mechanical analogies. Int. J. of Computing Anticipatory Systems. 2004. – Vol. 15. – P. 217–225.

Alexander Makarenko, Head of Applied Nonlinear Analysis Department, Institute of Applied System Analisis at National Technikal University of Ukraine (Igor Sykorski Kyiv Politechnic Institute), 03056, Kyiv, 37, Prosp. Peremohy, 35, Kyiv, Ukraine
E-mail: makalex51@gmail.com
ORCID: http://orcid.org/ 0000-0001-6728-3058

A METHODOLOGICAL APPROACH TO THE DEVELOPMENT OF SPATIAL DECISION SUPPORT SYSTEMS FOR TERRITORIAL PLANNING

Svitlana Kuznichenko

Abstract. The paper proposes approaches to building a model of the territory based on the determination of a quantitative indicator of the spatial and functional impact of objects on the adjacent territory. The use of expert assessments and continuous value functions to determine the significance of quantitative properties in models of territories has been substantiated. Approaches to determining the integral properties of the territory are described. The functional diagram of the prototype of the spatial decision support system for territorial planning, which implements the proposed methodological approach is presented.

Keywords: spatial decision support system, geoinformation technologies, multi-criteria decision making, territory model, methods of spatial modeling.

Introduction and statement of the problem

The effectiveness of decisions made on the management of territories is determined by the accuracy, completeness and efficiency of information available to the decision-maker (DM). The absence or incompleteness of the initial data, as well as the impossibility of an objective assessment of the consequences of the decisions made, is the main source of errors leading to negative and often catastrophic consequences, such as economic damage and environmental pollution.

In this regard, spatial decision support systems are gaining relevance, allowing to take into account spatial factors when managing territories. Such systems are in demand when planning the development of cities and regions as infrastructurally rich and equipped (urbanized) territories.

As a rule, spatial decision support systems are built on the basis of models that take into account the ecological, economic and social factors of the problem under consideration using the principles of a systems approach. The decision-making process consists in converting information about the

state of the territory into control information, performed by the decision-maker in the formation and selection of alternatives (decision options).

To form and select alternatives, it is necessary to have a goal and criteria for assessing the effectiveness of management, taking into account resource constraints. At the same time, to select the most preferable from a set of options (alternatives) according to a certain criterion or a set of criteria for assessing management efficiency, methods of multi-criteria decision-making based on matrices of expert assessments are often used.

In a generalized form, the decision-making problem is represented by a tuple of sets of conditions:

$$\langle A, C, F, P; D \rangle, \tag{1}$$

where $A = \{a_1, a_2, \ldots, am\}$ is a finite set of alternatives; $C = \{C_1, C_2, \ldots, Cn\}$ is the set of criteria by which alternatives are evaluated; F is criterion evaluation procedure; P is *DM's* benefits system, contains information on the evaluation of alternatives for each criterion; D is decision rule, sets the procedure for performing the desired action on a set of alternatives (selection, ranking, sorting of alternatives).

In the context of this article, a group of decision-making problems will be considered, which is reduced to the class of discrete problems with a finite set of explicitly specified alternatives. The class of such problems is called MADM – Multi-Attributive Decision Making. Examples of such tasks are the placement of industrial enterprises of a certain type, social facilities, transport routes, the determination of the boundaries and zones of the spread of natural disasters and man-made disasters, etc.

The class of problems of multi-objective decision making (MODM – Multi-Objective Decision Making), or more briefly – multi-objective optimization, is characterized by a sufficiently large or infinite set of implicitly specified alternatives [1, 2].

To solve discrete multicriteria problems such classical methods as MAVT, MAUT, AHP, PROMETHEE, ELECTRE, TOPSIS, etc. are used [3, 4]. Multipurpose problems are solved using various optimization methods, including a wide class of evolutionary / genetic algorithms [5–7].

The spatial nature of the tasks of territorial planning determines the use of geoinformation technologies. Modern geographic information systems (GIS) are an important component of decision support systems due to the developed functions of storing, processing and analyzing geodata, modeling tools and the availability of visualization tools. However, most modern

general-purpose GIS does not contain built-in full-featured tools that can implement a complex MCDA procedure. The use of separate software tools and tools and the lack of a unified system for processing expert knowledge leads to an increase in the duration of pre-project work, that is, to an increase in the life cycle of decision-making, and, accordingly, to an increase in the probability of erroneous results at its various stages. One of the possible ways to overcome the above problems is the development and integration of software tools into GIS that implement the MCDA procedure.

Integration of methods for multi-criteria decision analysis MCDM, Multiple-Criteria Decision Making or MCDA, Multiple-Criteria Decision Analysis [8–10] allows you to expand the capabilities of GIS, namely: to structure the problem of decision-making in the geographic space, to take into account value judgments (there are preferences regarding criteria and / or decision alternatives), ensure transparency of the decision-making procedure for decision makers, as well as the ability to take into account both qualitative and quantitative criteria for a comprehensive assessment of all alternative decision options.

Separate attempts to fully integrate MCDA and GIS tools within the framework of a common interface have found problems associated with the lack of flexibility and interactivity of such systems, which cannot provide the necessary freedom of action for analysts [11]. Therefore, the choice of the procedure and the corresponding MCDA methods that can provide the best solution to a specific problem is an urgent task for developers.

Analysis of recent studies and publications shows that the combination of MCDA and GIS is a fundamental tool for solving spatial problems in many areas [12–14]. Over the past few decades, significant progress has been made in the development of methods for multi-criteria analysis of the suitability of territories [15–17] and the choice of locations for the placement of spatial objects [18–21].

The purpose of this paper is to create a methodological approach to the construction of models and methods of multicriteria decision analysis for assessing the properties of territories and the implementation of these methods in the form of a spatial decision support system built on the basis of GIS.

Materials and Methods

If we consider the territory as a complex system, then the decision-making process can be reduced to an assessment of the model representation of

the system and its properties, which are most consistent with the real state of the territory in the given conditions (Fig. 1). At the same time, in accordance with (1), the goals of assessment, methods and scales of assessment should be defined; evaluation criteria and evaluation procedure. The technology for making managerial decisions is the receipt or generation of alternatives, their comparison according to certain criteria and, depending on the management objectives, their ranking and selection of the best (optimal) alternative.

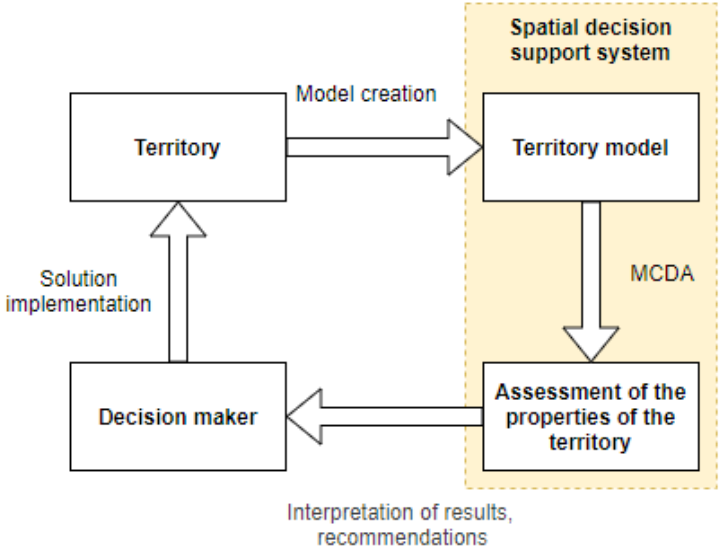

Figure 1. Decision process diagram

In the case of solving the problem of the most rational territorial location of industrial enterprises, social facilities and infrastructure, the properties of an urbanized territory can be considered as a result of the action (influence) of objects belonging to this territory:

$$T \subset O \times H, \tag{2}$$

where $O=\{o_j\}$, $j = 1 \div m$ is the set of objects belonging to the study area; $H = \{h_i\}$, $i = 1 \div n$ is the set of elementary areas into which the territory is divided.

Representation of the territory model as a system of elements and connections between them is as follows:

$$O \xrightarrow{F\mu} P, \tag{3}$$

where $F_{\mu} = \{F_{\mu ij}\}$, $j = 1 \div m$, $i = 1 \div n$ is the set of functions of influence of j-th objects on the i-th elementary areas of the territory; P is the territory property.

Assessment of the properties of a territory is defined as an ordered set of properties of elementary areas:

$$P = \left\{ P_i \mid P_i = \left\{ P_{ij} \right\} \right\}, i = 1 \div n,\ j = 1 \div m, \tag{4}$$

where P_i is the set of properties of elementary areas h_i of the territory, P_{ij} is the value of the influence of the j-th object at the i-th point or elementary area h_i of the territory.

$$P_{ij} = P_j \cdot F_{\mu j}\left(r_{ij}\right), \tag{5}$$

where P_j is thr value of the influence of the j-th object at its location; $F_{\mu j}$ is the influence propagation function of this object; r_{ij} is the distance between the i-th point (elementary area) of the territory and the j-th object.

The influence of a set of objects O on the i-th point (elementary area) of the territory is determined by aggregating the values of the influence of individual objects:

$$P_i = F_{AGG}\left(P_j \cdot F_{\mu j}\left(r_{ij}\right)\right), \tag{6}$$

In general, the influence aggregation function is non-linear and can include logical operations.

The set of elementary cells H is a set of points (pixels) of the study area. point is defined as $i(n\Delta x, m\Delta y)$, according to the x, y coordinates. Therefore, the model of the properties of the territory is a two-dimensional discrete system:

$$H = \left\{ h_{m,n} \mid m \in M, n \in N \right\}, \tag{7}$$

where indices n and m – discrete coordinate values of the position of the raster cells along the axis X (set N) and along the axis Y (set M). To shorten the notation, a couple of numbers m, n denoted by one index i – raster cell number: $H = \{h_i \mid i = 1; N \cdot M\}$.

With this in mind, the property of the territory can be represented as:

$$P_{x,y} = f_p(x, y), \tag{8}$$

Thus, based on (8), a territory raster can be constructed, each point of which, as an attribute, contains the value of the territory property at this point.

One will consider stationary point objects of the territory with constant properties. Then the value of the significance of the property of the object P_i from (4) will depend on the attributes that determine the proper-

ties of the object as an element of the territory. While the function of influence F_μ depends on a variety of properties of the territory (relief, slope, soil type, etc.), as well as on the distance r_{ij} between the *j*-th object and the *i*-th point of the territory.

The territorial influence function F_μ can be set analytically, for example, on the basis of equations describing known physical processes (models of pollution transfer, illumination propagation, etc.). Function F_μ can also be defined as a value function based on expert judgment.

The value function for the continuous range of the estimated parameter $X = \{x\}$ can be defined as follows:

$$f(x) = \mu(x) \to [0,1], \ \forall x \in X, \quad X = \{x\}. \tag{9}$$

The meaning of the value function equal to zero denotes the absolute, based on the expert's intuition, unacceptability of the corresponding value xi, and belonging equal to one – absolute preference. Studies have shown that in the overwhelming majority of cases it is possible to confine oneself to four typical types of preference functions (monotonically increasing, monotonically decreasing, having a maximum or minimum function) containing coefficients, the selection of which allows more or less accurately describe the changing judgments and establish the range of acceptable values of the functions.

For example, it is required to locate a production, one of the location factors of which is distance from settlements. In other words, settlements are objects that influence the location of production. The function of spreading the influence of these objects of the territory is given in the form of an expert value function (Fig. 2).

Figure 2 shows that the most favorable for the location of production according to the criterion of distance from settlements are areas located at a distance of 20 to 30 km from the facility. At a distance of more than 30 km, the influence of the object decreases, and more than 40 km, it is completely absent. Similarly, an increase in influence can be observed at a distance of 10 to 20 km from the object (settlement). The property of the territory P according to this criterion varies from 0 (complete absence of influence) to 1 (maximum influence).

The raster of territory properties for the criterion under consideration can be built using methods and tools of spatial modeling and GIS analysis, for example, geo-tools of the Spatial Analyst Tools libraries of the ArcGIS10.5 package.

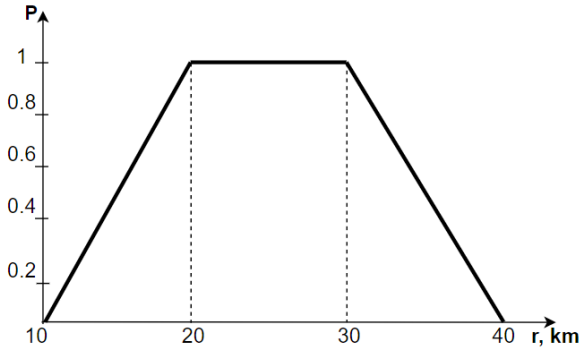

Figure 2. Expert-derived value functions for industrial site selection

For a fragment of a map with a settlement, a raster of Euclidean distances was initially built (Fig. 3 a), then the raster was reclassified in accordance with the influence function in (Fig. 2). The attribute of each cell of the raster in (Fig. 3 b) is equal to the value of the function of the influence of the settlement on the location of production.

In the general case, when constructed in accordance with the function of the spatial and functional influence of the territory raster, the attribute acts as an indicator of the territory's property. More specifically, an attribute is a measurable quantity or quality of the influence of objects on a given area of the territory.

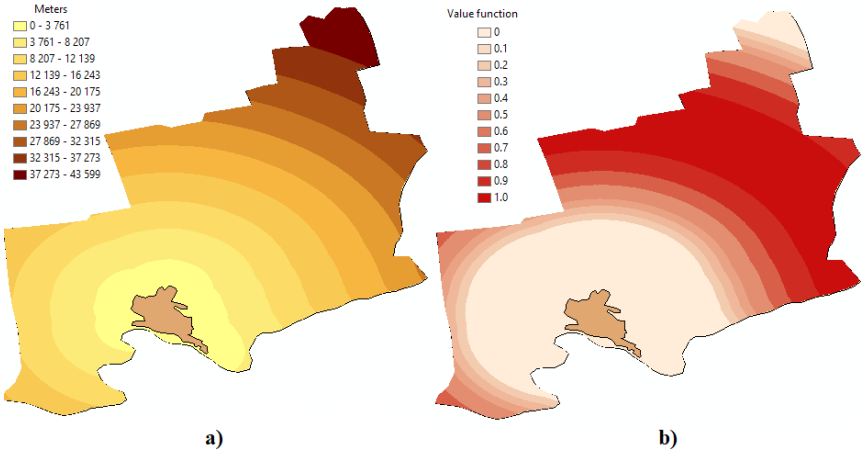

Figure 3. Rasters: Euclidean distance from a pixel to the city centers (a); value functions for industrial site selection (b)

The task of assessing or determining the property of a territory in the simplest case, when one thematic layer is taken, is to sum up at each point of this layer the influence from each of the objects of this layer:

$$P_i^r(n,m) = \sum_{j=1}^{J_r} w_j P_{ij}^r(n,m), \tag{10}$$

where P_i^r is the value of the property estimate for the elementary cell h_i of the thematic layer r; P_{ij}^r is the value of the estimate of the property of the element h_i from the influence of the j-th object that is part of the layer r; Jr is the number of objects contained in the r layer that affect the i-th point; w_j is the weight of the j-th object.

Since a digital map or model of territory properties consists of several thematic layers, the resulting (integral) property of the territory will be determined by the expression:

$$P(n,m) = F_{AGG}\left(P^r\left(n,m\right)\right) \tag{11}$$

The weighted sum operator can be used as an aggregation function. Then (11) can be represented as:

$$P(n,m) = \sum_{r=1}^{R} w_r P^r(n,m), \tag{12}$$

where w_r – the weight of the r-th thematic layer, R – the number of thematic layers from which the integral model of the territory properties is formed.

In the general case, combining the influence of objects in a thematic layer and combining models for evaluating the properties of thematic layers is not limited to the weighted summation function. As noted above, the aggregation function F_{AGG} can be represented by a variety of operations, including fuzzy logic operations.

Based on the above approach, the procedure for making decisions on territorial planning can be represented in two stages (Fig. 1), namely, building a model of the territory and determining the integral properties for the constructed model of the territory based on (11).

Building a model of the territory. To build a territory model, it is necessary to structure the problem and define goals. It is important to prepare geodata, as well as to take into account the factors that characterize or describe the spatial problem, influence the decision and must be taken into account. At least the following steps are required to obtain a model of the territory (Fig. 4):

1) Determination of the geographical area, study area. At this stage, it is important to determine the boundaries of the territory and the

step of its quantization. The value of the quantization step plays an important role in spatial analysis and can lead either to an increase in computational costs with an unreasonably small step, or to an increase in the modeling error – with an excessively large step. It is necessary to optimize the sizes of the elementary cells Δx and Δy, making them as large as possible without losing useful information. In accordance with (1), the selected elementary cells of the territory are alternative solutions.

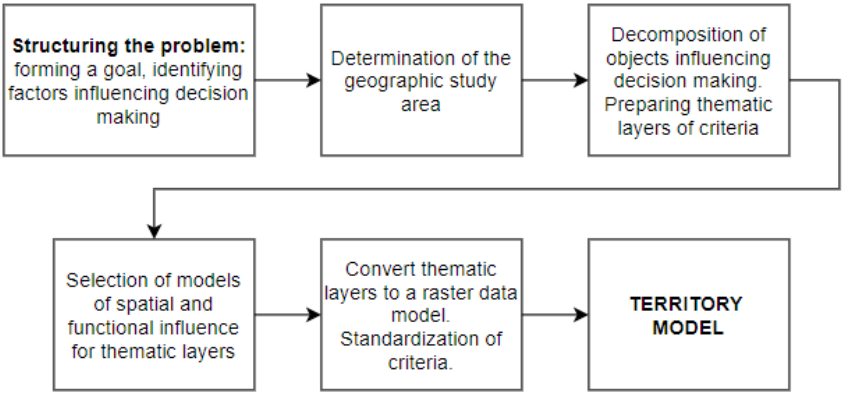

Figure 4. Territory model building process diagram

2) Formation of thematic layers for the study area, depending on the nature of the decision-making problem being solved (formation of the set R). At this stage, the decomposition of the set of objects O, which determine the properties of the territory and influence the decision-making, is performed on the subset of objects O_r of separate thematic layers:

$$O = \bigcup_{r=1}^{R} O_r, \tag{13}$$

where R is the set of properties of the territory (the number of thematic layers) that must be taken into account when solving the problem of decision making. According to (1), each thematic layer is formed on the basis of a certain criterion, according to which alternatives are evaluated.

3) Selection of models of spatial and functional influence P_{ij}^{r} and determination of their parameters. As noted above, the model of spatial-functional influence can be determined using the expert value function (8) or the function of membership in a fuzzy set.

4) Getting thematic layers in the raster data model in the form of elementary cells h_i. Applying the influence function to spatial data allows you to build a raster of a territory, in which the attributes are indicators of the properties of the territory according to the appropriate criterion. Discretization of vector thematic layers into a raster can also be performed using various methods of GIS analysis, for example, geostatistical interpolation, fractal analysis [22], calculating distance using the Euclidean metric, etc.

Determination of the integral properties of the territory. Territory model *M* is actually the set of thematic layers $P^r(n,m)$ built in accordance with the given criteria:

$$M = \left\{ P^r(n,m) \right\}, r = \overline{1,R}, \tag{14}$$

where *r* is number of the thematic layer of the model *M*.

Based on the existing model of the territory *M,* a layer of integral properties of the territory P(*n*, *m*) can be obtained. For this, as a rule, various multicriteria decision-making methods are used, in particular, the abovementioned multicriteria decision analysis methods: MAVT, MAUT, ANR, PROMETHEE, ELECTRE, TOPSIS, etc. (Figure 5) shows a diagram of the process of constructing a layer of integral properties of the territory, consisting of the following stages:

1) Determining the weights of the importance of the criteria w_j. A weight is a value assigned to an evaluation criterion that indicates its importance relative to the other criteria under consideration. A vast majority of the GIS-MCDA applications have use one of the three weighting methods: ranking, rating, and pairwise comparison [6, 10]. They are based on the assumption of spatial homogeneity of preferences. Consequently, they assign a single weight to each criterion. These methods require that the decision making agents specify their preferences with respect to the evaluation criteria. The entropy-based method provides an alternative criteria weighting approach. Unlike the ranking, rating, and pairwise comparison techniques, the entropy method is based on measuring information contained in the criterion values [10]. The weight coefficients of the criteria w_1, w_2,…, w_k,…, w_n must meet the following requirements: $0 \le w_k \le 1$ и $\sum_{k=1}^{n} w_k = 1$. The greater the weight, the more important is the criterion in the overall value/utility. Since the meaning of weights is dependent on multicriteria decision, the weights may have widely differing interpretations for different methods and decision contexts.

2) Determination of the aggregated (integral) assessment of the properties of the territory $P(n, m)$ based on the combination rules. Aggregation is combining criteria attributes according to certain decision-making rules (that is, building a generalized indicator for evaluating alternatives) using overlay operations. In GIS, various aggregation operators can be used: minimum, maximum, arithmetic mean, weighted sum [23]. It is important that the aggregation operator that will be used takes into account the forms of trade-off between the assessments of alternatives according to various criteria that are acceptable for the decision maker. An example of such an aggregation operator is the OWA Yager operator [23].

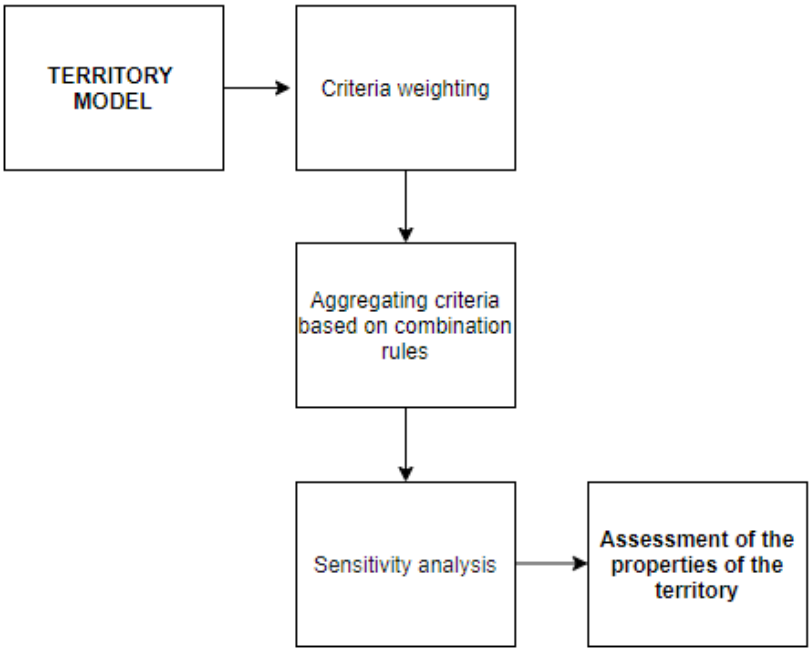

Figure 5. Diagram of the process of constructing a layer of integral properties of the territory

3) Sensitivity analysis allows you to assess the impact of changes in the initial parameters of the model on its final characteristics and actually check the reliability of the solution.

4) Reasonable recommendations for solving the problem. for the decision-maker can be given on the basis of the resulting map of the integrated properties of the territory.

Decomposition of the decision-making procedure into two stages makes it possible to unify approaches to the construction of a layer of integral properties of a territory and to consider them independently of the models of territories. The model of the territory is considered in this case as a certain set of thematic raster layers, the attributes of which are quantitative indicators of the properties of the territory according to a certain criterion. For example, when solving the problem of placing spatial objects is an indicator of the level of suitability of a territory for placing an object according to a certain criterion. In this case, a prerequisite is the standardization of attribute values in the range [0,1], that is, from a complete absence of influence (value, suitability) to maximum influence (value, suitability).

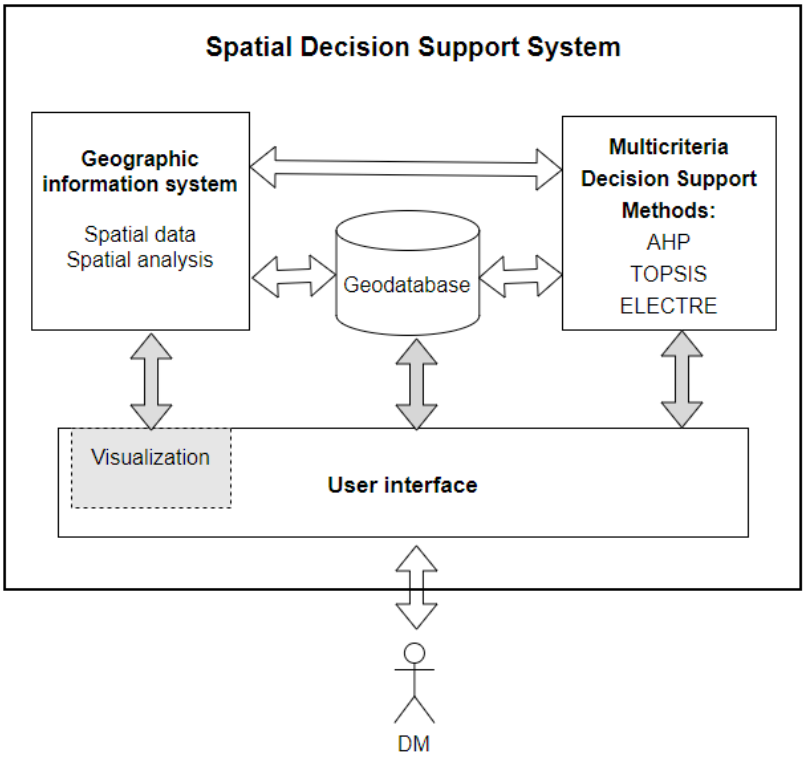

Figure 6. Functional diagram of the spatial decision support system for territorial planning

Methods of spatial modeling and GIS analysis can be used to build a model of territories. Methods of multi-criteria decision-making can be

used to build a layer of integrated properties of territories. At the same time, it is possible to apply the same aggregation procedure to different models of territories. Or, conversely, apply different aggregation procedures to the same territory model.

In (Fig. 6) shows the functional diagram of the spatial decision support system, which implements the proposed approach. The decision support system can be built as an add-on to a geographic information system. Built-in libraries and tools for spatial modeling and GIS analysis can be used to build a model of territories. The separately developed special tools for multi-criteria decisions analysis can be used to build a layer of integrated properties of territories.

An example of similar GIS-based multicriteria spatial decision support systems for planning urban infrastructures is presented in [24], and for the placement of municipal solid waste objects in [25].

Conclusion

To build a decision support system for the development of territories, it is advisable to use the methodology for assessing the ecological and socio-economic state of the territory as its aggregate property to ensure the implementation of production, economic and social activities. This potential of the territory is determined both by the properties of the territory itself, and by the physical, ecological and socio-economic impact on this territory of the entire set of objects located on this territory and beyond.

The paper proposes approaches to building a model of the territory based on the determination of a quantitative indicator of the impact of objects on the adjacent territory. To determine the significance of quantitative properties in models of territories using expert assessments, the use of continuous preference functions is justified.

The approaches to determining the integral properties of the territory are described. It is shown that the decomposition of the decision-making procedure into two stages makes it possible to unify the approaches to the construction of a layer of integral properties of the territory and to consider them independently of the models of territories. The functional diagram of the spatial decision support system for territorial planning, which implements the proposed methodological approach based on the assessment of the properties of the territory, is presented.

References:

1. *Malczewski J.* GIS and multicriteria decision analysis. – New York: Wiley, 1999. – 408 p.
2. *Hwang C.L., Yoon K.* Multiple attribute decision making: Methods and applications. – Berlin: Springer,. 1981. URL: http://dx.doi.org/10.1007/978-3-642-48318-9.
3. *Gwo-Hshiung Tzeng, Jih-Jeng Huang* Multiple Attribute Decision Making: Methods and Applications. Chapman and Hall/CRC, 2011. – 352 p.
4. *Velasquez M., Hester P. T.* An Analysis of Multi-Criteria Decision Making Methods. International Journal of Operations Research – 10(2). 2013. – P. 56–66.
5. *Fonseca C.* Multiobjective Genetic Algorithms with Application to Control Engineering Problems. Ph.D. thesis, University of Sheffield. 1995.
6. *Coello C.C.* 20 years of evolutionary mültiobjective optimization: What has been done and what remains to be done. Computational Intelligence: Principles and Practice: IEEE Computational Intelligence Society, 2006. – P. 73–88.
7. *Srinivas N., Deb K.* Multiobjective Optimization Using Nondominated Sorting in Genetic Algorithms. Evolutionary Computation, – 2(3). 1994. – P. 221–248.
8. *Chakhar S., Martel J.M.* Enhancing geographical information systems capabilities with multicriteria evaluation functions, Journal of Geographic Information and Decision Analysis, 2003. – Vol. 7. – No. 2. – P. 69–71.
9. *Malczewski J.* GIS-based multicriteria decision analysis: a survey of the literature. International Geographical Information Science, – 20(7). 2006. – P. 703–726.
10. *Malczewski J., Rinner C.* Multicriteria Decision Analysis in Geographic Information Science, 2015. Springer, – New York.
11. *Lidouh K.* On themotivation behind MCDA and GIS integration, Int. J. Multicriteria Decision Making, 2013. – Vol. 3. – No. 2/3. – P. 101–113.
12. *Afshari Ali, Vatanparast Mahdi, Ćoćkalo Dragan.* Application of multi criteria decision making to urban planning – A review, Journal of Engineering Management and Competitiveness (JEMC), 2016. – Vol. 6/03. – P. 46–53.
13. *Kuznichenko S., Kovalenko L.,* Buchynska I, Gunchenko Y. Development of a multicriteria model for making decisions on the location of

solid waste landfills. Eastern-European Journal Of Enterprise Technologies, – 2(3, 92). 2018. – P. 21–30. URL: https://doi.org/10.15587/1729-4061.2018. 129287

14. *Mardani A., Jusoh A.,* MD Nor K., Khalifah Z., Zakwan N., Valipour A. Multiple criteria decision-making techniques and their applications – a review of the literature from 2000 to 2014, Economic Research, 2015. – Vol. 28. – No. 1. – P. 516–571.
15. *Lashari Z., Yousif M., Sahito N., Brohi S., Meghwar S., Khokhar U. D., Land Q.* Suitability Analysis for Public Parks using the GIS Application, Sindh University Research Journal (Science Series), 2017. – Vol. 49(09). – P. 505–512.
16. *Joerin F., Theriault M., Musy A.* Using GIS and outranking multicriteria analysis for land-use suitability assessment, Int. j. of geographical information science, 2001. – Vol. 15. – No. 2. – P. 153–174.
17. *Malczewski J.* GIS-based land-use suitability analysis: a critical overview. Progress in Planning, – 62. 2004. – P. 3–6.
18. *Giovanni De Feo, Sabino De Gisi.* Using MCDA and GIS for hazardous waste landfill siting considering land scarcity for waste disposal. Waste Management. 2014. – No. 34. – P. 2225–2238.
19. *Kuznichenko S., Buchynska I., Kovalenko L., Tereshchenko T.* Integrated information system for regional flood monitoring using internet of things. CEUR Workshop Proceedings, 2019. – 2683. – P. 1–5.
20. *Kuznichenko S., Buchynska I., Kovalenko L., Gunchenko Y.* Suitable site selection using two-stage GIS-based fuzzy multi-criteria decision analysis. Advances in Intelligent Systems and Computing, 2020. – 1080 AISC, – P. 214–230.
21. *Rikalovic A., Cosic I., Lazarevic D.* GIS Based Multi-Criteria Analysis for Industrial Site Selection, Procedia Engineering, 2014. – Vol. 69. – No. 12. – P. 1054–1063.
22. *Mikolaj Karpinski, Svitlana Kuznichenko, Nadiia Kazakova, Oleksii Fraze-Frazenko and Daniel Jancarczyk.* Geospatial Assessment of the Territorial Road Network by Fractal Method. Future Internet, 2020. – 12(11). – 201 p. Doi:10.3390/fi12110201
23. *Kuznichenko S., Buchynska I.* Selection of aggregation operators for a multi-criteria evalution of sutability of territories// Cybersecurity: education, science, technology, – Vol. 1(№ 5). 2019. – P. 25–32.

24. *Coutinho-Rodrigues J.* et al. "A GIS-based multicriteria spatial decision support system for planning urban infrastructures." Decis. Support Syst. – 51. 2011. – P. 720–726.
25. *Kuznichenko S., Buchynska I.* Models, methods and tools for multi-criteria decision analysis in geographic information systems. Monograph. – Odessa: OSENU, 2020. – 202 p.

Svitlana Kuznichenko, PhD, Associate Professor, Head of the Information technologies department, Odessa State Environmental University, 15 Lvivska Str, Odesa Ukraine
E-mail: skuznichenko@gmail.com
ORCID: https://orcid.org/0000-0001-7982-1298